IMPLEMENTATION OF LOSS MINIMIZATION CONTROL FOR HIGH PERFORMANCE AC MOTOR DRIVES

RONG-SHEN LU

Implementation of Loss Minimization Control for High Performance AC Motor Drives

by

©Rong-shen Lu, B.Sc.

A thesis submitted to the School of Graduate
Studies in partial fulfillment of the
requirements for the degree of
Master of Engineering

Faculty of Engineering and Applied Science
Memorial University of Newfoundland

May 1993

St. John's Newfoundland Canada

ISBN 0-315-82644-4

Abstract

AC motors have been used in a wide range of power ratings to date and are playing a prominent role in drive applications. However, their highly non-linear dynamic structure with strong dynamic interactions requires more complex control schemes than dc motors.

The conventional linear techniques can no longer satisfy the stringent requirement placed on high-performance ac motor drive applications. Modern control techniques, such as optimal control and adaptive control, are applied in motor drive systems. But the realization of these techniques is generally difficult because of large time-critical computation requirements. Typical field-oriented control of ac motors uses current loop sampling rates of 5 to 10 KHz. This implies that the controller must process the control algorithms within 100 to 200 μs. Thus, for high-performance ac drives, some powerful microcomputers, such as Transputers, and parallel processing techniques are used in ac motor drive systems. On the other hand, reducing the energy losses in adjustable-speed electric motor drives is becoming increasingly important due to the high cost of energy.

Transputer-based parallel processing of high performance ac motor drives can be a good solution for fast dynamic calculation, flexible architecture and interactive control in order to achieve both requirements of high performance and loss minimization of ac motor drives.

The purpose of this study is to investigate and apply multiple Transputers in parallel processing of indirect field-oriented vector control employing loss minimization for high performance ac motor drives. A new scheme is proposed based on the use of multiple Transputers for real-time parallel processing implementation of the

indirect field-oriented control scheme incorporating the loss minimization strategy. Losses in ac motor drives are studied and verified by experiments. Computer simulation results of trials using five Transputers and experimental results of using four Transputers for parallel processing are presented in the thesis. It is shown that high performance as well as significant energy savings for ac motor drives can be achieved by the proposed scheme.

Acknowledgement

I would like to express my most sincere gratitude and appreciation to my supervisors Dr. R. Venkatesan and Dr. J.E. Quaicoe, for their guidance throughout the research and the preparation of this thesis.

I would also like to express my sincere thanks to other professors in the faculty of Engineering at Memorial University of Newfoundland for many valuable discussions and useful suggestions.

Help from the technical staff at the Faculty of Engineering and Applied Science is gratefully acknowledged. Assistance of fellow graduate students is appreciated.

I also like to take this opportunity to acknowledge the financial support through my supervisors' research grant which made this work possible.

Finally, my dedication is due to my mother, my wife as well as my daughter for their encouragement and support.

Contents

List of Figures

List of Tables

Notation

i_{ds}, i_{qs}	direct- and quadrature-axis stator currents in the synchronous rotating reference frame
i_{dr}, i_{qr}	direct- and quadrature-axis rotor currents in the synchrono rotating reference frame
u_{ds}, u_{qs}	direct- and quadrature-axis stator voltages in the synchronous rotating reference frame
u_{dr}, u_{qr}	direct- and quadrature-axis rotor voltages in the synchronous rotating reference frame
i_α, i_β	alpha- and beta-axis stator currents in the stationary reference frame
u_α, u_β	alpha- and beta-axis stator voltages in the stationary reference frame
ω_s	stator angular frequency
ω_r	rotor angular frequency
ω_{sl}	slip angular frequency
ψ_{dr}	rotor flux component in d axis
ψ_{qr}	rotor flux component in q axis
$\psi_{\alpha s}$	stator flux component in α axis
$\psi_{\beta s}$	stator flux component in β axis
$\psi_{\alpha r}$	rotor flux component in α axis
$\psi_{\beta r}$	rotor flux component in β axis
λ_{dr}	rotor flux linkage in d axis
λ_{qr}	rotor flux linkage in q axis
φ	airgap flux

θ_s	stator electrical angle
θ_r	rotor angle
θ_{sl}	slip angle
$*$	superfix denoting the reference value
R_r	rotor resistance
R_s	stator resistance
L_r	rotor inductance
L_s	stator inductance
L_m	mutual inductance
D	viscous friction coefficient
J	total inertia
T	motor torque
T_l	load torque
T_e	electrical torque
n_p	number of pole pairs
N_p	number of pole
s	slip
V	terminal voltage
f	stator frequency
rpm	revolution per minute

Chapter 1

Introduction

Electrical motors have been available for nearly a century and are playing a very important role in today's industrial automation. Several kinds of electrical motors — dc motors, induction motors, synchronous motors (in brushless dc form), step motors, and switch reluctance motors — are used in automatic control system.

DC motors have traditionally dominated the domain of drive systems. Although ac motors are superior to dc motors with respect to size, weight, rotor inertia, efficiency, maximum speed, reliability, cost, etc., because of their highly non-linear dynamic structure with strong dynamic interactions, the ac motors require more complex control schemes than the dc motors. During the last three decades, there has been intense research on the development of ac drive technology. With the rapid developments in the field of power electronics, microelectronics and microcomputers, the cost and performance of ac drives have been improved considerably, which made ac drives viable alternatives to dc drives in many applications. AC drives have been used in a wide range of power ratings to date, for both low-performance as well as high-performance system, and will continue to play a prominent role in drive applications in the future[1].

Today's motion control is an area of technology that embraces many diverse disciplines, such as electrical motors, power semiconductor devices, converter circuits, dedicated hardware signal electronics, control theory, microcomputers, VLSI circuits and sophisticated computer-aided design techniques[2] (Figure 1.1). Each of the component disciplines is undergoing an evolutionary process, and is contributing to the total advancement of motor control technology.

The conventional linear controllers such as PI (proportional - integral), PID (proportional - integral - derivative) have been used in many applications. However, since these controllers with fixed parameters are sensitive to plant parameter variations and load disturbance, performance of the motor drives varies with operating conditions, and it is also difficult to change controller parameters both on-line and off-line. Therefore, the conventional linear control techniques can no longer satisfy the stringent requirement placed on high-performance drive applications, such as fast response, loss minimization, fault tolerance, parameter-insensitivity and robustness. In recent years, research papers have extensively discussed the use of modern control techniques, such as optimal and adaptive control theories, and powerful microcomputers, such as the Transputer, in motor drive systems.

Field-oriented control techniques are now being accepted almost universally for high performance ac motor drives. Compared with the direct field-orientation method, the indirect field-orientation method avoids the requirement of flux acquisition by using known motor parameters to compute the appropriate motor slip frequency to obtain the desired flux position. Therefore, this scheme is simple to implement than the direct method.

Optimal control theory, such as Pontryagin's minimum principle, or the dynamic

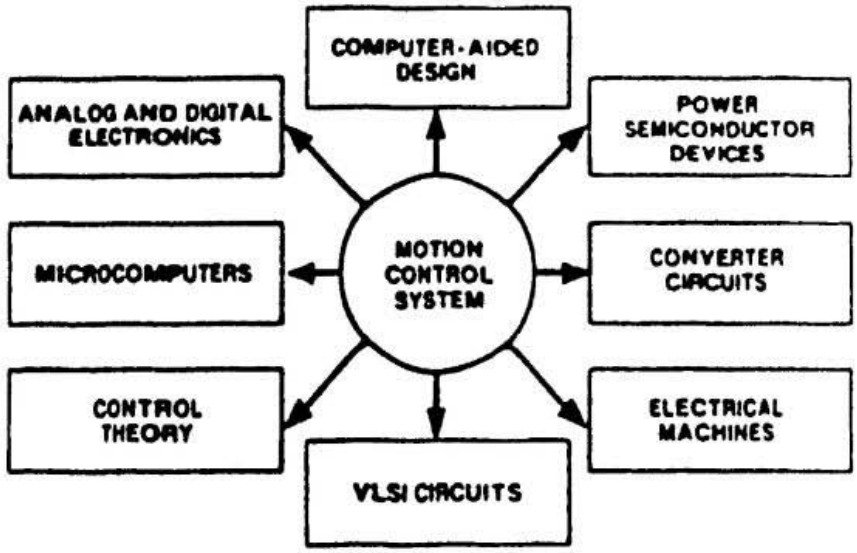

Figure 1.1: Motor control system—An interdisciplinary technology. [2]

programming technique, which is based on extensive iterative computation, can be generally applied to a single optimal profile of the drive system. The optimal precomputed profile can be generated, for example, on the basis of minimum time of transit or minimum energy consumption subject to a number of control constraints[2].

It is becoming increasingly important to reduce the energy losses in adjustable-speed electric motor drives of industrial and transportation systems due to the high cost of energy. Typical field-oriented control of ac motors uses current loop sampling rates of 5 to 10 KHz. This implies that the controller must process the control algorithms within 100 to 200 μs[3]. Modern control techniques, such as optimal control and adaptive control, can meet the needs of high-performance drive applications, but the realization of these techniques is generally difficult because of large time-critical computation requirements. Thus, some interesting architectures of 32-bit machine such as the Transputer can considerably enhance the capabilities of mi-

crocomputers. Since the Transputer allows high-resolution signal processing, it is useful in high-performance drives using modern control theories and is likely to play an increasingly important role in future imbedded control implementations[1].

The Transputer is a powerful microprocessor which has been specifically designed for parallel processing. The speed of parallel processing techniques has the potential of creating a flexible and high performance controller [4]. Therefore, Transputer-based parallel processing of high performance ac motor drives can be a good solution for fast dynamic calculation, flexible architecture and interactive control in order to achieve both purposes of high performance and loss minimization of ac motor drives.

The aim of this study is to investigate the application of multiple Transputers in parallel processing of indirect field-oriented vector control employing loss minimization for high performance ac motor drives. A new scheme is proposed based on the use of a multiple Transputer system for the real-time parallel processing implementation of the indirect field-oriented control scheme incorporating the loss minimization strategy. Losses in ac motor drives are studied and verified by experiments. Computer simulation results of trials using five Transputers and results of experiments using four Transputers for parallel processing are presented in the thesis. It is shown that high performance as well as significant energy savings can be achieved by the proposed scheme.

This thesis is organized into six chapters as follows:

Chapter 2 presents a review of the previous work on energy efficient control of ac motor drives as well as the Transputers and parallel processing for ac motor drives. The fundamental principle of indirect field-oriented control of ac motor drives is also briefly addressed in this chapter.

In Chapter 3, losses in ac motor drives are studied in detail by theoretical derivation and experimental verification. The results of the study show that significant energy savings can be achieved for operation at light torque loads for all speeds, and for torque loads near the rated value under low-speed operation. An indirect field-oriented control method incorporating a loss minimization control strategy in an adaptive control technique is proposed. The model of an ac motor for the field-oriented control is also presented. It is shown that an indirect field-oriented control scheme with a variable frequency loss minimization control system can meet the needs of high-performance drive applications.

Chapter 4 proposes a new scheme of using multiple Transputers for the parallel processing implementation of the proposed indirect field-oriented control scheme employing the loss minimization strategy. The fundamental principles of parallel processing and the Transputer are presented. The hardware and software details of a parallel processing scheme using five T800 Transputers are proposed to emulate the partitioned algorithms for real-time control studies. Execution times of the control process using one (and five) Transputer(s) are also investigated. It is shown that the multiple Transputer system can be a good solution for parallel processing to fully explore the inherent advantages of real-time digital control of ac motor drives.

Chapter 5 provides the digital simulation and experimental results of the proposed Transputer-based parallel processing scheme for ac motor drives. It demonstrates that the proposed scheme can achieve both the potential for high performance of ac motor drives and significant energy savings.

In Chapter 6, conclusions and suggestions for further research are made.

Chapter 2

Review of Literature

In this chapter, a survey of previous work on energy efficient control of ac motor drives as well as the Transputers and parallel processing for ac motor drives is presented. The survey is divided into four sections: the review of energy efficient control of ac motors, field-oriented control, loss minimization based on the field-orientation and adaptive control schemes, and the review of Transputers and parallel processing for high performance ac motor drives.

2.1 Energy Efficient Control

The subject of how to reduce the energy losses in adjustable-speed ac motor drives used in industrial and transportation systems has been studied for several decades. In 1970, Tsivitse and Klingshirn[5] originally introduced the idea of improving the efficiency of ac motors and showed that the optimum efficiency of ac motor drives can be found by combination of stator voltage and frequency for a given speed and load torque. Though they made a lot of assumptions for simplifying the complex problem, the general trend of their results was correct.

Nola[6][7] further investigated the subject and suggested that energy could be saved at light load by restoring the proper balance between no-load losses and losses under load. He introduced a Triac ac voltage controller at the input to a single-phase motor[8]. When a motor was operating in steady state, the controller reduced the motor voltage as a function of load (stator current), consequently reducing the air gap flux density, iron loss, magnetizing current and stator copper loss. The success of this technique was simplicity of both the control strategy and the converter, and effective for motors that operate with a varying load torque.

Galler[9] proposed a feedback control system for energy efficient control of an induction motor driven vehicle. The block diagram of the system is shown in Figure 2.1. He used a linear torque control technique and linear optimal control method in the development of a minimum energy loss controller. Simulation results were presented to show that the scheme could improve the energy utilization by the use of maximum efficiency slip frequency. But he neglected the core losses, and his technique relied heavily on the knowledge of the component values of his equivalent circuit of the induction motor.

Jian et al.[10] studied the relationship between maximum efficiency and motor slip. They used the motor slip as a control quantity and showed that with a linear model of ac motor, there exists for all values of the load torque a unique value of the slip which maximizes efficiency. However, their model did not account for the influence of saturation on the motor parameters.

In 1983, Kusko et al.[11] presented a general survey reporting theoretical analysis of the loss minimization in ac motor drive systems. They proposed that the maximum efficiency could be achieved at any speed and torque operating point by

enforcing a precalculated relation between three motor variables: stator voltage, stator frequency and slip. They also suggested an open-loop controller as given in Figure 2.2. Their controller tried to solve the optimization problem, and measured the power input to the drive and adjusted the output of the controller until the optimum point was reached. Although a solution to the loss minimization problem was achieved, they also neglected the influence of saturation.

Park et al.[12] calculated a sub-optimal value of the slip frequency for a slip controlled current source inverter to achieve the maximum efficiency of ac motor drives. They also calculated the relationship between the dc link current and the slip frequency, which minimizes the motor losses at light load. The experimental results obtained with this system showed substantial power savings.

Park et al.[13] reported the use of microprocessor for optimal efficiency drives. Their scheme was designed to operate at the optimal efficiency slip tracking by adjusting the voltage to frequency ratio. All the control loops in the scheme were implemented using Z-80 microprocessors.

Recently, Famouri et al.[14] presented a practical adaptive control method for loss minimization control of induction motor while maintaining any particular torque-speed load point. Figure 2.3 shows the block diagram of the adaptive controller. This method was suitable for nonlinear torque-speed characteristics, such as a fan or pump load.

Since the field-oriented control of ac motor drives can decouple the two components of stator current and provide independent control of torque flux as in separately excited dc motor, it can achieve both satisfactory steady-state and transient performance. Comparing direct and indirect field-oriented methods, the later is con-

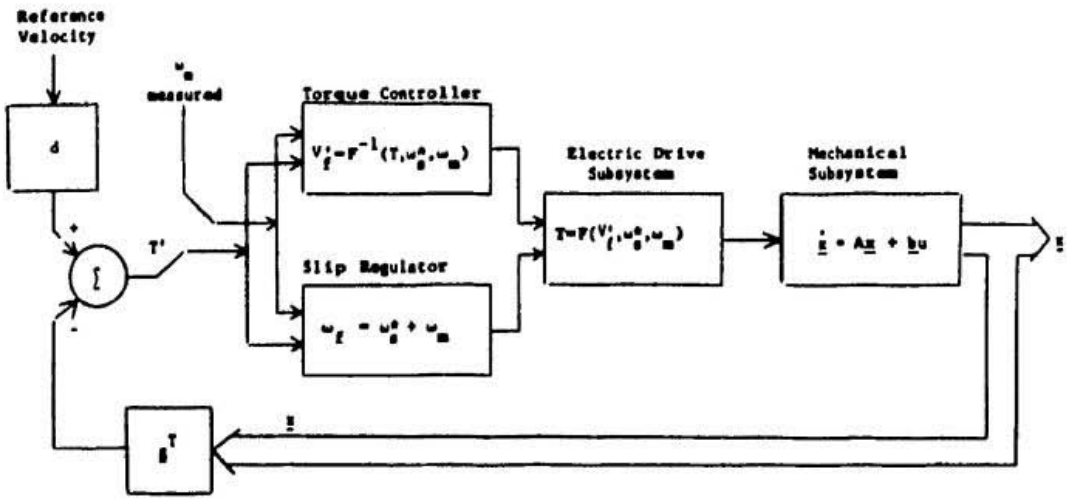

Figure 2.1: Block diagram of the vehicle propulsion and control system. [9]

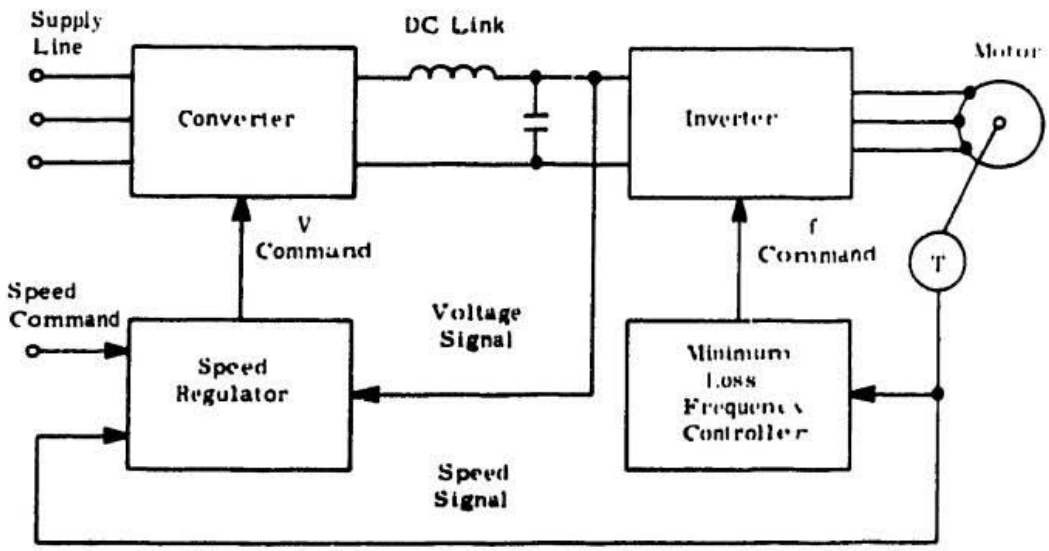

Figure 2.2: Block diagram of the open-loop minimum-loss controller. [11]

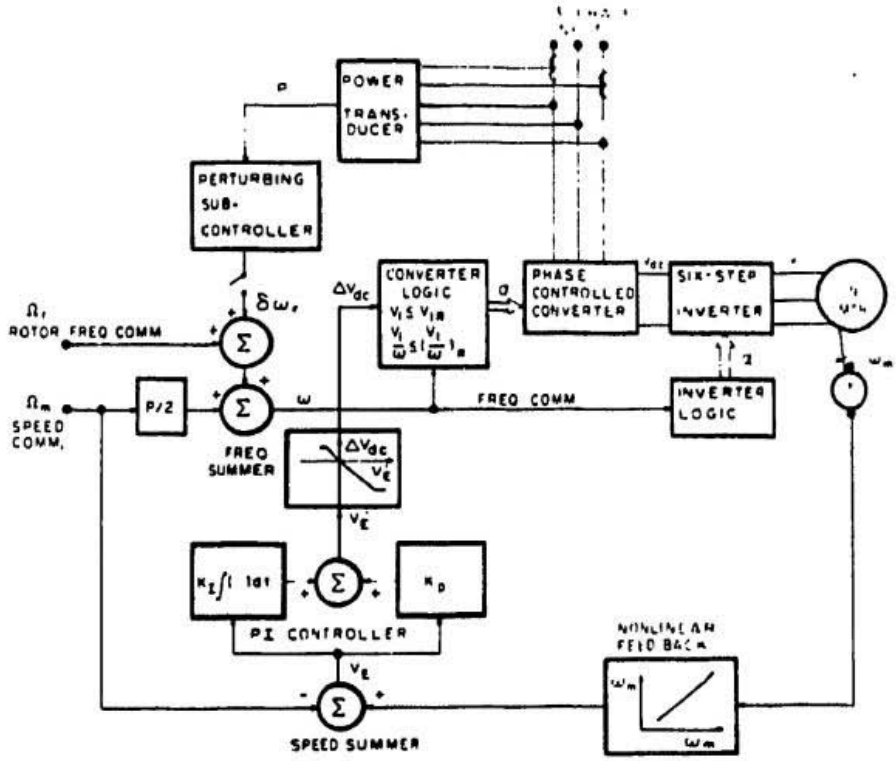

Figure 2.3: Block diagram of the adaptive controller. [14]

sidered as the most practical system due to its various merits such as no required flux sensor and higher reliability of flux measurement, etc.

In the next section, the fundamental principle of the conventional field-oriented drive system is briefly discussed. More papers concerning field-orientation based loss minimization control will be reviewed in Section 2.3.

2.2 Principles of Indirect Field-Oriented Control of AC Motors

Field-oriented control techniques are now being accepted almost universally for high performance ac motor drives. Such control methods were developed in Germany in the early 1970's. Blaschke[15] originally introduced the direct method of field-oriented control and Hasse[16] developed the indirect method. Numerous contributions have been made in these areas to date[18]-[43].

The concept of field-oriented control is based on decoupling the stator current into torque and magnetizing components to give the equivalent of dc motor control characteristics. Vas[40] discussed in detail three types of field-oriented control, namely, the rotor-flux-, the stator-flux-, and the magnetizing-flux-oriented control including the details of the direct and indirect implementations.

Since the general principle of field-oriented control is well established in the literature, only the the basic equations of the control methods are presented here. The more detailed expression and derivation of the principles can be found in several related references [40] and [41].

It is well known that an ac motor can be represented by the following nonlinear dynamic differential equations in $d-q$ axes fixed in the stator with the reference axes rotating at synchronous speed ω_s:

$$u_{qs} = R_s i_{qs} + \frac{d\lambda_{qs}}{dt} + \omega_s \lambda_{ds} \tag{2.1}$$

$$u_{ds} = R_s i_{ds} + \frac{d\lambda_{ds}}{dt} - \omega_s \lambda_{qs} \tag{2.2}$$

$$0 = R_r i_{qr} + \frac{d\lambda_{qr}}{dt} + (\omega_s - \omega_r)\lambda_{dr} \tag{2.3}$$

$$0 = R_r i_{dr} + \frac{d\lambda_{dr}}{dt} - (\omega_s - \omega_r)\lambda_{qr} \tag{2.4}$$

$$\lambda_{qs} = L_s i_{qs} + L_m i_{qr} \tag{2.5}$$

$$\lambda_{ds} = L_s i_{ds} + L_m i_{dr} \tag{2.6}$$

$$\lambda_{qr} = L_m i_{qs} + L_r i_{qr} \tag{2.7}$$

$$\lambda_{dr} = L_m i_{ds} + L_r i_{dr} \tag{2.8}$$

$$T_e = \frac{L_m}{L_r}(\lambda_{dr} i_{qs} - \lambda_{qr} i_{ds}). \tag{2.9}$$

If the rotor flux vector is entirely aligned with the d-axis, then the rotor flux has only a d-axis component. That is,

$$\lambda_{qr} = 0 \tag{2.10}$$

Thus, equation 2.7 becomes

$$i_{qr} = -\frac{L_m}{L_r} i_{qs} \tag{2.11}$$

Substituting equation 2.10 into 2.9 gives,

$$T_e = \frac{L_m}{L_r} \lambda_{dr} i_{qs} \tag{2.12}$$

Equations 2.4, 2.8 and 2.10 yield a relation between i_{ds} and λ_{dr}:

$$(R_r + \frac{dL_r}{dt})\lambda_{dr} = R_r L_m i_{ds} \tag{2.13}$$

Equations 2.12 and 2.13 completely describe the dynamic behaviour of the ac motor.

In the steady state, equation 2.13 becomes,

$$\lambda_{dr} = L_m i_{ds} \tag{2.14}$$

Substituting equation 2.14 into equations 2.9 gives,

$$T_e = \frac{L_m}{L_r}\lambda_{dr} i_{qs} = \frac{L_m^2}{L_r} i_{ds} i_{qs}. \tag{2.15}$$

Equation 2.15 is similar in characteristic to dc shunt motors in which torque and flux can be controlled by i_{ds} and i_{qs}, respectively.

Equations 2.3 and 2.11 give the value of slip frequency needed to keep this orientation of the reference frame. Substituting equations 2.10 and 2.11 into 2.3, and assuming constant i_{ds}, the relation for the slip frequency can be obtained,

$$\omega_{sl} = (\omega_s - \omega_r) = \frac{L_m}{L_r}\frac{R_r i_{qs}}{\lambda_{dr}} = (\frac{R_r}{L_r})\frac{i_{qs}}{i_{ds}}. \tag{2.16}$$

The implementations of field-oriented control of ac motor drives are classified according to the method used to realize the orientation condition, equation 2.10. In the indirect field-oriented control, measured values of ω_r and i_{qs} are used to calculate the stator frequency ω_s from equation 2.16. This particular choice of instantaneous stator frequency aligns the d-axis of the reference frame with the rotor flux and equation 2.10 results.

Two types of typical indirect field oriented control system are shown in Figures 2.4 and 2.5. Figure 2.4 is commonly used for a controlled current source, and figure 2.5 is used for a controlled voltage source.

In field-oriented control systems, the flux command i_{ds}^{*} is commonly kept constant to maintain a constant flux level. A speed (or position) loop is used that regulates the torque command i_{qs}^{*} to obtain proper torque to satisfy the output speed (or position).

2.3 Loss Minimization Based on Field-Oriented Control

Several papers concerning field-orientation based loss minimization control have been published.

In 1983, Peak et al.[44] designed a sub-optimal control strategy to reduce the total losses in a field-oriented induction motor drive systems. They analyzed in detail the losses in the ac motor and the current-fed PWM inverter, and calculated a sub-optimal value of the slip frequency and hence a flux versus torque program for the drive system.

Kim et al.[46] presented an optimal efficiency drive scheme for a current source inverter-fed induction motor by flux control. The efficiency can be substantially improved when the motor is running under light loads. The air-gap flux can be indirectly controlled by adjusting the stator current and slip frequency in the drive system. But their schemes required an accurate knowledge of the motor parameters as in [9][11][13][44] and [45]. Because maximum efficiency slip is more sensitive to

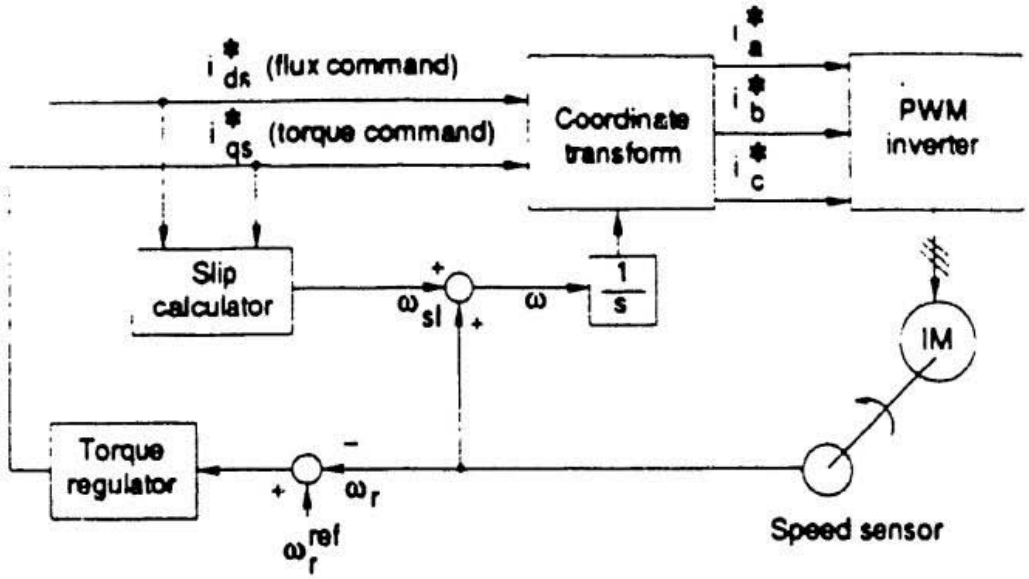

Figure 2.4: Current source indirect field-oriented control system. [35]

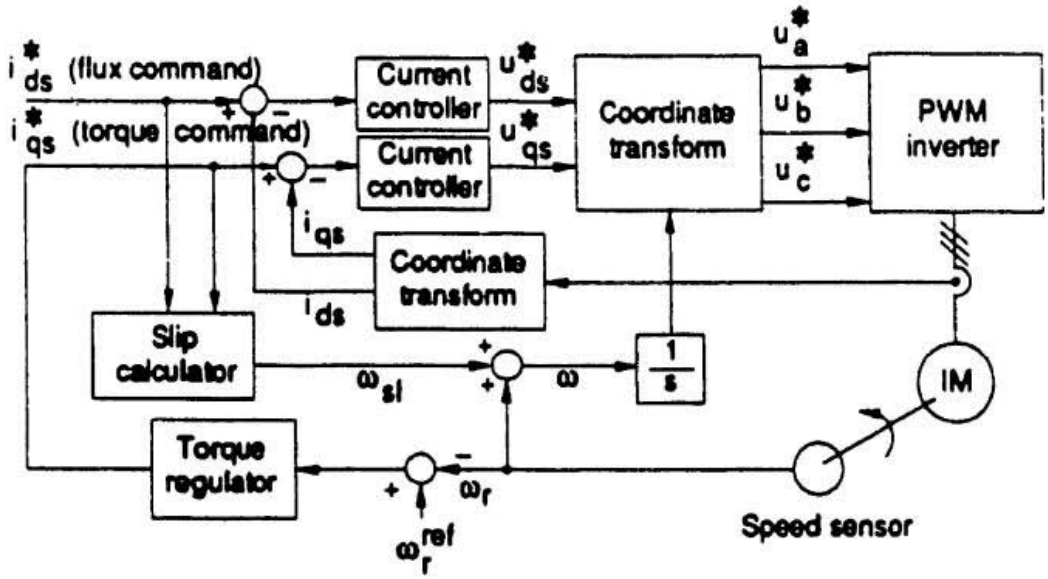

Figure 2.5: Voltage source indirect field-oriented control system. [35]

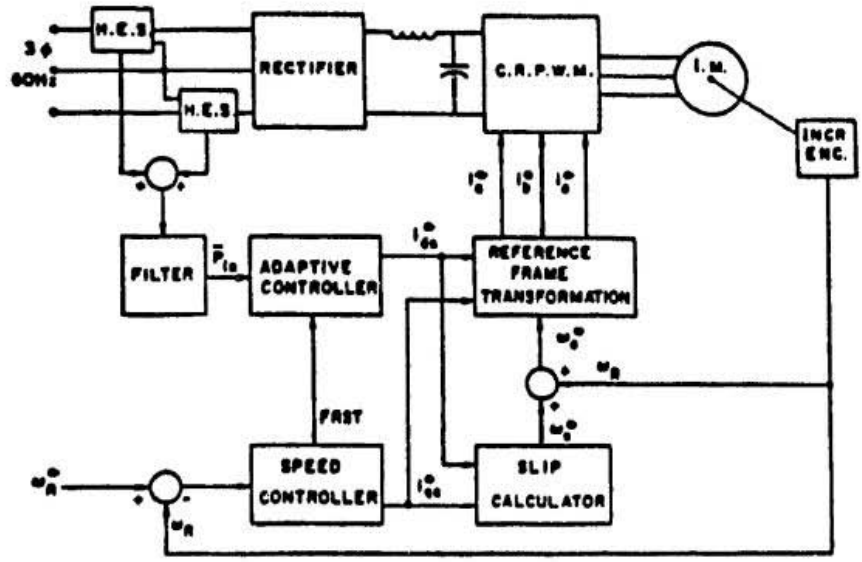

Figure 2.6: Block diagram representation of the prototype system (H.E.S.: Hall-effect sensor, FRST: Flux reset command).[47]

the value of rotor resistance, and dynamic measurement of its value is quite difficult, and the implementations of their schemes are not easy.

Using a direct measurement of the power input and an adaptive control strategy, Kirschen et al.[47] described the implementation of a testing or perturbing controller for minimum loss operation of an indirect field-oriented controlled induction motor. The block diagram representation of the prototype system is shown in Figure 2.6. The principle of the scheme was that for a given load, if the shaft torque or speed is maintained constant, the efficiency of the drive would be maximum when the power measured at the input of the system was minimum. This scheme did not require knowledge of the machine parameters and it yielded a true optimum at any load torque and speed. Two Intel 8085 microprocessors were used for the implementation, and because of the limitation of the sampling cycle, it was difficult to achieve a high

performance of field-oriented controlled motor drive system.

There have been several papers recently published on the subject. Chen et al.[48] applied variable-voltage variable-frequency (VVVF) for the open and closed-loop efficiency analysis and experiment of ac motor. Dynamic programming schemes were used by Lorenz et al. for optimum efficiency closed-cycle operation of field-orientation ac motor drives[49], and for optimally selecting the minimum size machine and/or obtaining optimal time performance from a given machine[50].

Stringent performance requirements for high performance ac motor drive applications are difficult to achieve using conventional microprocessors because of the limitation of their sampling rate. Transputer-based parallel processing in ac motor drives provides fast dynamic calculation thus allowing complex and efficient loss minimization strategies to be implemented in high performance applications.

2.4 Transputers and Parallel Processing for AC Motor Drives

The Transputer is a powerful microprocessor specifically designed for parallel processing. Several researchers have recently focused their efforts on transputer-based parallel processing for electric motor drives. In 1988, Jones et al.[59][60] originally presented a scheme which used Transputers for ac motor control. They divided the calculations of the control algorithm into three independent parts:

1. voltage generation,

2. current transformation and control, and

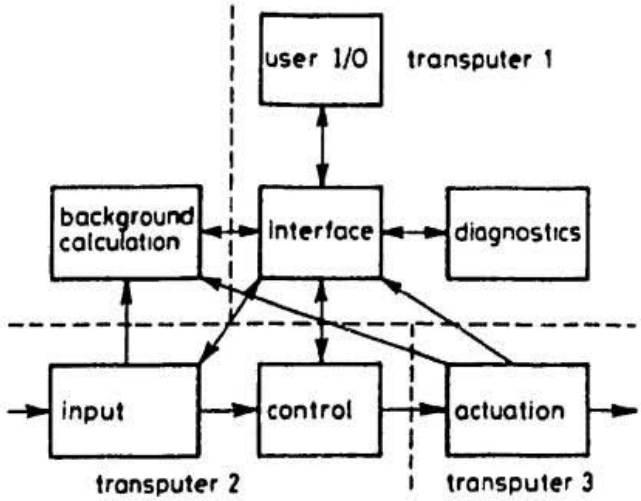

Figure 2.7: Tasking scheme for motor control (with transputer mapping for vector control) [64]

3. decoupling computation and speed control.

These three parts were processed in parallel over two or three transputers and the sampling time of the current loop was 250 μs.

Asher et al. [64] developed a parallel processing scheme which used two T212 and one T400 transputers for the implementation of vector control schemes, including two methods of PWM generation. The proposed general motor drive tasking scheme is shown in Figure 2.7. The low level in the figure consists of signal input, conditioning, control processing and actuator output for the power convertor. The next level covers the drive's intelligence, supervision and memory. The highest level is user input/output.

They implemented three indirect vector control schemes, namely,

1. impressed stator voltages with open-loop stator dynamic compensation,

impressed stator voltages with current control, or the current-controlled V-type[23], and

3. impressed current method or *I*-type[26].

Figures 2.8 and 2.9 show the implementations of transputer-based V-type (Methods 1 and 2) and I-type vector control strategies (Method 3), respectively.

In their implementations, the Transputer 1 ($T1$) is a T414 mounted on a B004 board resident in an expansion slot of an IBM AT host computer. It works as a "supervisor" and oversees diagnostic storage and user interface, the parallelism allowing transient performance data to be passed to the host for display, while reference and control parameters can be user input and passed to the control transputer also during drive operation. The host computer acts as a file handler and editor. The Transputers 2 and 3 ($T2$ and $T3$) handling the control and actuation are 16 bit T212 devices. $T2$ handles speed and line current acquisition, speed control, slip and inverter frequency calculation, and current acquisition for monitoring. Speed is sampled every 5 ms while currents are sampled at 250 μs for all the three methods. The outputs of $T2$ are the inverter frequency f, and the reference $d-$ and $q-$axis voltages, and these are transmitted to $T3$ every 250 μs. $T3$ implements an asynchronous symmetrically sampled PWM generator running with a 2 kHz carrier, with the modulating waveforms being derived from the 2-3-phase transforms. Sine and cosine lookup tables are stored in internal RAM and the transputer is fast enough to compute pulsewidths in real time, making for a highly programmable PWM generator. The pulse times for 3 phases are downloaded via link adapters to three 16 bit counters for PWM waveform synthesis.

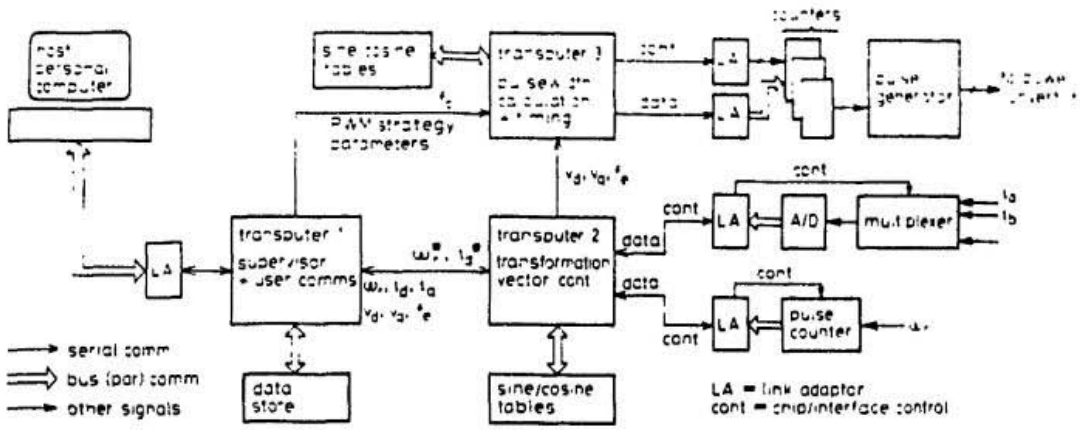

Figure 2.8: Implementations of transputer-based V-type vector control strategies. [64]

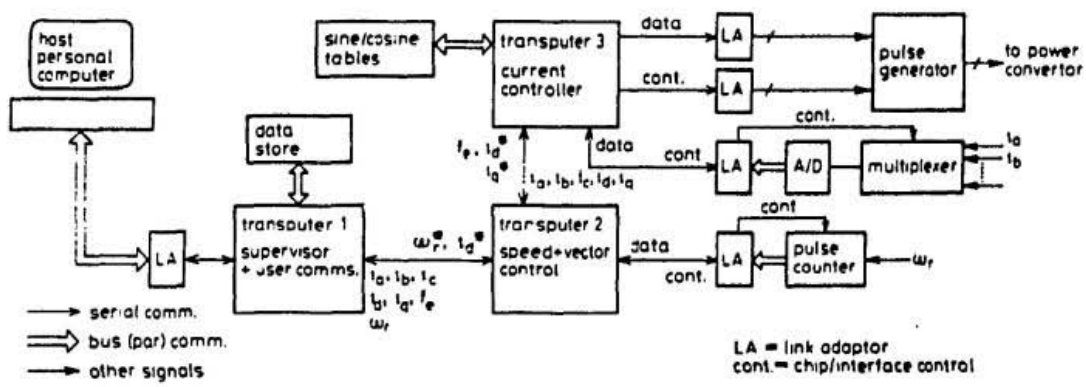

Figure 2.9: Implementations of transputer-based I-type vector control strategies. [64]

Sampling times in the above schemes are too large, and it can be reduced by applying several methods, for example, using newer enhanced Transputers such as the T424 and T800 with a serial link speed of 20 Mbit/s, instead of the T212 they used, which operates at 10 Mbit/s.

Harley et al. [3] proposed a three transputer-based parallel processing for a field oriented controlled ac servo drive. They investigated how the field-oriented control scheme and space vector modulation algorithm can be partitioned for parallel processing, then increasing the system's sampling rate and trying to add other features for enhancing the drive system. The diagram of the controller and the software distribution is shown in Figures 2.10 and 2.11, respectively.

The implementation of the hardware, which is an AIL (analog in loop) system developed by Stellenbosch University in South Africa, has some problems, since the AIL system has a limited sampling delay of 125 μs per channel. Therefore, the AIL system is not suitable to implement control systems of the required bandwidth, due to slow I/O and poor interrupt facilities.

In 1991, Harley et al.[4] addressed some issues in the use of the transputer for real-time applications of a high performance ac motor drive. These issues included event response times, scheduling strategies, I/O and real-time kernel performance. They were still trying to make the real-time kernel to form a platform to support a highly programmable and configurable drive controller, including features such as parameter sampling and user interaction, which were required in high performance ac drive controllers to facilitate, fault tolerance, self-tuning and user friendliness.

Li [43] proposed a scheme using five transputers for parallel processing simulation of indirect field-oriented control of an induction motor. Based on simulation

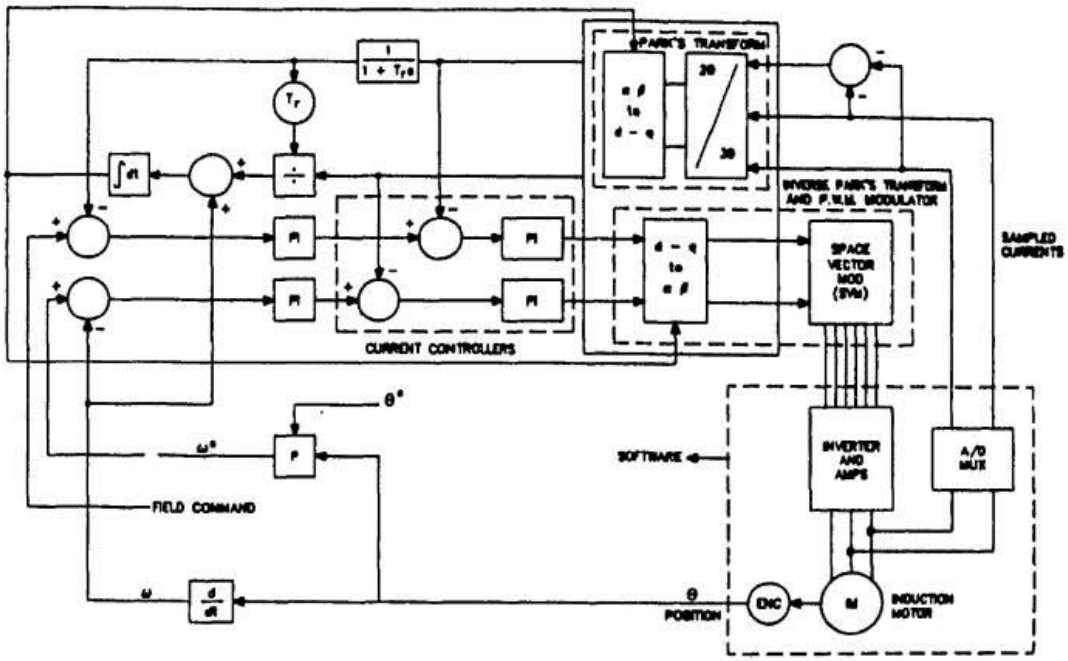

Figure 2.10: Diagram of the field oriented control and space vector modulation controller. [3]

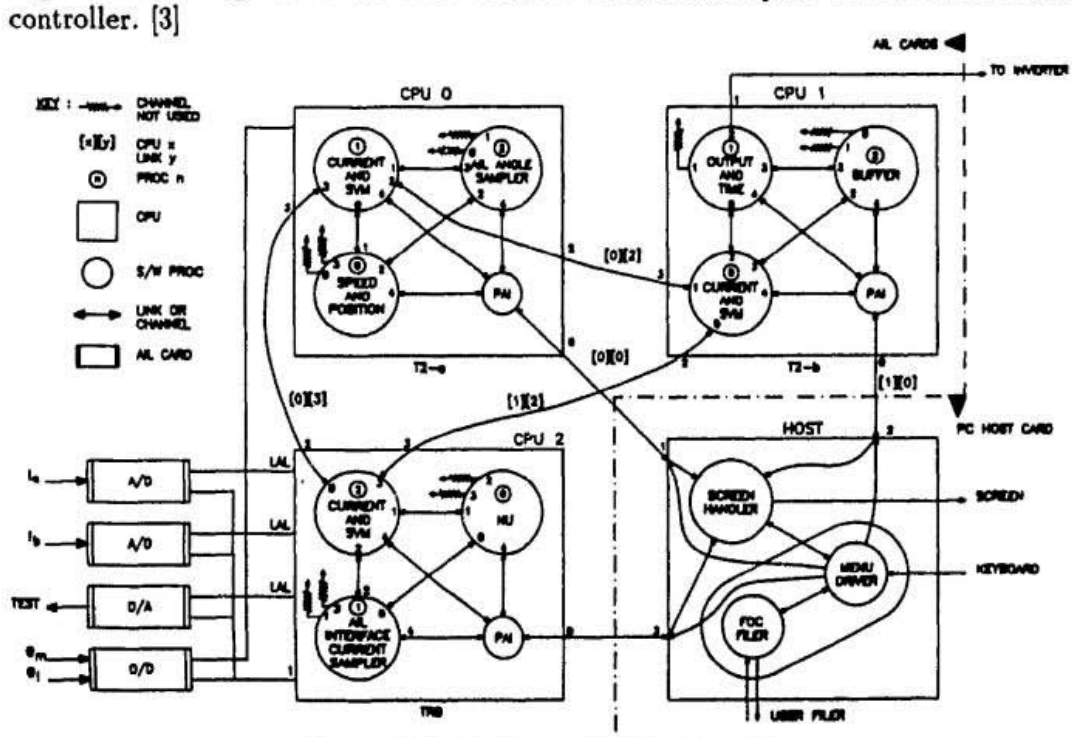

Figure 2.11: Software distribution [3]

trials, measured execution times showed that his scheme could achieve very short processing times thus meeting fast dynamic control demands. Certain fault tolerance tests for Transputer communication link failures or processor failures were also reported.

Bowes et al. presented two transputer-based control schemes for inverter drives. One was for harmonic-elimination PWM control [67] and another was for optimal PWM control [68]. In [67], the authors used the INMOS transputer-based parallel processing for a new harmonic-elimination PWM strategy for ac drives, and emphasized the concurrent programming ability of the transputer for PWM generation. Experimental results of transputer-controlled PWM inverter driver were presented there. In [68], the implementation of the INMOS transputer-based optimal PWM strategy for inverter-induction motor drive system were addressed. Li and Venkatesan [69] proposed a new simulation scheme of five transputer-based parallel processing for indirect field-oriented control of ac motor.

It can be seen from the survey of previous work that, due to the high cost of energy and the needs of high performance of ac motor drives, it is necessary to develop a Transputer-based parallel processing scheme for field-oriented control incorporating loss minimization for ac motor drives. This subject will be discussed in detail in the rest of the thesis.

Chapter 3

Loss Minimization Control of AC Motor Drives

From the previous chapter, we know that significant energy savings of ac motor drives can be achieved by several schemes. In this chapter, losses in ac motor drives have been studied in detail by theoretical derivation and experimental results. Since the maximum efficiency of ac motor drive is a complex function of the motor parameters, it is therefore necessary to apply an adaptive controller to achieve the efficiency optimization. It is also shown that a proposed loss minimization control scheme, which incorporates an adaptive control technique in an indirect field-oriented control method, can achieve the aim of significant energy savings for ac motor drives. The model of an ac motor are briefly addressed and the parameters of the ac motor for the experiment are also calculated in this chapter.

3.1 Losses in AC Motor Drives and Loss Minimization

Consideration of motor losses is important for at least three reasons[37]:

- Losses determine the efficiency of the motor and appreciably influence its operating cost;
- Losses determine the heating of the motor and hence the rating or power output that can be obtained without undue deterioration of the insulation;
- The voltage drops or current components associated with supplying the losses must be properly accounted for in a motor representation.

Motor efficiency is given by

$$Efficiency = \frac{output}{input} \tag{3.1}$$

which can also be expressed as

$$Efficiency = \frac{input - losses}{input} = 1 - \frac{losses}{input} \tag{3.2}$$

or

$$Efficiency = \frac{output}{output + losses} \tag{3.3}$$

In general, there are several kinds of losses in an ac motor, and they can be categorized into three parts as follows:

- The copper losses in stator and rotor windings, and the stray-load loss. These losses are proportional to the square of the rotor current;
- The iron loss which is caused by hysteresis and eddy currents, and the mechanical losses due to friction and windage;
- The effect of some other nonideal factors, such as saturation, skin effect and source harmonic.

This section details losses in ac motor drives and demonstrates by theoretical derivation that potential energy savings can be achieved.

3.1.1 Potential Energy Savings

The behaviour of an ac motor drive can be described by three independent variables, namely, the speed N, the terminal voltage V and frequency f_s, and by the parameters of the motor and its power supply. In a field-oriented control scheme, the speed of the ac motor is adjusted by voltage, current and/or frequency. The loss minimization of the drive and potential energy savings can be found at any speed and torque operating point.

Figure 3.1 shows the steady state speed versus torque characteristics for a given operating point, and Figure 3.2 shows the efficiency and loss curves for a particular operating point. It can be seen from the figures that for each load speed and torque, there exist many different combinations of stator voltage V and stator frequency f_s in an induction motor operating in the steady state at an output power characterized by a speed ω_r and a load torque T_l. The efficiencies are different for different combinations and the minimum power input to the ac motor must exist among all the possible solutions.

The power input to a motor can be minimized for a given speed and torque load, if a proper balance is established within the various losses. The flux level must be at the center of this optimization process. The core loss is directly a function of the flux, and flux variation changes the amount of current for a given torque, thus affecting the stator and rotor losses.

Kusko et al.[11] examined the general problem of loss minimization and described

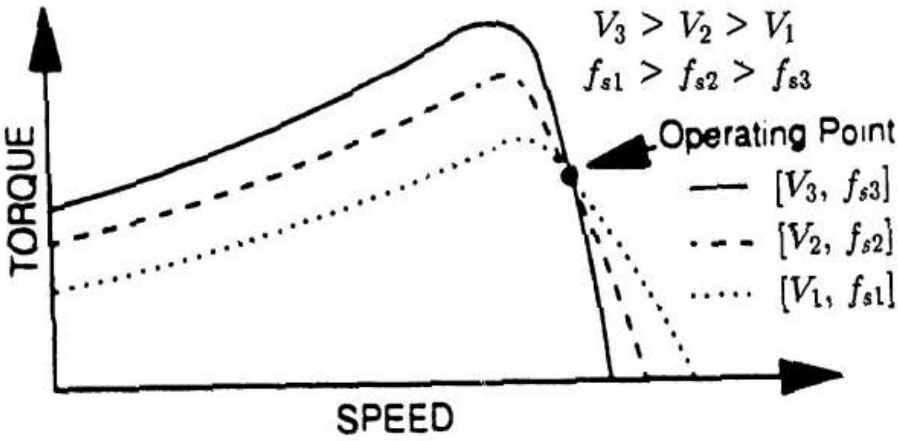

Figure 3.1: The operating point on torque-speed curve. [56]

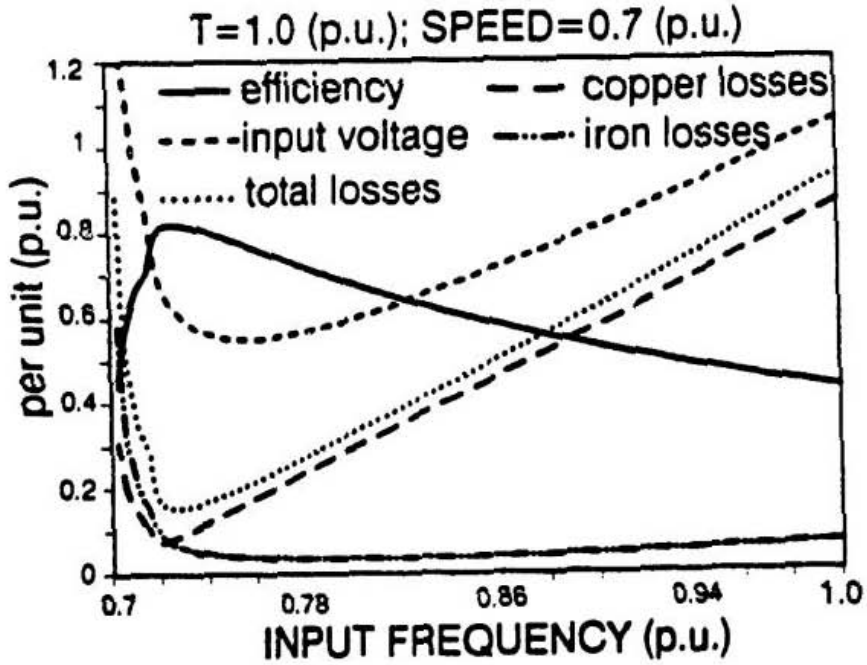

Figure 3.2: The efficiency and losses curves of the operating point. [56]

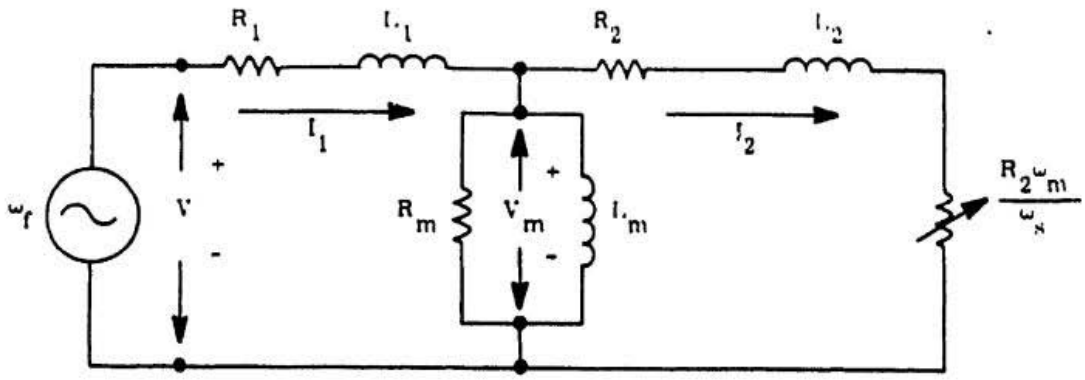

Definitions

$Z_1 = R_1 + j\omega_f L_1$
$Z_2 = R_2\omega_f/\omega_s + j\omega_f L_2$
$Z_m = R_m j\omega_f L_m/(R_m + j\omega_f L_m)$
$Z_T = Z_1Z_2 + Z_1Z_m + Z_2Z_m$
$Z = Z_T/(Z_2 + Z_m)$

ω_f = $2\pi f$
ω_m = $2\pi 60N/N_s$
ω_s = $\omega_f - \omega_m$
N_s = Rated speed
N = Speed (r/min)

Figure 3.3: Per-phase equivalent circuit and definitions used for ac motor analysis. [11]

qualitatively the nature of the solution. They used the equivalent circuit of Figure 3.3 to derive the total controllable loss P_t and showed that P_t is a function only of the frequency for a given speed and torque.

Assuming that the friction, windage and the stray load losses are independent of torque at constant speed, the stator and rotor copper losses and the core loss can be minimized at a given torque because they are controlled by the stator voltage and frequency. Using equivalent circuit (Figure 3.3) of the ac motor, the total controllable loss P_t, which includes rotor and copper loss and core loss, can be expressed as:

$$P_t = |I_1|^2 R_1 + |I_2|^2 R_2 + \frac{|V_m|^2}{R_m} \tag{3.4}$$

Equation 3.4 can be rewritten as:

$$P_t = V^2 \left[\left| \frac{Z_2 + Z_m}{Z_T} \right|^2 R_1 + \left| \frac{Z_m}{Z_T} \right|^2 R_2 + \left| \frac{Z_m Z_2}{Z_T} \right|^2 / R_m \right] \tag{3.5}$$

where the impedances are as defined in Figure 3.3. Z_2 and Z_T are functions of the frequency and the slip, hence P_t is a function of V, f_s and N.

For steady state, we assume that the speed N be constant. That is to say, only f_s and V can be varied to reduce the loss. For a given speed and torque operating point, f_s and V are dependent. This dependence is expressed as,

$$T = f(V, f_s, N) \tag{3.6}$$

or

$$T = V^2 f_T(f_s, N) \tag{3.7}$$

and

$$V^2 = \frac{T}{f_T(f_s, N)}. \tag{3.8}$$

Equation 3.8 can be expressed in terms of the motor parameters (from Figure 3.3) as,

$$V^2 = \frac{T\omega_s}{N_p R_2} \left| \frac{Z_T}{Z_m} \right|^2 \tag{3.9}$$

Inserting equation 3.9 into equation 3.5, the controllable loss is obtained as,

$$P_t = \frac{2\pi T(f - 60N/N_s)}{R_2 N_p} \left[\left| \frac{Z_2 + Z_m}{Z_m} \right|^2 R_1 + R_2 + \frac{|Z_2|^2}{R_m} \right]. \tag{3.10}$$

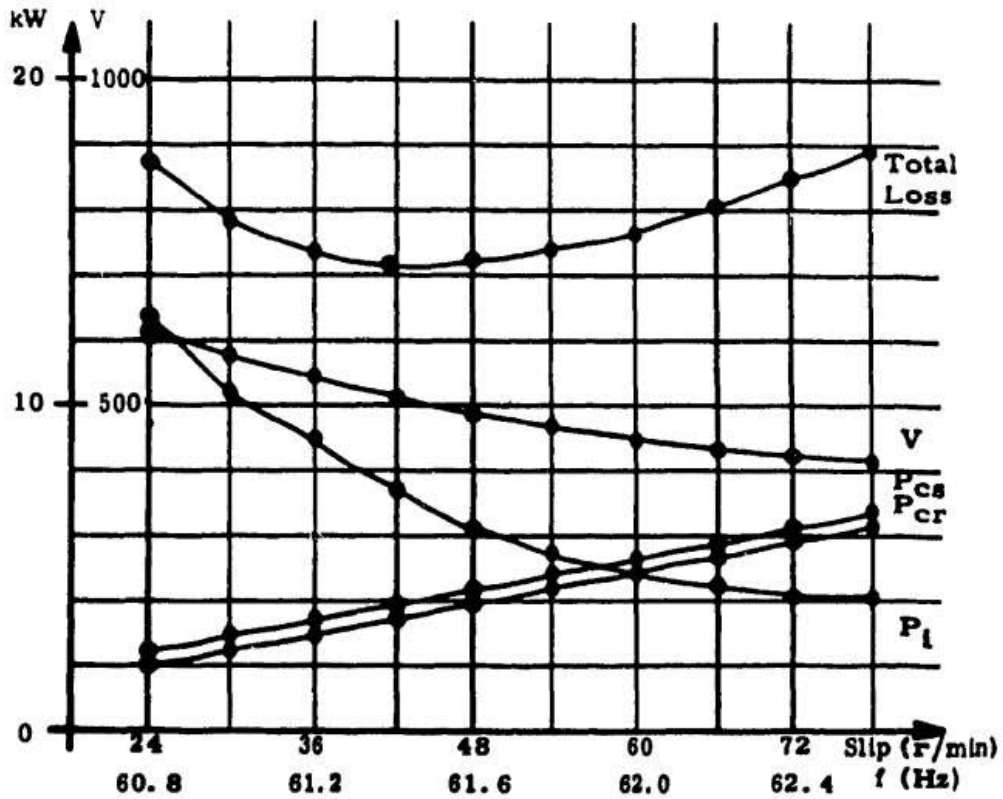

Figure 3.4: Loss-components for 100-hp induction motor as function of slip rpm. B=1800 rpm, T=1.0 p.u. [11]

The expression shows that the controllable loss P_t is a function only of the frequency for a given operating point.

Figure 3.4 shows the behaviour of P_t for a 100-hp motor at constant speed and torque, where the voltage is varied as shown to maintain constant torque. It is clear that there is a minimum loss point at 61.4 Hz.

Now, we can try to achieve the minimum P_t by setting equation 3.10 as,

$$\left|\frac{\partial P_l(T, f, N)}{\partial f}\right|_{T,N} = 0 \tag{3.11}$$

Solving equation 3.11 for f_s as a function of torque T and speed N, the minimum loss operation can be achieved. But this equation is too difficult to solve. We have to neglect the core loss in equation 3.11 in order to simplify the problem and obtain a closed-form expression. Then the solution to equation 3.11 can be achieved as,

$$f_s = 60\frac{N}{N_s} + \frac{1}{2\pi}\sqrt{\frac{R_1 R_2^2}{R_1(L_2 + L_m)^2 + R_2 L_m^2}}. \tag{3.12}$$

Finally, the numerical results of the frequency for loss minimization can be obtained as

$$f_s = 60\frac{N}{N_s} + (aN + b) \tag{3.13}$$

where a and b are constants. The first term in equation 3.13 corresponds to the rotor speed and the second term is a linear function of the slip frequency which varies with motor speed. If $a = 0$, it means that the frequency for minimum loss is that the slip frequency f_s is a constant. The constants a and b can be found numerically and programmed into a controller. Due to the use of linear motor model, equations 3.12 and 3.13 are not functions of torque T, and the values of the components in Figure 3.4 are functions only of N and f.

Figures 3.5 and 3.6 show the loss components and total controllable loss for an induction motor (75 kW) at 1.0 pu (1800 rpm) speed and variable torque. An open-loop minimum loss controller is applied for the demonstration. Figure 3.5 shows the losses for conventional operation, in which the voltage and frequency are adjusted together (constant V/Hz). As the figure shows, the largest loss component is the core loss P_{cr} as the torque is reduced. Figure 3.6 demonstrates the losses for

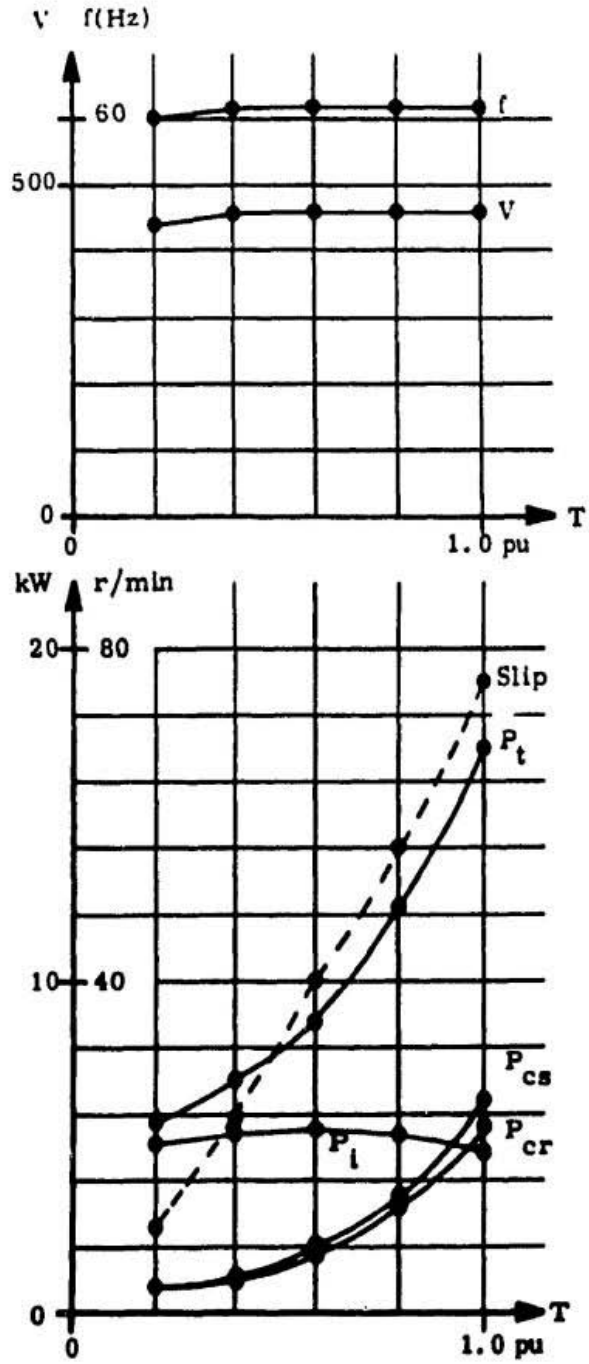

Figure 3.5: Power loss for constant V/Hz operation at constant speed.[11]

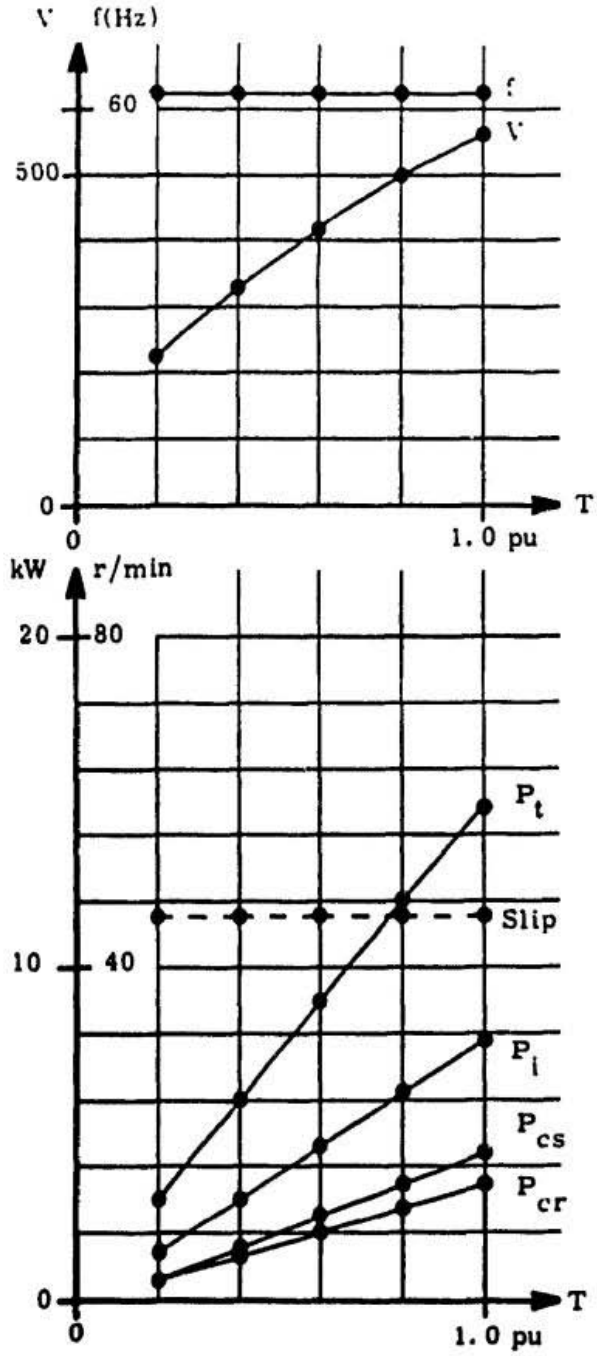

Figure 3.6: Power loss for minimum loss operation at constant speed.[11]

minimum loss operation. The voltage is reduced as the torque is reduced. The loss components remain in balance: core loss equals stator plus rotor copper losses.

Comparing Figure 3.5 with Figure 3.6, we can find that the total controllable losses P_t in the former vary from 17 kW at 1.0 pu torque to 6 kW at 0.2 pu torque, as well as P_t in the latter vary from 15 kW at 1.0 pu torque to 3 kW at 0.2 pu torque. These figures also demonstrate that if the loss components remain in balance (e.g. core loss equals stator plus rotor copper loss), the loss minimization operating point can be achieved.

3.1.2 Losses in AC Motor Drives

Since the losses in ac motor drives is a complex problem, it is difficult to comprehend the problem intuitively. If some nonideal factors, e.g. core saturation, skin effect and source harmonics, are taken into account, the mathematical relations become highly involved. Several researchers have studied this problem[57] [48]. Using a modified equivalent circuit of induction motor, Kirschen[57] developed a steady state equivalent circuit which includes saturation, stray load losses, harmonic losses, skin effect in the rotor bars and the dependence of the core losses on frequency. Figure 3.7 shows the equivalent circuit. In the following, we discuss further the losses in ac motor drives. More details concerning this subject can be found in [34] [38] and [57].

A. Core losses

The core loss is the sum of the eddy current losses and the hysteresis losses in the stator and rotor of an ac motor. The expression for the eddy current losses in the stator can be described as,

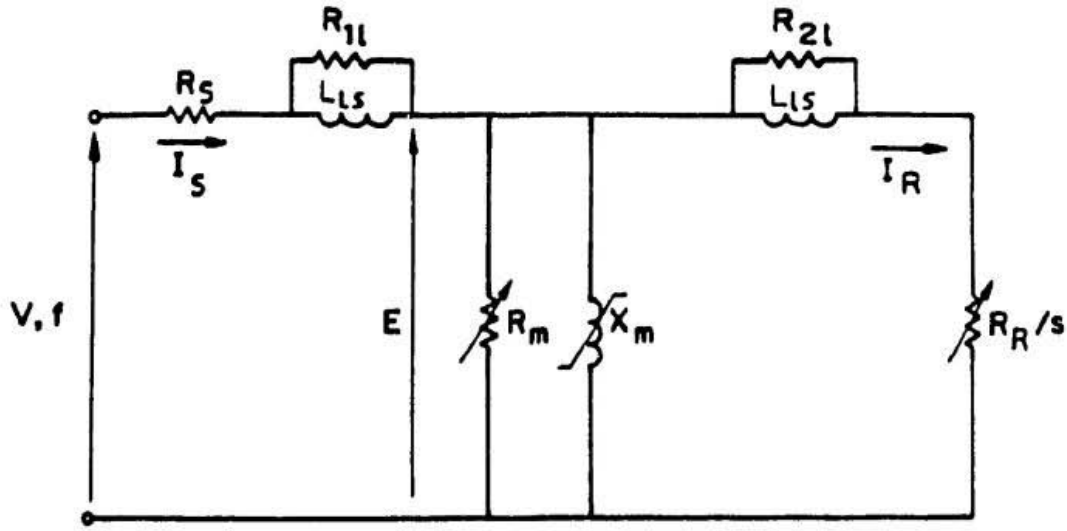

Figure 3.7: Modified equivalent circuit of induction motor.[57]

$$W_{es} = \beta_e f^2 \varphi^2 \tag{3.14}$$

and the hysteresis losses in the stator as,

$$W_{hs} = \beta_h f \varphi^n \tag{3.15}$$

where,

φ — airgap flux.

n — empirical coefficient varying between 1.5 and 2.5.

β_e — per-unit stator eddy current loss at rated frequency and 1 p.u. airgap flux.

β_h — per-unit stator hysteresis loss at rated frequency and 1 p.u. airgap flux.

Here β_e and β_h are dependent on the type of magnetic material and proportional to the volume of the stator. Replacing the stator frequency f by the rotor frequency sf, the eddy current loss in the rotor can be obtained as,

$$W_{er} = \beta_e (sf)^2 \varphi^2 \tag{3.16}$$

and the rotor hysteresis losses is given by,

$$W_{hr} = \beta_h s f \varphi^n. \tag{3.17}$$

Assuming $n = 2$, the total rotor core loss is obtained as,

$$W_m = W_{er} + W_{hr} = \beta_h (1+s) f \varphi^2 + \beta_e (1+s^2) f^2 \varphi^2 \tag{3.18}$$

B. Saturation Effect

Since the magnetic materials in motors are not ideal, an increase in flux results in a decrease in the magnetic permeability. Consequently, the effectiveness of the magnetic material contributing to the overall flux density in the motor decreases. The influence of saturation on motor performance is introduced in the form of correction factors on the magnetizing reactance and the equivalent core loss resistance. In order to incorporate the effect of core saturation in the analysis, the circuit parameters R_m and X_m in the equivalent circuit are evaluated by no-load test for the range of airgap flux level under consideration. Figure 3.8 shows the experimental results for the saturation coefficients C_{rm}, C_{xm} of R_m and X_m[56].

$$C_{rm} = -0.5895(flux)^4 - 0.0088(flux)^3 + 0.2882(flux)^2 + 0.7983(flux) + 0.47 \tag{3.19}$$

and

$$C_{xm} = -4.8156(flux)^4 + 10.4226(flux)^3 - 9.27(flux)^2 + 3.831(flux) + 0.6825. \tag{3.20}$$

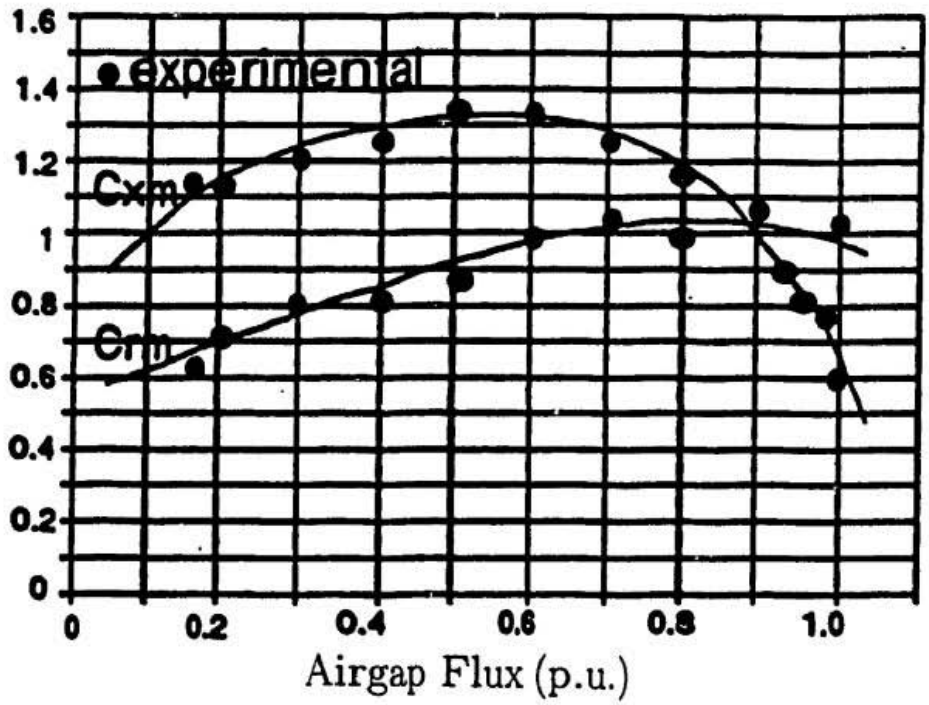

Figure 3.8: Saturation coefficient curves.[56]

C. Harmonic Losses

Voltage and current harmonic losses in ac motor drive are due to the non-sinusoidal nature of the pulse width modulation (PWM) inverter output waveform. The harmonic losses in the steady state can be calculated by the Fourier series method with an equivalent circuit at each frequency until the contribution of the higher harmonics becomes negligible. The harmonics occur at the positive and negative sequences of the k-th order, where $k = 6n \pm 1$ with n = positive integers. The harmonic slip of the k-th order S_k thus is,

$$S_k = \frac{\pm kf - f_r}{\pm kf} = 1 \pm \frac{1 \mp s}{k} \tag{3.21}$$

where f_r is the mechanical speed. The negative sign applies to the forward rotating harmonic fields and the positive sign to the backward rotating harmonic field.

D. Skin Effect

When the alternating current travels through the conductor, the cross effect of the magnetic and electric fields will cause the current to concentrate its density toward the surface. The higher the input frequency, the more pronounced the skin effect will be.

Skin effect influences the value of the rotor resistance and leakage reactance and could have a significant impact on the motor losses[84]. For caged induction motors, skin effect will result in the increase of rotor resistance and decrease of rotor inductance with slip frequency. The benefits are the increase of the starting torque and the reduction of the copper loss in the rotor at steady state[52].

E. Stray Load Losses

Stray load losses consist of the losses arising from nonuniform current distribution in the copper and the additional core losses produced in the iron by distortion of the magnetic flux by the load current. The stray load losses have only a small impact on motor performances when supplied by a sinusoidal source. But their influence becomes more significant and comparable to the harmonic copper losses if the motor is fed by an inverter[84]. Honsinger[18] suggested a model of these losses using resistances connected in parallel with the stator and rotor leakage reactances. He showed that at the fundamental frequency, the additional losses are small (about 1 % of rated output power) and concentrated in the stator since the slip is small.

Using a numerical search procedure, Kirschen et al. [47] calculated the combination of stator voltage and frequency which produces the minimum amount of losses for a given value of speed and load torque. Figure 3.9 presents the difference between the power input obtained with conventional constant volts per hertz control and the minimum power input at various load torques and speeds for a specific 7.5 hp motor. Figure 3.10 shows the same data in terms of the relative reduction in losses. Figures 3.9 and 3.10 demonstrate that when motors operate outside the rated load condition, the losses are higher, and therefore the most significant energy savings can be obtained at light loads.

3.2 Experimental Results of the Losses and the Parameters in an AC Motor

According to references [36] [37] and [38], the procedures of no-load and blocked-rotor tests for ac motor are addressed in this section. Thus, experimental test results are presented to calculate the parameters of an ac motor for the experiment and to study the losses in the motor.

3.2.1 Procedures of No-load and Blocked-Rotor Tests

From no-load and blocked-rotor tests, all values in the equivalent circuit of an induction motor in Figure 3.11 can be obtained.

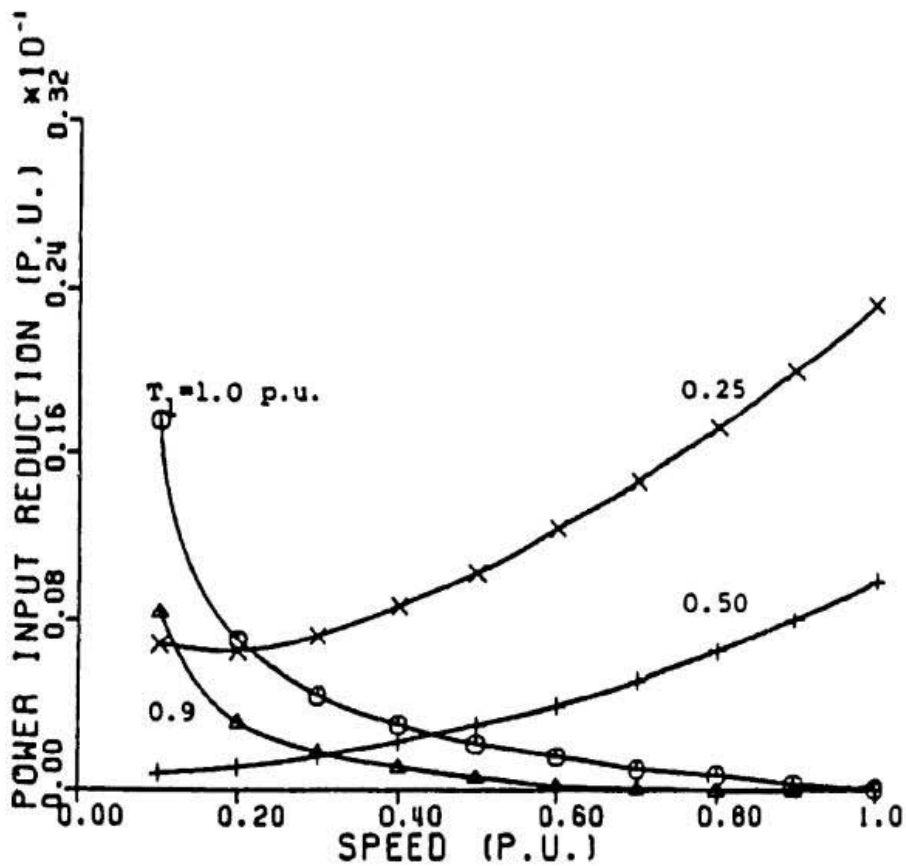

Figure 3.9: Calculated reduction in power input for a 7.5 hp test motor (in p.u.). [47]

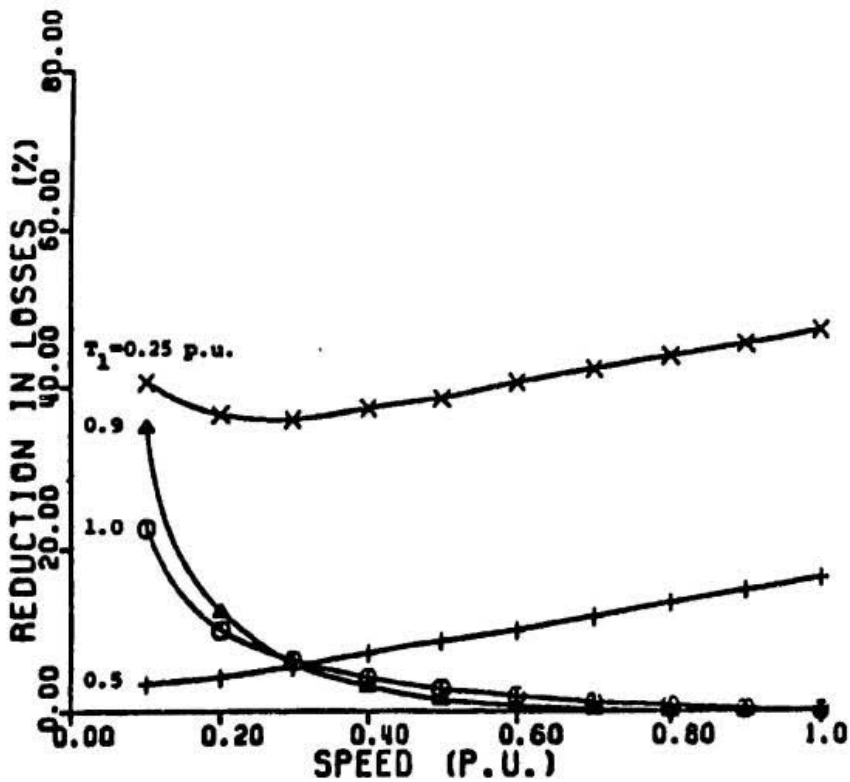

Figure 3.10: Calculated relative reduction in losses for a 7.5 hp test motor. [47]

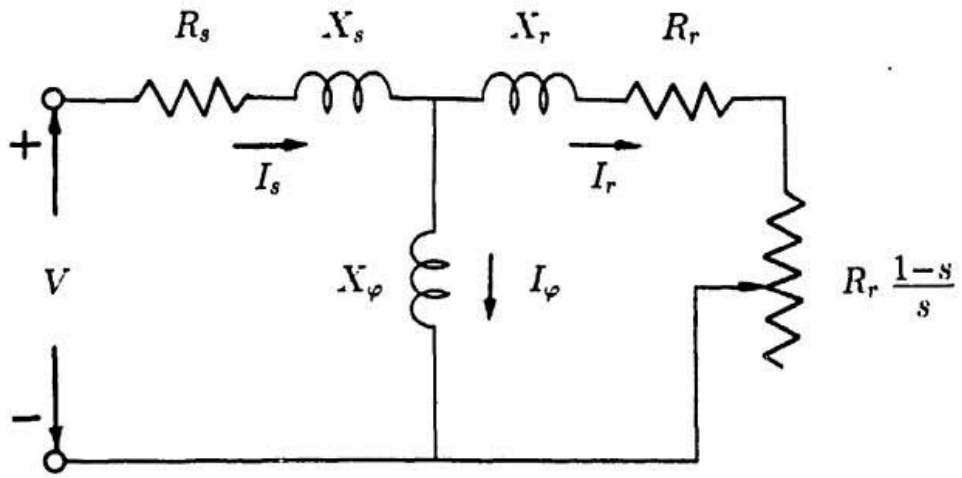

Figure 3.11: Equivalent circuit of an induction motor.

No-Load Test

The no-load test on an induction motor gives information with respect to exciting current and no-load losses. The test is ordinarily done at rated frequency and with balanced polyphase voltages applied to the stator terminals. Readings are taken at rated voltages, after the motor has been running long enough for the bearings to be properly lubricated. The total rotational loss at rated voltage and frequency under load usually is considered to be constant and equal to its no-load value.

At no load, the rotor current is only the very small value needed to produce sufficient torque to overcome friction and windage. The no-load rotor I^2R loss therefore is negligibly small. The rotational loss P_R for normal running conditons is

$$P_R = P_{nl} - q_1 I_{nl}^2 R_s \tag{3.22}$$

where P_{nl} = total polyphase power input at no load

I_{nl} = current per phase at no load

q_1 = number of stator phases

R_s = stator resistance per phase

Because the slip at no load is very small, the reflected rotored rotor resistance $\frac{R_r}{s_{nl}}$ is very large. The parallel combination of rotor and magnetizing branches then becomes jX_φ shunted by a very high resistance, and the reactance of this parallel combination therefore nearly equals X_φ. Consequently the apparent reactance X_{nl} measured at the stator terminals at no load very nearly equals $X_s + X_\varphi$, which is the self-reactance X_{11} of the stator, that is

$$X_{11} = X_s + X_\varphi = X_{nl} \tag{3.23}$$

The self-reactance of the stator can therefore be determined from the instrument readings at no load. For a 3-phase ac motor with star-connection, the magnitude of the no-load impedance Z_{nl} per phase is

$$Z_{nl} = \frac{V_{nl}}{\sqrt{3}I_{nl}} \tag{3.24}$$

where V_{nl} = line-to-line terminal votage in the no-load test.

The no-load resistance R_{nl} is

$$R_{nl} = \frac{P_{nl}}{3I_{nl}^2} \tag{3.25}$$

and

$$X_{nl} = \sqrt{Z_{nl}^2 - R_{nl}^2} \tag{3.26}$$

Usually the no-load power factor is about 0.1, so that the no-load reactance very nearly equals the no-load impedance.

Blocked-Rotor Test

The blocked-rotor test provides information on the leakage impedances. The rotor is blocked and balanced polyphase voltages are applied to the stator terminals.

The leakage impedance of an induction motor may be affected by magnetic saturation of the leakage-flux paths and by rotor frequency. The blocked impedance may also be affected by rotor position, although this effect generally is small with cage rotors. The blocked-rotor test should be taken under conditions of current and rotor frequency approximately the same as those existing in the operating condition.

A frequency of 25 percent of rated frequency is suggested in [36]. The total leakage reactance at normal frequency can be obtained from this test value by considering the reactance to be proportional to frequency. The blocked impedance can be measured directly at normal frequency.

If the exciting current is neglected, the blocked-rotor reactance X_{bl}, corrected to normal frequency, equals the sum of the normal-frequency stator and rotor leakage reactances X_s and X_r. The performance of the motor is relatively little affected by the way in which the total leakage reactance $X_s + X_r$ is distributed between stator and rotor. Table 3.1 shows the empirical distribution of leakage reactances in induction motors.

The magnetizing reactance X_φ can be obtained from the no-load test and the value of X_s as

$$X_\varphi = X_{nl} - X_s \tag{3.27}$$

Because R_s can be considered as its dc value, R_r then can be calculated as follows.

Table 3.1: Empirical distribution of leakage reactances in induction motors. [36]

Motor class	Description	Fraction of $X_1 + X_2$	
		X_1	X_2
A	Normal starting torque, normal starting current	0.5	0.5
B	Normal starting torque, low starting current	0.4	0.6
C	High starting torque, low starting current	0.3	0.7
D	High starting torque, high slip	0.5	0.5
Wound rotor		0.5	0.5

From the blocked-rotor test, the blocked resistance R_{bl} can be computed by means of a relation similar to equation 3.25. The difference value R between the blocked resistance R_{bl} and the stator resistance R_s can be determined from test data. That is

$$R = R_{bl} - R_s \tag{3.28}$$

From the equivalent cicuit (Figure 3.11), with $s = 1$, R is the resistive part of the combination of $R_r + jX_r$ in parallel with jX_φ; thus

$$R = R_r \frac{X_\varphi^2}{R_r^2 + X_{22}^2} \simeq R_r \left(\frac{X_\varphi}{X_{22}}\right)^2 \tag{3.29}$$

where $X_{22} = X_r + X_\varphi$ is the self-reactance of the rotor. if X_{22} is greater than $10R_r$ as is usually the case, less than 1 persent error results from using the approximate form of equation 3.29. Substituting it into equation 3.28, R_r can be obtained as,

$$R_r = R\left(\frac{X_{22}}{X_\varphi}\right)^2 = (R_{bl} - R_s)\left(\frac{X_{22}}{X_\varphi}\right)^2 \tag{3.30}$$

From the equations 3.22 - 3.30, all the parameters in the equivalent circuit of the induction motor (Figure 3.11) are obtained. These parameters can be used to

compute the motor performance under load. In Chapter 5, these parameters will be used in real-time control of the indirect field-orientation scheme employing loss minimization strategy.

3.2.2 Test Results of the Parameters and the Losses in an AC Motor

According to the testing procedures addressed above, experimental results are presented to calculate the parameters of an ac motor for the experiment and to study the losses in the motor as follows.

Parameters of An AC Motor

The nameplate data of the tested motor are list in Appendix A-1. Using Type 2503 Digital AC Power Meter and 8010A Digital Multimeters, several test data are obtained as follows:

1. Test 1: No-load Test at 60 Hz:

   Applied voltage V_{ll} = 208 V, Average line current I_{nl} = 2.93 A,
   Power P = 429 W, Speed = 1792 rpm.

2. Test 2: Blocked-Rotor Test at 15 Hz:

   V_{ll} = 52 V, I = 14.02 A, P = 885 W.

3. Test 3: Blocked-Rotor Test at 60 Hz:

$$V_{ll} = 208 \text{ V}. \qquad I = 41.55 \text{ A}. \qquad P = 8745 \text{ W}.$$

4. Test 4: DC Resistance Per Stator Phase:

Using HP 4328A milliohmmeter, the average dc resistance per stator phase is measured as:

$$R_s = 1.04\ \Omega \text{ / phase (Y connection)}$$

Based on the above test results and the equations 3.22 - 3.30 as well as Table 3.1, all the parameters in the equivalent circuit (Figure 3.11) are calculated:

From Test 1 and equation 3.22, $P_r = 331$ W.

From Test 1 and equations 3.24 - 3.26,

$$Z_{nl} = 41.00\ \Omega\text{/phase Y}, \qquad R_{nl} = 16.66\ \Omega, \qquad X_{nl} = 37.46\ \Omega.$$

From Test 2,

$$Z'_{bl} = 2.14\ \Omega\text{/phase at 15 Hz}, \qquad R_{bl} = 1.50\ \Omega, \qquad X'_{bl} = 1.53\ \Omega \text{ at 15 Hz},$$

and $X_{bl} = 6.12\ \Omega$.

As usual, we choose the motor with normal starting torque low starting current type. According to Table 3.1, this is design class B, thus,

$$X_s = 2.448\ \Omega\text{/phase}, \qquad X_r = 3.672\ \Omega\text{/phase},$$

and by equation 3.27, $X_\varphi = 35.5\ \Omega$/phase.

From test 4 as well as equations 3.28 and 3.30:

$$R = 0.46\ \Omega\text{/phase}, \qquad R_s = 0.562\ \Omega\text{/phase}.$$

The equivalent circuit parameters of the motor are listed in Appendix A-1.

Losses in An AC Motor

1. Test 1: Test with Mechanical Load:

   V_{ll} = 208 V, I = 3.36 A, P = 615 W, Speed = 1785 rpm.

   Since the power of no-load test is 429 W, the mechanical load T_m is

   $$T_m = 615 - 429 = 186 \text{ W}.$$

2. Test 2: Power Input for Different Speeds:

   Figure 3.12 shows the test of the power input for different speeds of the ac motor with mechanical load and 420 W electrical load. The input voltage is reduced as the speed is reduced. The speed is changed from 866 rpm (The supply frequency is 30 Hz.) to 1723 rpm (This is rated speed.). The figure shows the input power varies from 909 W to 1939 W.

3. Stator I^2R losses: 129.6 W.

4. Air-gap power P_g: $P_g = 8745 - 129.6 = 8615.4$ W.

5. Caculated Internal Starting Torque T_{start}:

   Since ω_s = 188.5 rad / s, $T_{start} = \frac{P_g}{\omega_s} = 45.7$ N m.

In Chapter 5, some more test results are presented.

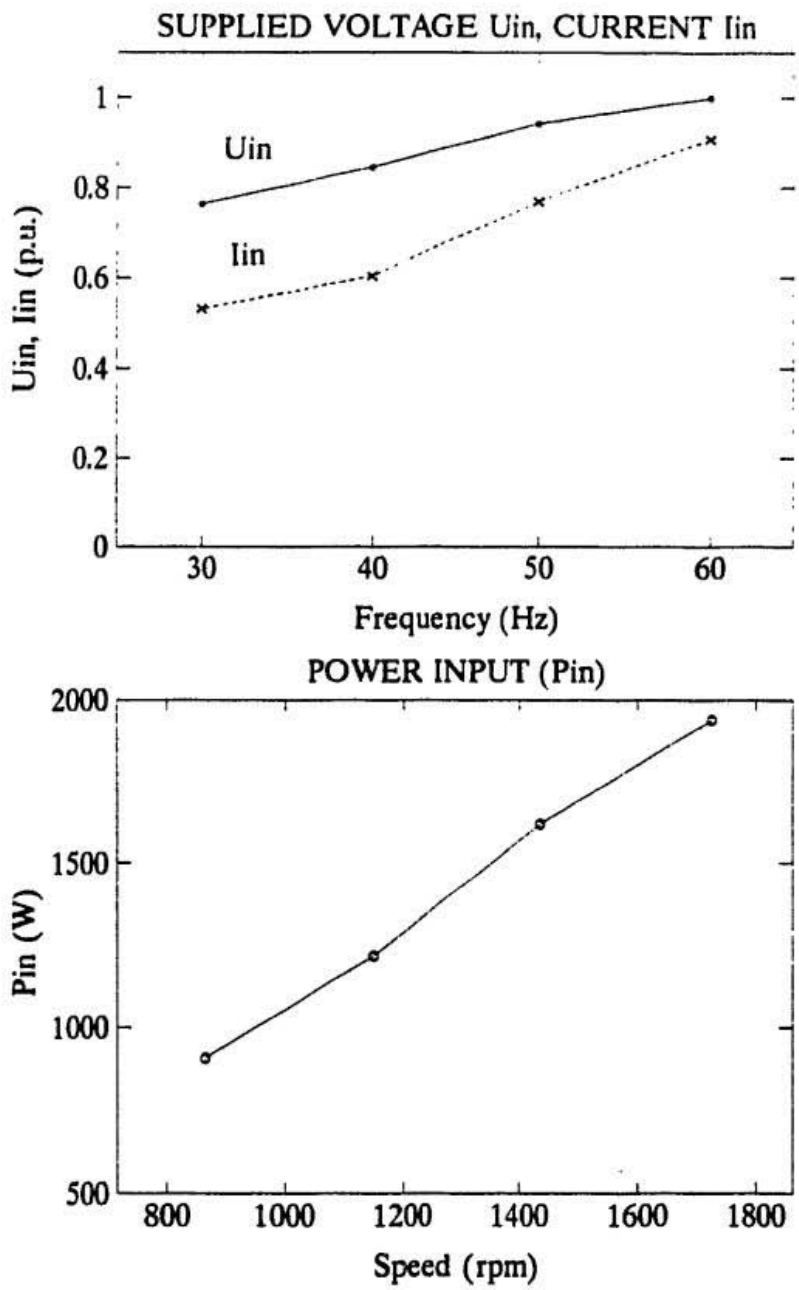

Figure 3.12: Power input for different speeds

3.3 Loss Minimization of AC Drive System Using Adaptive Controller

From the previous analysis and experimental results we can conclude that significant energy savings can be achieved, if an ac motor works at the optimal operating point. However, the optimal combination of airgap flux and slip frequency (and hence of stator voltage and frequency) is a complex function of the load torque and speed as well as the motor parameters.

Since the objective of optimal control is to minimize the losses for a given output power, the best results can be obtained when the input power is measured and considered as the controlled variable. But conventional feedback control system cannot solve the complex problem, because there is no an input power signal as one of the system's input reference values. Therefore, in order to achieve the efficiency optimization, it is necessary to apply an adaptive controller, which is able to adjust an actuating variable until it detects a minimum in the input power.

Figure 3.13 shows a simple block diagram of the proposed loss minimization control system which incorporates an adaptive control technique in an indirect field-oriented control scheme[53].

In this section, the model of an ac motor is briefly addressed. The operation of field orientation with variable flux control system, and the proposed loss minimization control system which incorporates an adaptive control technique in an indirect field-oriented control scheme are further discussed.

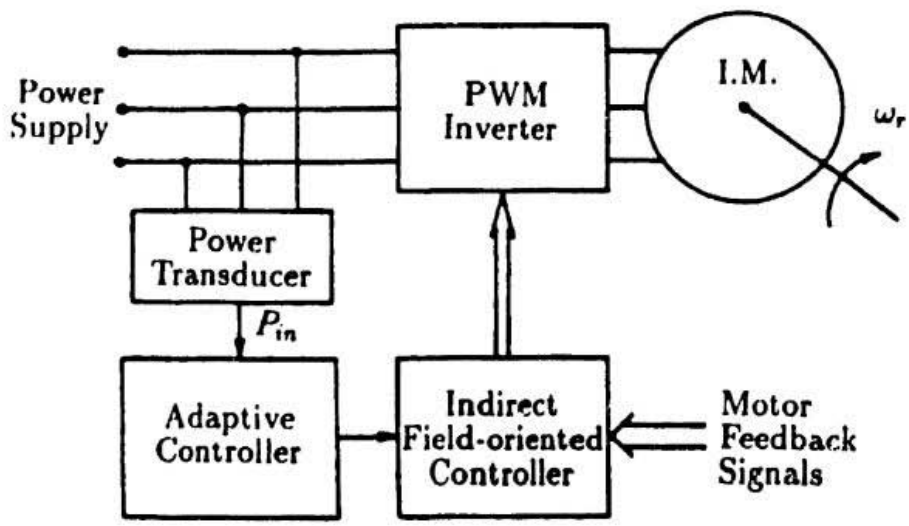

Figure 3.13: Brief block diagram of the loss minimization control scheme.

3.3.1 Modelling of Indirect Field-Oriented Control of an AC Motor

For analyzing the field orientation of ac motor drives, it is useful to digitally simulate the overall ac motor control schemes. Hence, it is necessary to obtain a model of the ac motor. The electrical dynamics of an ac motor can be represented by a fourth-order nonlinear equation which may be either in a stationary reference frame (Stanley equation), or in a synchronously rotating reference frame[25].

Several researchers have studied the subject of models of ac motors and/or field orientation of ac motor drives [20][28][31][32][35] and [43]. In the following, a model of field-oriented control of a voltage-fed ac motor for simulation is derived, which is referred from [43].

Usually, the motor model is represented in the two-axis system, α-β reference frame. An N-pole induction motor with a short-circuited rotor circuit is characterized by the following equations:

$$\begin{bmatrix} u_\alpha \\ u_\beta \\ 0 \\ 0 \end{bmatrix} = \begin{bmatrix} R_s + pL_s & 0 & pM & 0 \\ 0 & R_s + pL_s & 0 & pM \\ pM & w_r M & R_r + pL_r & w_r L_r \\ -w_r M & pM & -w_r L_r & R_r + pL_r \end{bmatrix} \begin{bmatrix} i_\alpha \\ i_\beta \\ i_{\alpha r} \\ i_{\beta r} \end{bmatrix} \tag{3.31}$$

$$\frac{J}{n_p}\frac{dw_r}{dt} = T - T_l - D\frac{w_r}{n_p} \tag{3.32}$$

$$T = \frac{3}{2}Mn_p(i_\beta i_{\alpha r} - i_\alpha i_{\beta r}) \tag{3.33}$$

$$\frac{d}{dt}\psi_\alpha = u_\alpha - R_s i_\alpha \tag{3.34}$$

$$\frac{d}{dt}\psi_{\alpha r} = -R_r i_{\alpha r} - w_r \psi_{\beta r} \tag{3.35}$$

$$\frac{d}{dt}\psi_{\beta r} = -R_r i_{\beta r} + w_r \psi_{\alpha r} \tag{3.36}$$

$$\frac{d}{dt}\psi_{\beta} = u_{\beta} - R_s i_{\beta}, \tag{3.37}$$

where:

$$\begin{bmatrix} i_\alpha \\ i_{\alpha r} \\ i_{\beta r} \\ i_\beta \end{bmatrix} = \frac{1}{L_s L_r - M^2} \begin{bmatrix} L_r \psi_\alpha - M\psi_{\alpha r} \\ L_s \psi_{\alpha r} - M\psi_\alpha \\ L_s \psi_{\beta r} - M\psi_\beta \\ L_r \psi_\beta - M\psi_{\beta r} \end{bmatrix}. \tag{3.38}$$

In the indirect field-oriented control, the required stator voltages u_α and u_β are obtained by the following coordinate transformations:

$$\begin{bmatrix} u_\alpha \\ u_\beta \end{bmatrix} = \begin{bmatrix} cos\theta_s & -sin\theta_s \\ sin\theta_s & cos\theta_s \end{bmatrix} \begin{bmatrix} u_{ds} \\ u_{qs} \end{bmatrix}. \tag{3.39}$$

Three phase variables in ac motor can be easily transformed from two axes variables by the following transformations:

$$\begin{bmatrix} u_a \\ u_b \\ u_c \end{bmatrix} = \begin{bmatrix} 1 & 0 \\ -\frac{1}{2} & \frac{\sqrt{3}}{2} \\ -\frac{1}{2} & -\frac{\sqrt{3}}{2} \end{bmatrix} \begin{bmatrix} u_\alpha \\ u_\beta \end{bmatrix}. \tag{3.40}$$

The stator current i_α and i_β in the $\alpha - \beta$ reference frame can be transformed to field-oriented unidirectional quantities i_d and i_q with the following coordinate transformations:

$$\begin{bmatrix} i_\alpha \\ i_\beta \end{bmatrix} = \begin{bmatrix} 1 & 0 & 0 \\ 0 & \frac{1}{\sqrt{3}} & -\frac{1}{\sqrt{3}} \end{bmatrix} \begin{bmatrix} i_a \\ i_b \\ i_c \end{bmatrix} \tag{3.41}$$

and

$$\begin{bmatrix} i_{ds} \\ i_{qs} \end{bmatrix} = \begin{bmatrix} cos\theta_s & sin\theta_s \\ -sin\theta_s & cos\theta_s \end{bmatrix} \begin{bmatrix} i_\alpha \\ i_\beta \end{bmatrix}. \tag{3.42}$$

The frequency and phase of the voltage components u_α and u_β in the stationary reference frame for establishing the required rotor flux and stator current are controlled by the slip frequency ω_{sl} which can be calculated from equation 2.16.

The time domain model for indirect field-oriented control of ac motor - equations 3.31 to 3.38 -, and coordinate transformations - equations 3.39 to 3.42 - are used for digital simulation of the proposed loss minimization control scheme.

3.3.2 Field-Orientation with Variable Flux Control

Significant energy savings have been reported to date for operation at light torque loads at all speeds, and for torque loads near the rated value under low-speed operation.

The flux level must be reduced when the motor runs at light loads. This is different from the conventional field orientation, where the sole function of the flux regulator is to maintain the rotor flux as close as possible to its rated value. Since the rotor flux remains constant, the torque follows instantaneously and exactly the variations of the q-axis component of the stator current. However, the quantity of rotor flux affects directly the repartition of losses and is simply related to the d-axis component of the stator current. Therefore, it also can constitute an excellent tool for improving the efficiency of ac motor drives. Equations 2.13 and 2.14 reveal the relationship among these quantities.

But the reduction of the flux level slows down the system response to a load change and decreases the peak torque that can be developed by the motor. This

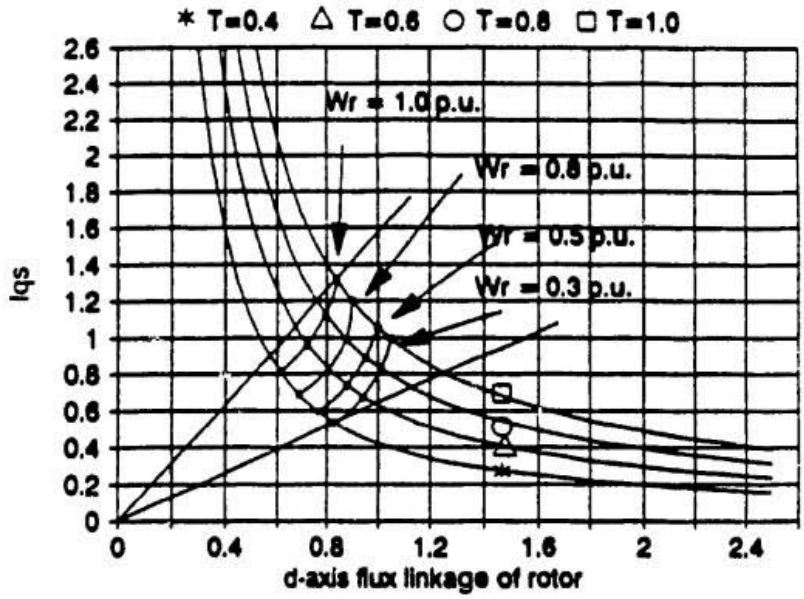

Figure 3.14: The optimal efficiency curves of dq frame for nonideal cases (saturation, harmonic, skin effect) included. [48]

problem must be solved properly if the system is to maintain high dynamic performance.

Based on equation 2.15, the relation between the torque current and the rotor flux was found and shown in Figure 3.14 with the torque as a parameter[48]. The figure shows the required torque current and rotor flux for various rotor speeds obtained from computer simulation taking nonideal effects into consideration. The corresponding field and torque currents are given in Figure 3.15. Figures 3.14 and 3.15 show that to control an ac motor from one set of torque and speed to another using field orientation for optimal efficiency at steady state, requires not only to change the torque current I_{qs}, but also the field current I_{ds}.

Therefore, for the loss minimization scheme which incorporates the control of

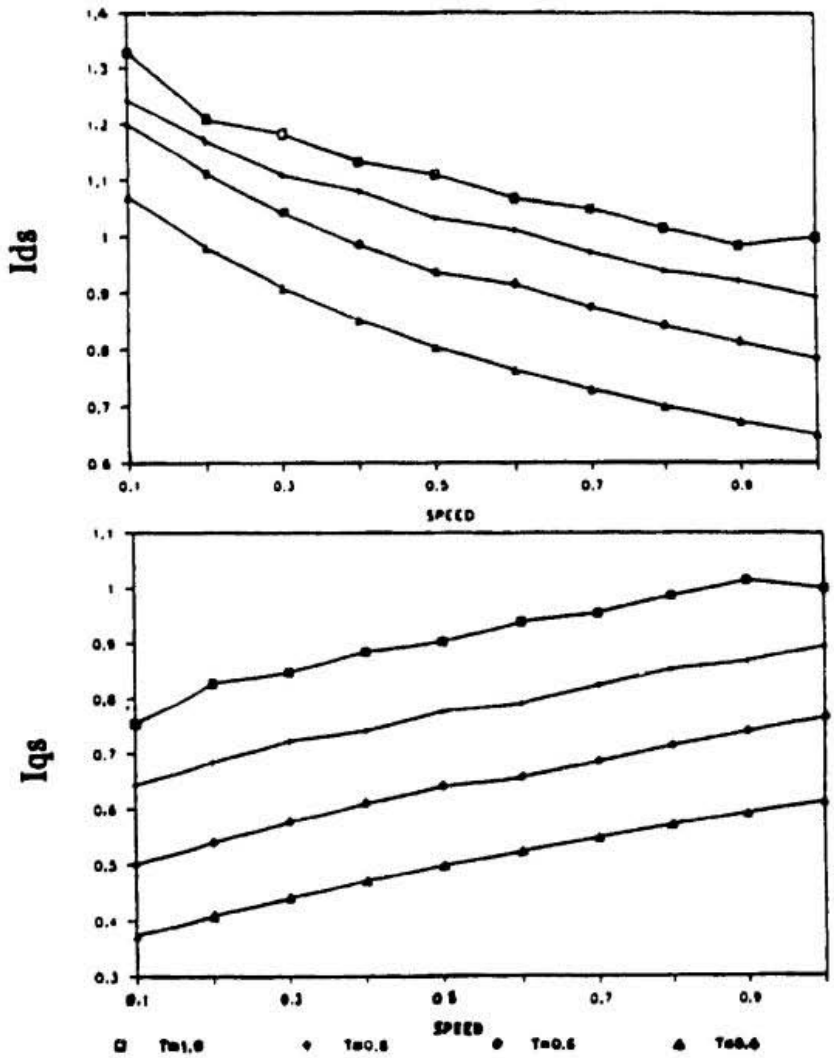

Figure 3.15: The optimal efficiency point of I_{ds} and I_{qs}.[48]

field current with field orientation, the flux level to assure sufficient torque and fast response in transient state must be considered. When a large increase occurs in torque due to a light load, low flux, maximum efficiency operating point can be achieved only by increasing both the q-axis component of stator current and the rotor flux. The speed of response of the q-axis stator current is only limited by the poles of the regulator and by the inverter voltage available to force a current through the stator circuit. Equation 2.13 also shows that the flux response involves the rotor time constant L_r/R_r in addition to the limitations of the current regulator. In Chapter 5, this subject will be discussed further, and simulation as well as experimental results will be presented to show how the problem is solved.

Several closed-loop loss minimization control schemes have been presented to date, such as Figures 2.6 and 2.3 mentioned in Chapter 2.

The derivation of transfer functions of a field-oriented control system is given in [47], along with analyses of the impact of flux level reduction on the damping of the speed controller and on the maximum torque. Assuming that the mechanical part of a drive system is governed by:

$$J\frac{d\omega_r}{dt} + B\omega_r = T_e - T_l \tag{3.43}$$

and the electromagnetic torque is,

$$T_e = \lambda'_{dr} i_{qs} \tag{3.44}$$

If the speed is controlled by a proportional plus integral (PI) controller using i^*_{qs} as the actuating variable, the following equation is obtained,

$$i^*_{qs} = K_p[(\omega^*_r - \omega_r) + K_i \int_0^t (\omega^*_r - \omega_r)dt]. \tag{3.45}$$

The small signal transfer function relating the speed to its reference in a field oriented drive can be derived as.

$$\Delta\Omega_r = \frac{\frac{K_p\lambda'_{dro}}{J}(S + K_i)\Delta\Omega_r^*}{S^2 + (\frac{B+K_p\lambda'_{dro}}{J})S + \frac{K_iK_p\lambda'_{dro}}{J}} \tag{3.46}$$

where

$$\lambda'_{dro} = \frac{L_m}{L_r}\lambda_{dro} \tag{3.47}$$

and λ_{dro} is the value of the flux around which the linearization is carried out.

Equation 3.46 shows that the damping of the system decreases with the rotor flux level. Due to the simplicity of the dynamics of field oriented control, it has been suggested in [19] that this reduction can be proportional to the gain of the speed controller.

Based on the previous work[53][55], the proposed loss minimization control scheme is presented here. In order to achieve the minimum losses in ac motor drives, an adaptive controller is designed for the proposed scheme. Figure 3.16 presents the block diagram of the proposed scheme which incorporates an adaptive controller in an indirect field orientation for simulation. Figure 3.17 shows the block diagram of the proposed scheme for experiment. This setup is explained in detail in Chapter 5.

The proposed loss minimization control system is based on the concept that for a given load, if the shaft torque or speed is maintained constant, the efficiency of the drive will be maximum when the power measured at the input of the system is minimum. An adaptive controller therefore can steer the system to its optimum operating point by iteratively adjusting a controlling variable until it detects a min-

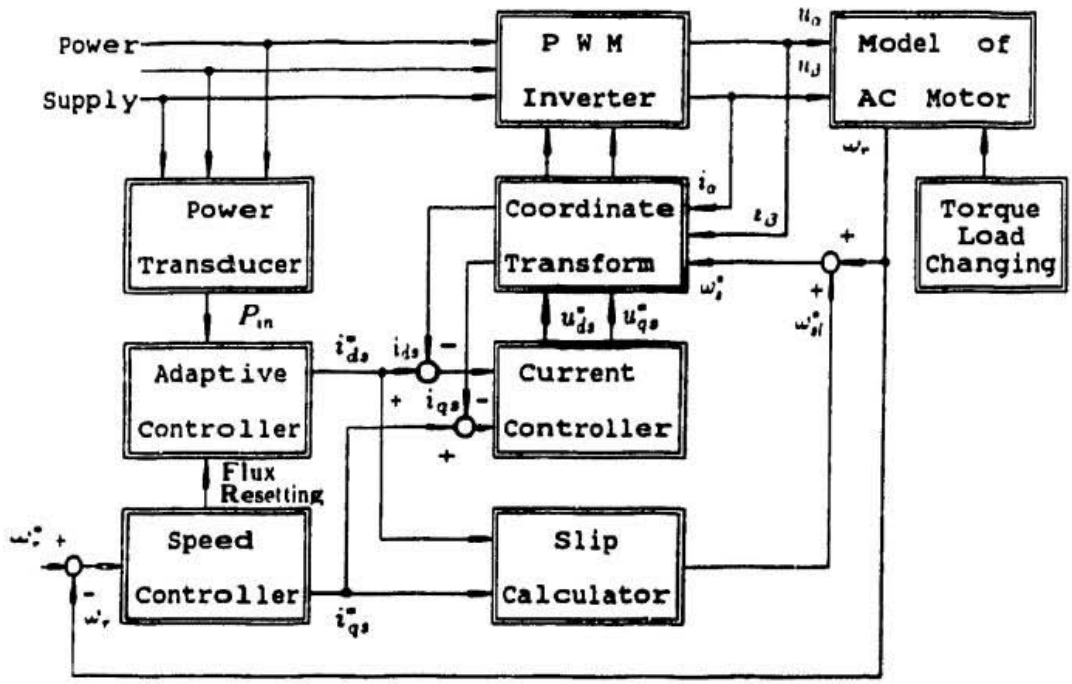

Figure 3.16: Block diagram of the proposed loss minimization control scheme for simulation.

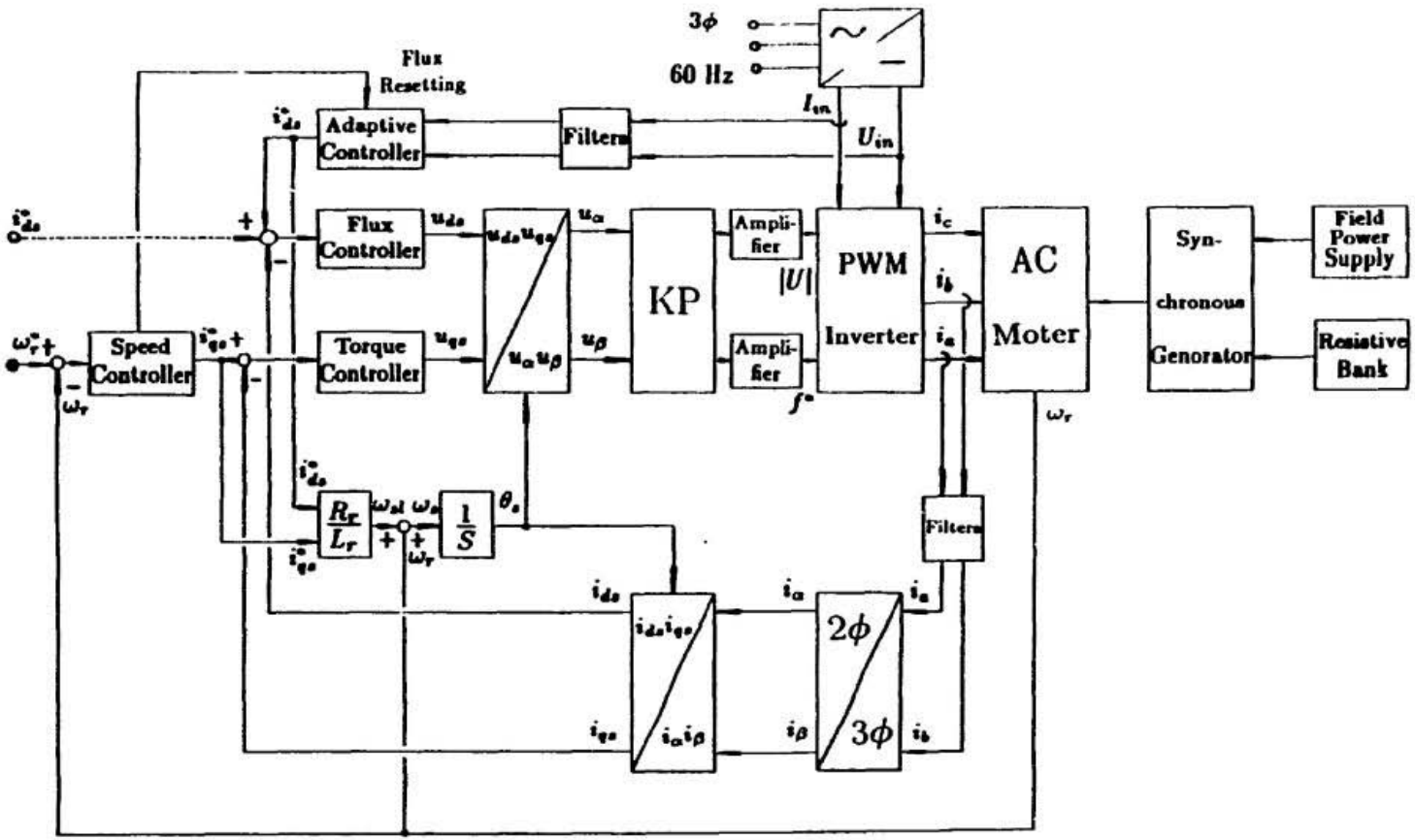

Figure 3.17: Block diagram representation of the proposed loss minimization control scheme for experiment

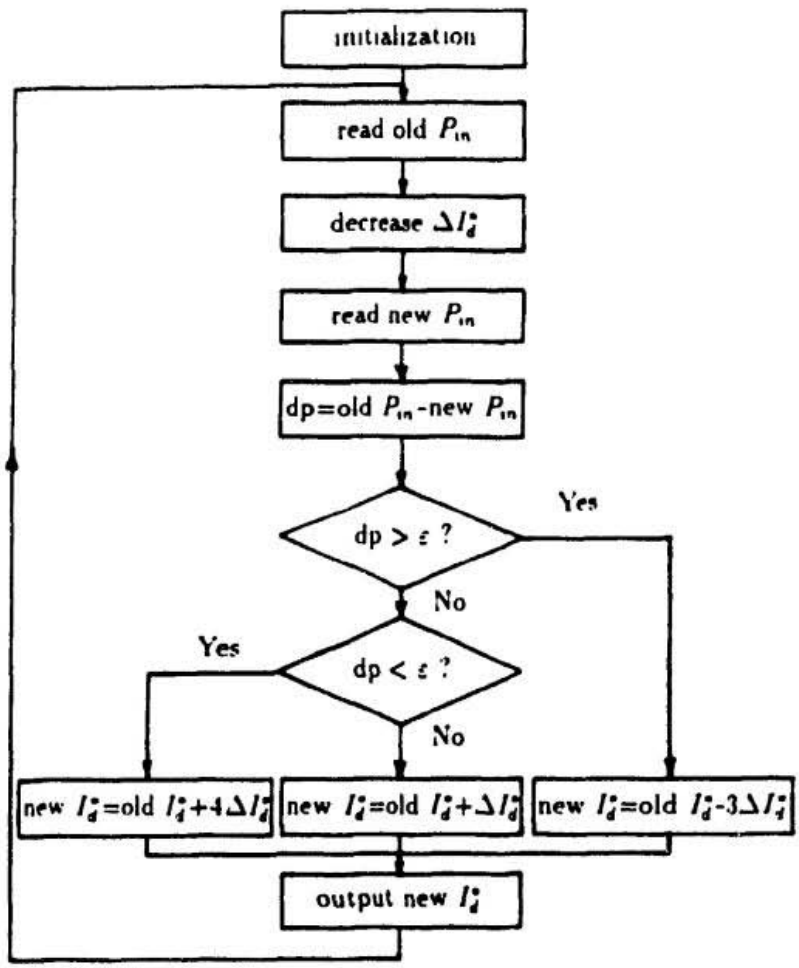

Figure 3.18: Brief flowchart of the adaptive controller program.

imum in the measured power input. Figure 3.18 shows the brief flowchart of the adaptive controller program.

This method does not require the knowledge of the motor parameters and loss minimization can be obtained for all speed and torque operating points. It can be readily implemented on any motor and with different types of inverters, and is perfectly robust and can adapt the variations in motor parameters such as an increase in rotor resistance possibly due to a rise in motor temperature.

The field-oriented controller in the proposed scheme is of the indirect type. It does not require a flux sensor, and thus is easy to implement. The controller relies on a measured value of the shaft speed and a calculated value of the slip frequency to realize the field orientation for the steady-state and transient operation.

The principle, digital simulation and implementation of the proposed scheme by transputer-based parallel processing will be further discussed in Chapters 4 and 5.

3.4 Summary

Based on the above analyses it is clear that significant energy savings can be achieved for operation at light torque loads for all speeds, and for torque loads near the rated value under low-speed operation. The rotor flux is indeed one of the controlled variables and provides direct control of the distribution of losses. Moreover, field-oriented control scheme realizes the best decoupling between the flux and torque control loops, simplifying greatly the design of the adaptive controller. A variable frequency loss minimization control system with an indirect field-oriented control scheme can meet the needs of high-performance drive applications. The dynamics

of a field-oriented control scheme are simple and the implications of operation at reduced flux can therefore be easily determined and remedial measures developed.

But the maximum efficiency is a complex function of the motor parameters. It is therefore necessary to apply an adaptive controller to achieve efficiency optimization. The proposed loss minimization control scheme, which incorporates an adaptive controller in an indirect field oriented control scheme, can potentially achieve significant energy savings for ac motor drives.

There has been a recent interest in applying modern control theories to ac motor control systems. However, the resulting complexity of control algorithms such as the indirect field-oriented control leads to a heavy computation burden on computers. In such cases, the execution time in a real-time control system becomes critical. Therefore, without parallel processing and/or fast real-time processors, applying modern control theory to ac motor control systems is in general difficult. The multiple Transputer system can be a good solution for parallel processing to fully explore the inherent advantages of real-time digital control of ac motor drives. This subject is discussed in detail in the next chapter.

Chapter 4

Transputer-Based Parallel Processing Realization of Motor Control

Microprocessor based digital control of high performance ac motor drives offers the potential for fast dynamic calculation, flexible architecture and interactive control tool. For field-oriented control of an ac motor, it has current loop sampling rates of 5 to 10 KHz. This implies that the controller must process the control algorithms within 100 to 200 μs[3]. Using five Transputers, simulation results in [43] demonstrated that this goal can be achieved. On the other hand, for high-performance drive applications, conventional linear controllers (PI, PID) cannot achieve the stringent performance requirements. Modern control techniques, such as optimal control and adaptive control, can meet the needs of high-performance drive applications, but require implementation of complex real-time signal processing algorithms. Because multiprocessor solutions based on Von Neumann architectures communicating via common resources—bus or shared memory—have certain disadvantages, the new parallel architecture of Transputer which suffers from none of these disadvantages is of interest for fully exploring the inherent advantages of real-time digital control

of ac motor drives. Transputer-based parallel processing of high performance ac motor drives offers the potential for fast dynamic calculation, flexible architecture and interactive control.

This chapter describes a new scheme using multiple Transputers for the parallel processing and implementation of field-oriented control including the loss minimization strategy. The fundamental principles of parallel processing and the Transputer are stated. The hardware and software of a parallel processor using five T800 Transputers for emulating the partitioned algorithms for real-time control studies and using four Transputers for real-time control experiment are presented. Execution times of the control process in one and five Transputers are also investigated.

4.1 Transputers and Parallel Architecture

Modern control techniques can explicitly improve the control system performance. However, the resulting complexity of control algorithms leads to a heavy computation burden on computers. In such cases, execution time in a real-time control system becomes critical. The solutions can come from parallel processing techniques.

Unlike the sequential computer systems based on the Von Neumann architecture, the new parallel architecture of the Transputer achieves its speed by dividing up the composite parts of a problem and working on them simultaneously.

The Transputers being used in the scheme are 32-bit(T800) single chip microcomputers which have their own local memory and communication links with clock speeds of 20 MHz. They are generally categorized as Multiple Instruction stream

Multiple Data (MIMD) computers.

Using Transputers, we can minimize the execution time of the control algorithms, thus increase the sampling frequency, which in turn enables implementation of control of systems with large bandwidths. Parallel processing systems can achieve real-time control, process a flexible control architecture and feature a high reliability.

4.1.1 Parallel Processing

The one of main objectives using computers for real-time control is to minimize the execution time of the control algorithms. There are several methods to achieve this aim:

- Using a single, fast CPU to increase the execution rate of the processing system, thus enabling it to realize the algorithms in the required time.
- Using some specific architecture, which are free from the overheads imposed by a generalized solution, to achieve the potential for the highest performance.
- Using a parallel or multi-processor method.

This thesis concentrates on the use of the parallel processing method.

In order for the system to satisfy the real-time constraints, i.e. regular sampling of the current, speed and torque at the required frequency, small latencies between each task over different Transputers are required. Therefore, partition of the software is very important, and careful consideration must be given to the dynamic coupling relations within the control algorithms in order to determine the optimal break-up of the system functions. Then, a control system which contains several nested

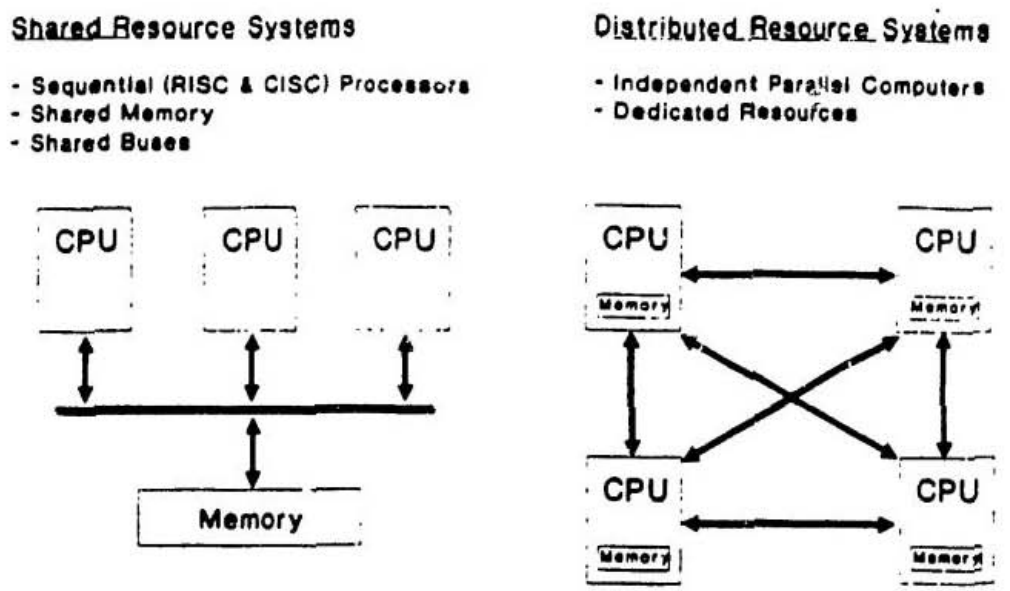

Figure 4.1: Distributed and shared resource systems.[73]

control loops, can be directly parallelized, and each control loop can be executed concurrently.

Conventional processors, both RISC (Reduced Instruction Set Computer) and CISC (Complex Instruction Set Computer), follow sequential architectures without parallelism. This means that one task must be completed before the next can begin. The parts of a problem are handled one at a time, even if they actually occur together and are interrelated. When parallel systems are modelled with sequential computers, the impact of real-time interactions between events is lost. Parallel computers achieve their speed by dividing up the composite parts of a problem and working on them simultaneously.

Parallel processing systems can be divided into two basic categories: *shared resource* and *distributed resource* systems[73], which are shown in Figure 4.1.

Shared resource systems execute the components of a problem on conventional CPU's. They are connected by a common bus to a shared memory. Concurrency is achieved by time sharing the memory. Sequential processors used in a shared resource system have a Von Neumann architecture. The performance improvement of the system may not be significant when more than just three of four processors are connected in parallel because memory access times begin to limit the speed at which a program can execute. It is only possible to speed up the system by using expansion memory that is much faster than the CPU's.

A distributed resource system gains speed by partitioning the parallel parts of a problem among the hardware nodes of the system. Each node runs its own program and includes a CPU with a local memory and facilities that support concurrency. Each machine operates sequentially by fetching an instruction from memory, reading an operand, executing the instruction and storing the result. One might attempt to overcome the limitation of memory access by adding some dedicated memory to each processor in addition to global memory. The problem of communication may be overcome by using more buses. The Transputer described below adopts this solution.

4.1.2 The Transputer

The Transputer is a family of 16-bit(T222) and 32-bit(T800) CMOS single chip microcomputers which have their own local memory and communication links; clock speeds are in the range 10 - 30 MHz. The Transputer is specifically designed for parallel processing. Transputers operate as stand-alone machines or as processing elements interconnected by their links to form computing arrays and networks. The architecture of the Transputer enables a modular design where an arbitrary num-

ber of Transputers can be used as processing elements interconnected by their links to support a broad range of applications; the inherent redundancy in multiprocessors can be utilized to achieve fault tolerance. Several processes can be defined and run concurrently with interprocess communication being achieved using defined communication channels.

Since the Transputers are Multiple Instruction stream Multiple Data (MIMD) computer, they are used to execute different operations on separate data at the same time. Figure 4.2 shows the architecture of the INMOS T800 Transputer. T800 is a 32 bit microcomputer with a 64 bit floating point unit and graphics support. It has 4 Kbytes on-chip RAM for high speed processing, a configurable memory interface and four standard INMOS communication links. It can directly access a linear address space of 4 Gbytes. The 32 bit wide memory interface uses multiplexed data and address lines and provides a data rate of up to 4 bytes every 100 *ns* (40 Mbytes/sec) under a 30 MHz clock. The links in the Transputer allow networks of Transputer family products to be constructed by direct point-to-point connections with external logic, and the standard operating speed is 10 Mbits/sec but can operate at 5 or 20 Mbits/sec. Each link can transfer data bi-directionally at up to 2.35 Mbytes/sec.

The T800 Transputer provides a direct implementation of the message-passing mode of parallel computation of loosely coupled systems, and its architecture has been designed for efficient execution of programs written in the parallel processing language Occam. The Transputer development system provides the environment of editing, compiling and configuring the processes to run on the Transputer network.

Parallel processing systems can achieve real-time control solution, flexibility of control architecture and high reliability of control system. But with the conventional

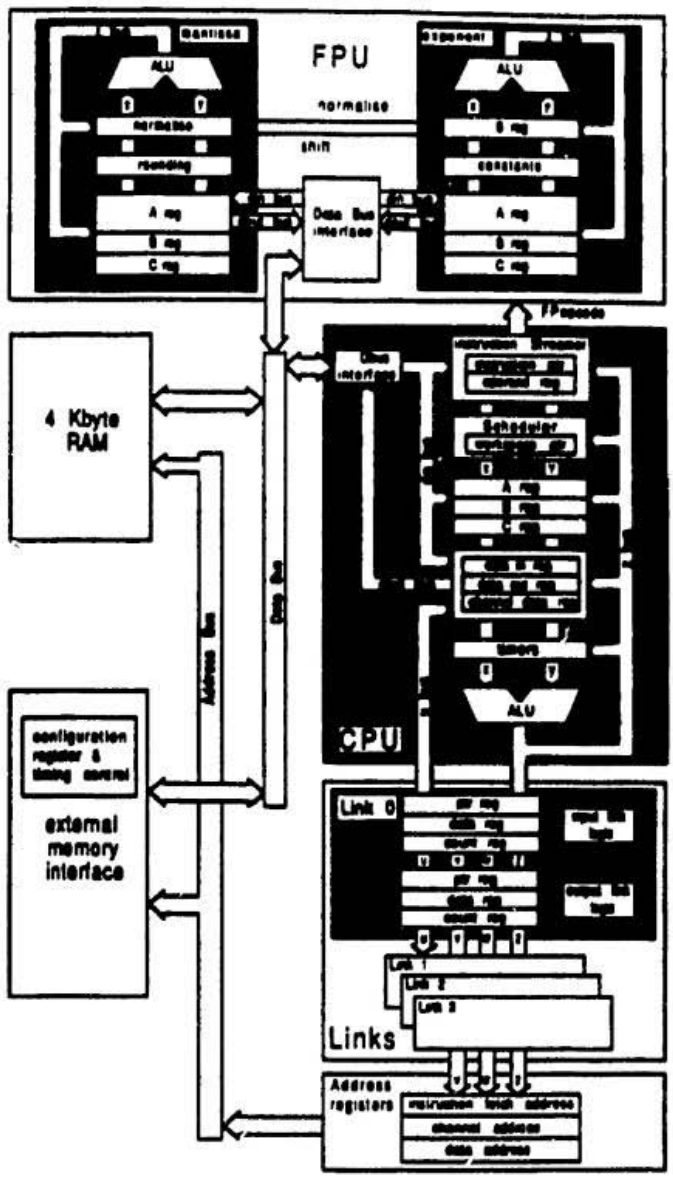

Figure 4.2: INMOS T800 architecture.[75]

multiprocessor architectures, the following disadvantages have to be considered[3][64]:

1. A shared resource becomes a bottleneck and therefore, limits system expansion.

2. Expansion of the system is difficult due to complexity.

3. Bus arbitration logic is necessary, which increases complexity, cost and chip count.

4. Multiprocessor bus layout suffers from high track densities, capacitance and cost problems.

5. Software development is cumbersome and it is left to the programmer to establish the parallelism using languages inherently designed for sequential processors and programs.

The Transputer suffers from none of the above disadvantages. It is a parallel microprocessor, generally categorized as an MIMD, with four standard serial communication links. Transputers do not share a common bus, but instead exchange messages through their own high-speed serial links. Each link is a fast, synchronous, full-duplex channel used to provide pairwise connection of Transputer nodes. These connections can be configured on a variety of topologies such as rings, arrays, and pipelines. More details about T800 Transputer can be found in [75].

4.1.3 Parallel Processing by Transputers

Performance maximization is necessary if the full potential is to be obtained from a particular Transputer implementation. The following has been suggested in

[63]:

- Making use of the on-chip memory. The internal memory cycles are approximately 5 times faster than the external memory cycles. Hence to maximize performance, the most frequently accessed variables should be placed in internal memory.

- Abbreviations. Abbreviations can be used to bring non local variables into scope, thereby removing static chaining. Abbreviations can also speed up execution by removing the necessity for range checking instructions.

- Retyping. This can speed up bit and byte extraction from a word.

- Decoupling communication and computation. To avoid the links waiting on the Transputer or vice versa the communication should be buffered.

- Load balancing. It is important to balance the processing time between communications on each Transputer to ensure maximum throughput. The programmer can adopt a simple methodology to ensure reasonable efficiency by measuring the execution time of each module of code, (either by inserting it into a timing harness, or by totalling the instruction execution times), and then manually adjust the instance of the code to improve the performance of the system. Static allocation of code to Transputers, with some measure of load balancing, appears at present to be the only way to extract maximum performance from a Transputer network. The overheads involved in dynamic task allocation imply inferior performance.

Li and Venkatesan [69][43] developed a simulation scheme of multiple Transputer-based parallel processing for field-oriented control of ac motors. Based on their

work. the proposed scheme for parallel processing is that several Transputers are connected in a parallel arrangement and a means of communication is provided between them. The software of the control algorithm is partitioned into several tasks, and distributed among the Transputers. Therefore, the partitions need to be carefully made considering the dynamic coupling relations within the control algorithms to determine the optimal breakdown of the system functions. The implementation of the hardware and software of the proposed scheme is described in the subsequent sections.

4.2 Hardware for Parallel Processing

In the hardware part of proposed scheme for digital simulation, an IBM-PC microcomputer (386 model) and five T800 Transputers are used. The IBM-PC microcomputer is connected to the five Transputers. The source program is written in C and compiled in the PC. The executable files, compiled and linked by the IBM-PC, are downloaded into each Transputer. Transputers with loaded files work individually unless communications are required between them. The Transputer communication works in such a way that when a processor performs input or output to a communication channel, the processor is blocked until the corresponding processor performs its respective output or input. That is to say, only when this communication has been accepted (handshaking is completed) can the process proceed. This acceptance occurs every sampling cycle.

The parallel processing architecture using five Transputers for the simulation and four Transputers for experiment of the proposed loss minimization scheme are

shown in Figures 4.3 and 4.4, respectively. In these diagrams, three of the Transputers ($T2$-$T4$) are used for controlling the motor drive. Transputer 1 ($T1$) is used for interface and communication with the host computer (IBM-PC) and the other Transputers. Transputer 5 ($T5$) in figure 4.3 is for modelling the dynamic behaviour of the ac motor. The IBM-PC in the figures are host computers. For a development rig, the host computer is normally of the form of a local keyboard/terminal for online commands, parameter modification, data display and software development. For commercial drives, it can be a user control panel or a remote communication link either to a modem or programmable controller. The RTI-815 in Figure 4.4 is a multifuction board with eight channels of analog to digital (A/D) and two channels of digital to analog (D/A) converters. The details of the architecture of the proposed Transputer-based schemes employed for simulation and experiment are addressed in the rest of this chapter and in the next chapter.

4.3 Software for Parallel Processing

For efficient operation, the partitioned tasks, each of which consists of several processes and is allocated to an individual Transputer, should use approximately the same amount of computing time per sampling cycle. This will ensure correct updating of system variables and avoid idle time in each calculation cycle.

Taking advantage of the inherent parallelism in motor control, the control program, written in C, is carefully partitioned and assigned to the Transputers making sure that they approximately expend the same amount of computing time in each sample period. The program is operated in the T800 Transputers at a clock speed

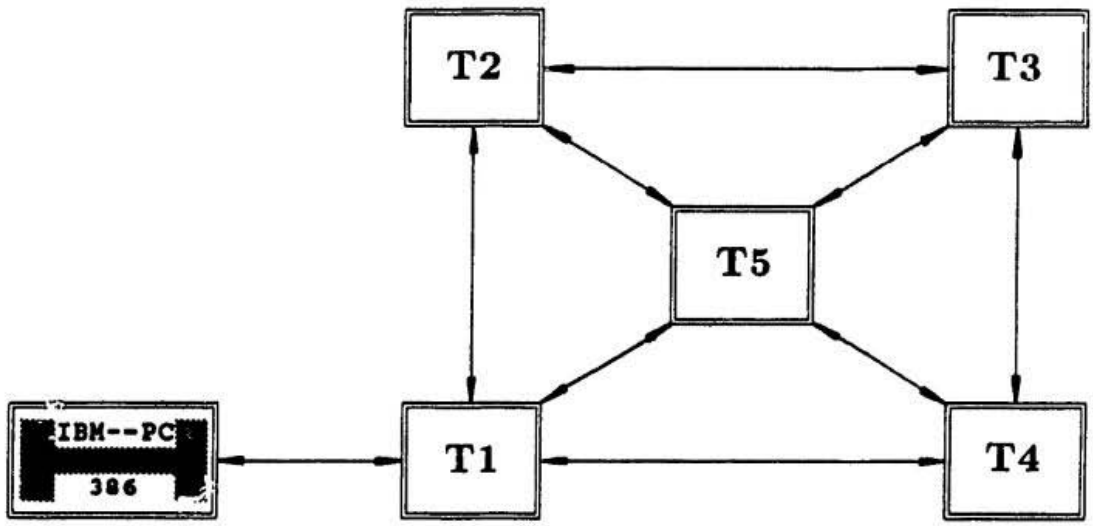

Figure 4.3: Diagram of the parallel processing architecture using five Transputers for simulation.

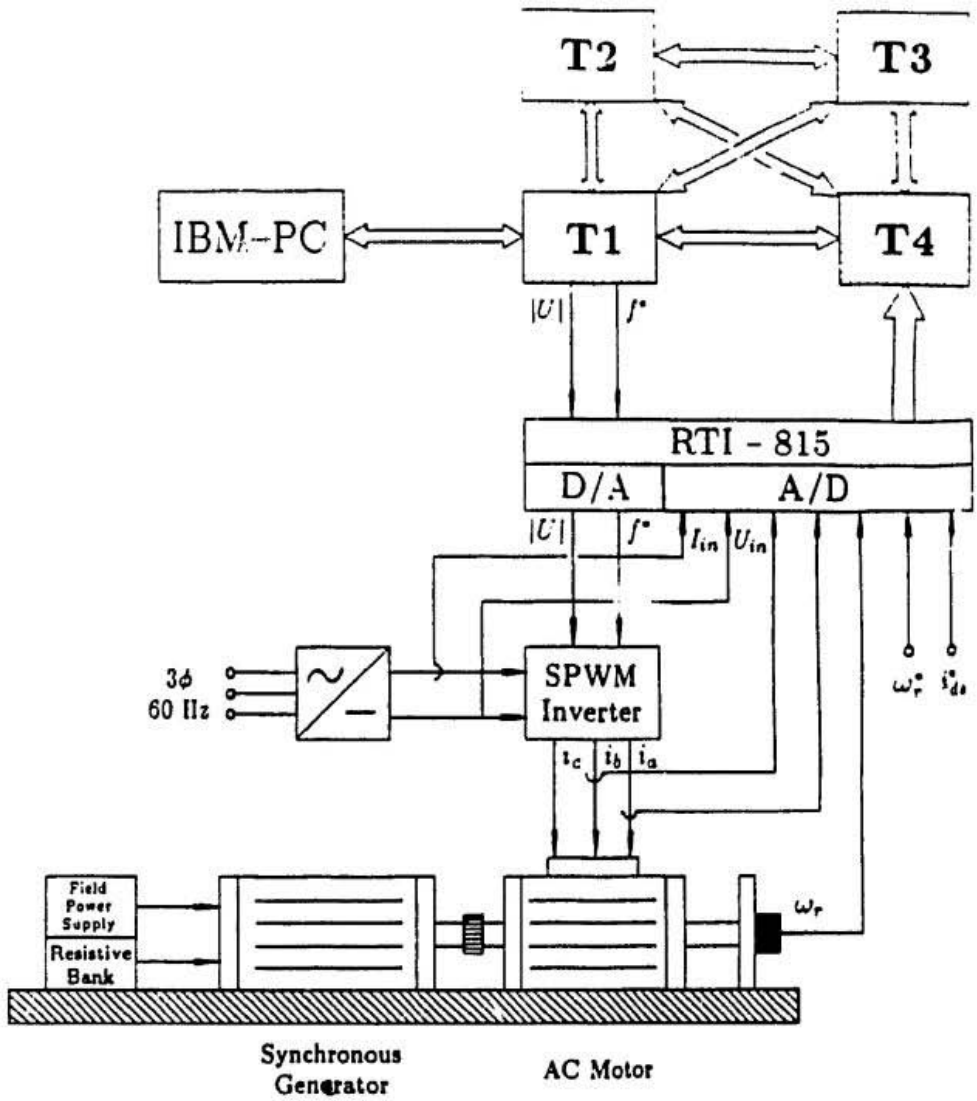

Figure 4.4: Diagram of the parallel processing architecture using four Transputers for experiment.

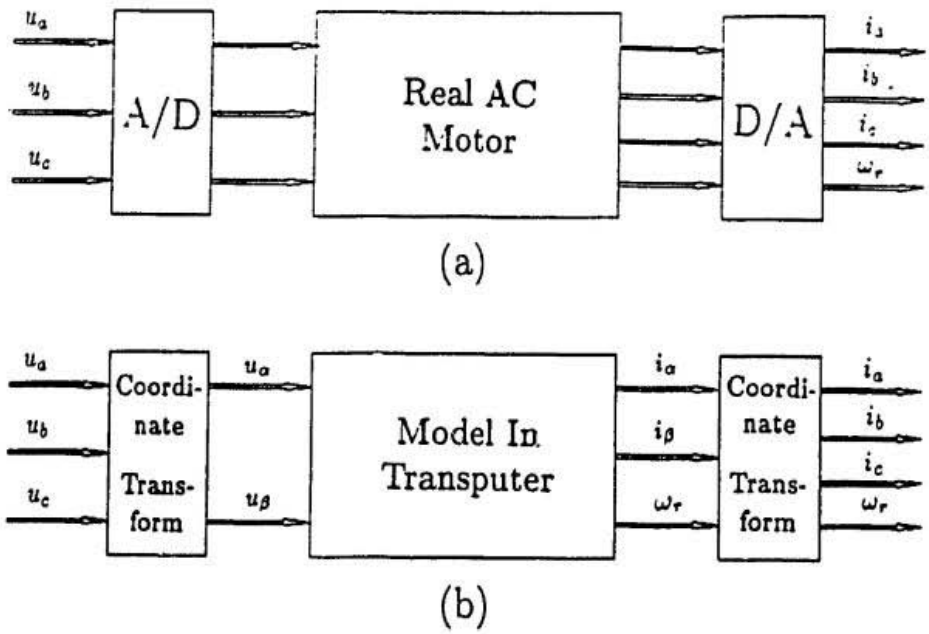

Figure 4.5: An ac motor control in field-orientation. (a) Real motor control, (b) Transputer-based real-time emulation of the ac motor control.

of 20 MHz.

The time domain model of ac motor for the simulation of loss minimization control is given by equations 3.31 - 3.38, and the coordinate transformations are given in equations 3.39 - 3.42. Figure 4.5 shows an ac motor control in field-orientation.

The transputer-based computer simulation program of parallel processing for indirect field-oriented control employing loss minimization of ac motor drives is partitioned into several parts as described below.

- Set-up Routine:

  The function of the set-up routine is to initialize each transputer. Commands from the host computer (IBM-PC) are passed to each individual transputer for setting input parameters.

- Parallel-1 (in Transputer 1):

  Works as an interactive interface: passes host computer (the IBM-PC) commands to other transputers, receives calculated results and status information from the other transputers and then sends them to the PC.

- Parallel-2 (in Transputer 2):

  Forms the speed PI controller, torque current limitation and slip frequency calculation, and handles the cosine triangle function of slip angle. The calculated speed PI controller output, slip frequency and cosine function are sent to Transputer 3.

- Parallel-3 (in Transputer 3):

  Deals with flux and the torque current PI control of field orientation, and calculates the sine triangle function of slip angle and coordinate transformations. Due to data dependency in the scheme, this routine plays a critical role in determining the overall control system sampling time, and it must be carefully decomposed from system control algorithms. For example, because the calculation of triangle function takes a long processing time (It will be shown later in Table 4.3), it has to be divided into two parts (sine and cosine triangle functions). Therefore, there is data dependency between the two parts.

- Parallel-4 (in Transputer 4): Calculates the measured power input from A/D converter, and then sends the results to the adaptive controller for loss minimization. It also deals with field orientation feedback control and calculates actual and reference torques. The calculated control signal is sent to Transputer 3 for calculating the slip frequency which determines the field orientation.

- Parallel-5 (in Transputer 5):

  Models the ac motor dynamic behaviour and responds as a real motor. For each computing loop, it sends out all the necessary motor state variables to other transputers which samples the required variables for the purpose of control.

In the program, all the control system state variables are reset to the initial values. The simulation results on the transputer are sent back to IBM-PC for storage in hard-disk.

There are some data dependencies in the control scheme. For example, real-time calculation of trigonometric functions can obtain more accurate values than the method of the look-up table for α-β to d-q and d-q to α-β coordinate transformations, but the real-time calculation takes too much processing time. Therefore, it has to be divided into two parts (sine and cosine trigonometric functions) and calculated in different transputers. Figure 4.6 shows the relations between processes in different transputers.

$P1$ through $P7$ present different control processes. $P1$ in transputer 2 is the motor speed controller, slip frequency calculation and communication to the motor. $P2$ is the Cosine function computing, and communications to transputer 3. $P3$ through $P5$ are in transputer 3. $P3$ presents the current controller, α-β to d-q coordinate transformation. $P4$ is the sine function calculation, and $P5$ is d-q to α-β coordinate transformation. In transputer 4, $P6$ and $P7$ present the power measurement and calculation, respectively. The lines between processes indicate the data dependencies. For instance, process $P5$ in transputer 3 cannot start until $P2$ in transputer 2 has been completed.

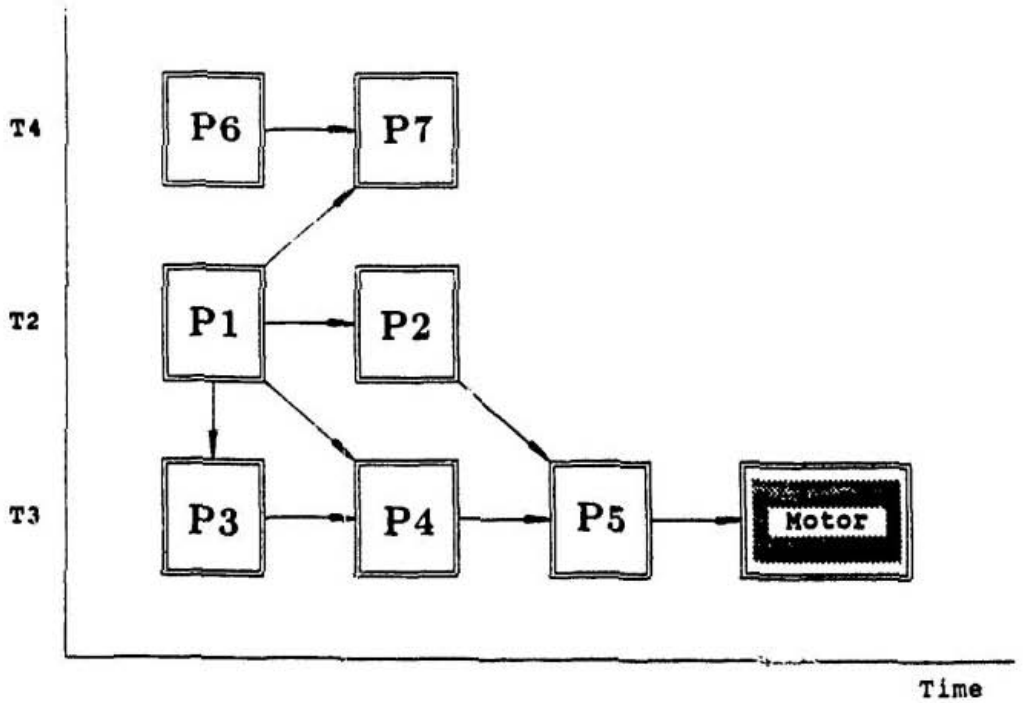

Figure 4.6: Control task dependency in the parallel processing.

Table 4.1: Simulation Computing Times for Each Sampling Cycle Over Different Computers (Time in Microseconds).

COMPUTER	SIMULATION COMPUTING TIME
IBM - PC (Model 386)	712
VAX 8530	558
One Transputer	315
Five Transputers	99

For speed comparison, we executed similar simulation programs in different computers. Table 4.1. shows the computing times for the testing and comparisons. The table clearly shows that computing times of the five transputer method is faster than one, as well as the one transputer method is faster than the others.

4.4 Execution Time

Since complexity of control algorithms leads to a heavy computational burden on computers, the execution time in a real-time control system becomes critical. For comparing conventional multiprocessor-based parallel processing systems with transputer-based one, Table 4.2[43] presented the different execution times on different parallel processors for field orientation of ac motor drives. The table shows that the multi-transputer control system offers the fastest processing speed.

To measure the calculation times of the different control algorithms and channel communications of the proposed parallel processing scheme, the T800 transputer internal timer with 1 μs is used. The measured execution times of simulation programs over five transputers are listed in Table 4.3.

Table 4.2: Comparison of Execution Times for Different Parallel Processors (Time in μs) [43] (In the figure: (a) Referred from [35]: (b) From [17]: (c) From [2]: (d) From [33]

Controller Type	Flexibility	Software Development	Parameter Adaptation Control	Sampling Time
Intel-8086 + signal processor NEC77720 (a)	No	Cumbersome	No	125
Inter-8086 + two Intel-8031 (b)	Yes	Cumbersome	No	2200
Four Inter-8086 (c)	Yes	Cumbersome	No	700
Three Transputers (T400) (d)	Yes	Easy	No	250
Five Transputer (T800)	Yes	Easy	Yes	92 or 83

Table 4.3: Execution Times

Transputer	Process	Function	Execution Time (μs)
T2	P1	Speed controller and slip frequency calculation	34
T2	P2	Cosine function computation	41
T3	P3	Current controller and α-β to d-q coordinate transformation	17
T3	P4	Sine function computation	32
T3	P5	d-q to α-β coordinate transformation	50
T4	P6	Power measurement and calculation	16
T4	P7	Adaptive control	38

Table 4.4 is redrawn from Table 4.3, so that we can easily calculate the total execution times for each transputer. The maximum execution time in the table is 99 μs, and it is also the sampling cycle of the proposed five transputer simulation scheme as given in Table 4.1.

According to the simulation results and the measured execution time, a conclusion can be made that since using multiple Transputer system, we are able to obtain sampling times of about 100 μs, which meets fast dynamic servo control requirements.

Table 4.4: Total Execution Times

	T2	T3	T4
P1	34		
P2	41		
P3		17	
P4		32	
P5		50	
P6			16
P7			38
Computation Time (μs) in each Transputer	75	99	54

4.5 Summary

This chapter describes a new scheme of multi-transputer-based parallel processing for indirect field-oriented control employing loss minimization strategy of induction motor drives to realize and implement real-time processing of a complex control scheme. The fundamental principles of parallel processing and transputer are stated. The hardware and software details of the parallel processing using five T800 transputers to emulate the partitioned algorithms for real-time control studies and using four Transputers for real-time control experiment are presented. Execution times of control process in one and five transputers are investigated to properly partition the control program for parallel processing. According to the test results, the following conclusions can be made.

1. Based on the adaptive controller in the indirect field-oriented scheme and parallel processing, the proposed scheme offers both the potential for significant energy savings and high performance of ac motor drives.

2. The execution times of the proposed scheme using one and five T800 transputers have been determined, and the effectiveness of the proposed scheme for parallel processing has been verified.

3. Since high performance and reliable motor drive systems often require additional features such as fault tolerance, self tuning, on-line diagnostics, protection, data capturing and user friendliness, and considering that modern control techniques constitute complex real-time signal processing algorithms, parallel processing using multiple Transputers is a good solution.

Chapter 5

Digital Simulation and Experimental Results

In this chapter, system descriptions for digital computer simulation and experiment are addressed. Open- and closed-loop tests for the proposed scheme are provided. Measured execution times using similar real time control programs over different computers are also reported. Digital computer simulation and experimental results demonstrate that the proposed scheme can achieve both the potential for significant energy savings and high performance of ac motor drives.

5.1 Digital Simulation Results

Digital computer simulation results are presented here to verify the theory of loss minimization and show the achievement of maximum efficiency by the proposed scheme. The dynamic performance is also analyzed.

5.1.1 System Description

Several simulation schemes for field-oriented control of ac motor drives and mathematical models of ac motor have been published [20][28][31][32][35]. A typical indirect vector control simulation scheme is shown in figure 5.1. Based on the work[13], a simulation scheme for loss minimization control with indirect field-orientation of ac motor drives has been shown in Figure 3.16. The fundamental principle of the field-oriented control and the derivation of the mathematical model of an ac motor have been discussed in Chapter 2, and are used in this simulation.

In this scheme (Figure 3.16 and 3.17), there are four controllers:

- Flux PID controller
- Torque PID controller
- Speed PID controller
- Loss minimum adaptive controller.

The flux, torque and speed PID controllers are part of the field-oriented control. The inner flux and torque control loops are faster than outer speed and adaptive control loops. The currents i_a and i_b are obtained from the output voltages u_a and u_b of the inverter. The $d-$ and $q-$axis components of the stator currents i_{ds}, and i_{qs} in the indirect field-oriented reference frame are obtained from the coordinate transformation, as given by equation 3.42. The difference between speed command ω_r^* and ω_r is the input to the speed controller, and the output of the speed controller i_{qs}^* to the inner torque control loop for controlling the speed. The difference between i_{qs}^* and i_{qs} is the input to the torque controller, which determines the reference value

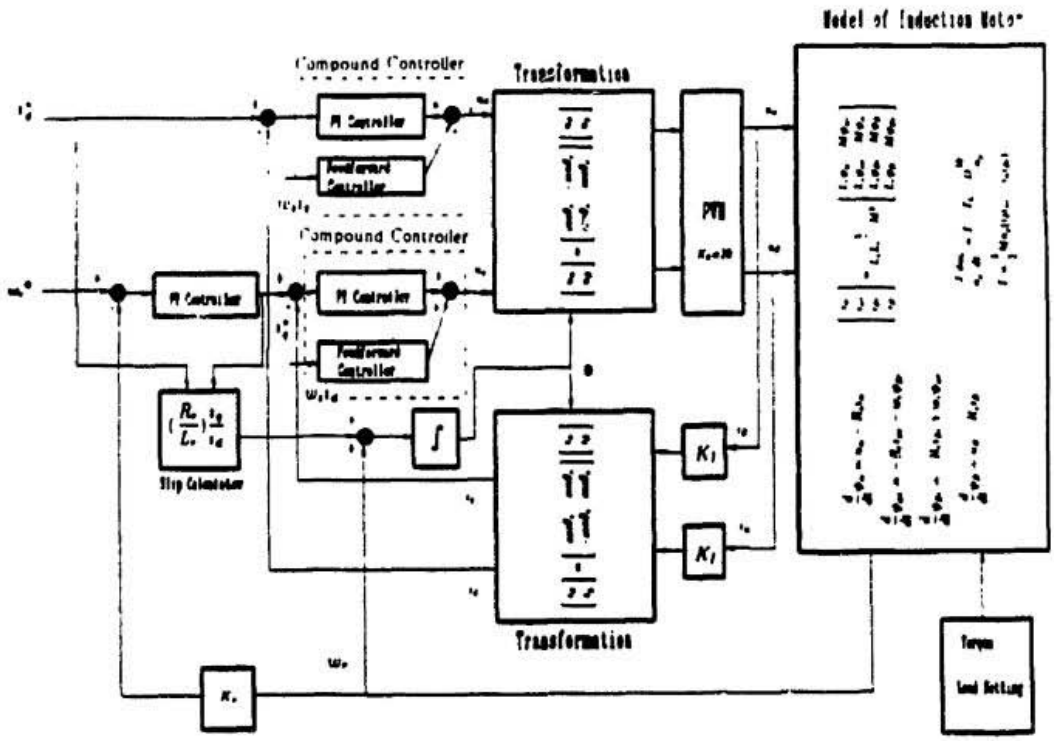

Figure 5.1: Time domain model of indirect field-oriented control system. [43]

of the torque producing component of stator voltage u_{1s}. The difference between i_{1s}^{*} and i_{1s} is the input to the flux controller, which produces the flux component of stator voltage u_{ds}. The coordinate transformation (equation 3.39) is applied to yield the reference stator voltages $u_{\alpha s}$ and $u_{\beta s}$ in the stationary reference frame; these voltages are applied to the PWM inverter to control the ac motor.

The adaptive controller implements loss minimization control. The principle of the adaptive control loop is based on the assumption that the loss minimization loop and the torque control loop are decoupled, although total decoupling is impossible. If this problem can not be solved satisfactorily, the torque control loop will be unable to maintain the power output at its original level. For decoupling the two loops well, we can make the response time of the torque loop much shorter than the interval of time separating two iterations of the adaptive controller. The simulation results demonstrate that this method is acceptable.

The purpose of the adaptive controller in the proposed scheme is that the controller adjusts the rotor flux reference component i_{ds} until the power input to the system P_{in} is minimum. The principle of the system is based on the concept that for a given load, if the shaft torque or speed is maintained constant, the efficiency of the drive will be maximum when the power measured at the input P_{in} of the system is minimum. The adaptive controller steers the system to its optimum operating point by iteratively adjusting a controlling variable i_{ds}^{*} until it detects a minimum in the measured power input P_{in}. A brief flowchart of the adaptive controller program is shown in Figure 3.18.

The computer also oversees the dynamic behaviour of the inner field-orientation system in case of a large load, speed and/or torque, change. If the load change

exceeds a given threshold, the loss minimization procedure is interrupted and the output of the adaptive controller i_{ds}^{*} is increased to its rated value to satisfy the large load command. After several seconds, the adaptive controller works again for the changed load until the new loss minimization operating point is achieved.

The losses in the drive are computed as mentioned in the Chapter 3 except for the harmonic and stray losses which are neglected. The parameters of an 1kW, 1710 rpm induction motor used in this simulation are listed in the Appendix A-2.

5.1.2 Open-Loop Test

Since this is an open-loop test, all the control loops in the proposed scheme are disconnected.

Figures 5.2-5.5 show the simulation results of the open-loop tests of the ac motor. Five seconds after the start, the flux current i_{ds} is decreased (Figure 5.2), and the input power P_{in}, which is plotted as instantaneous value, also decreases (Figure 5.4). It is clear that there is a loss minimization point for the given speed and torque at about 12 seconds. Beyond this point if i_{ds} is decreased, the input power will increase (Figures 5.3 and 5.4). This conclusion agrees with Figure 3.4. The results also show that if the input power decreases well beyond the loss minimization point, the system becomes unstable (Figures 5.3, 5.4 and 5.5).

5.1.3 Closed-Loop Test

Figures 5.6 and 5.7 show the simulation results of the control system with and without the adaptive controller. The figures show that after 10 seconds, the adaptive

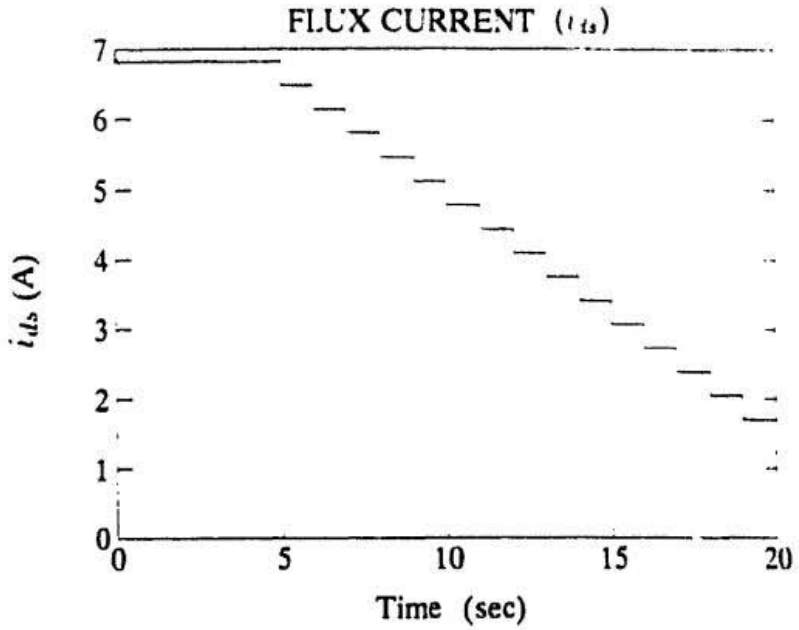

Figure 5.2: Simulation result of the open-loop test: Flux current i_{ds}.

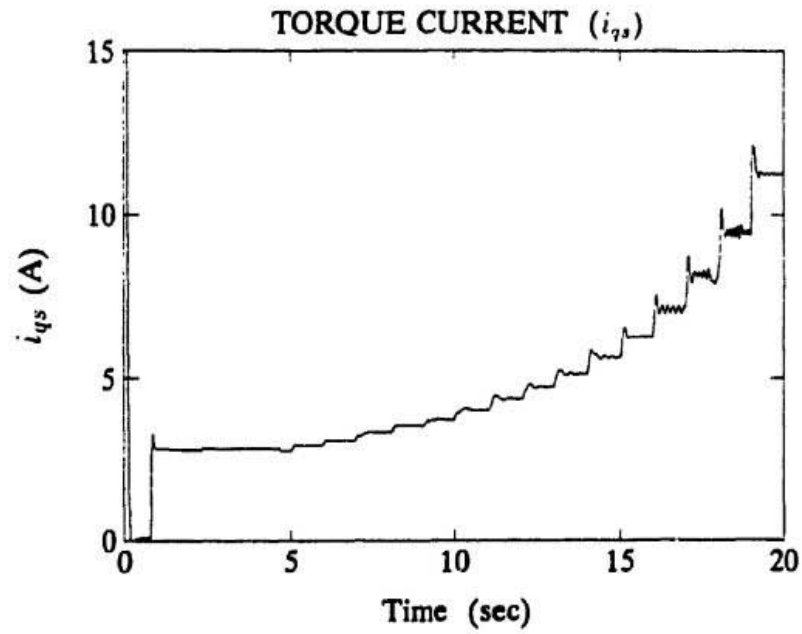

Figure 5.3: Simulation result of the open-loop test: Torque current i_{qs}.

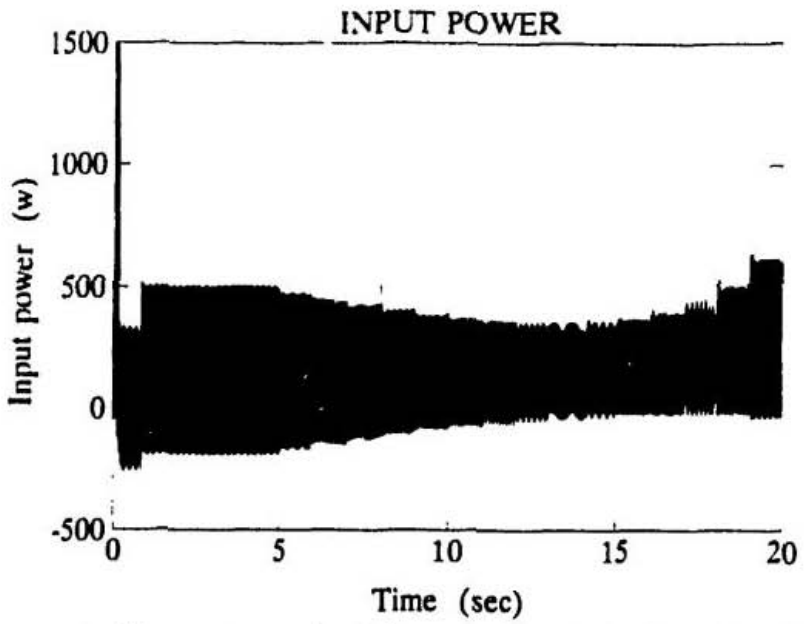

Figure 5.4: Simulation result of the open-loop test: Power input P_{in}

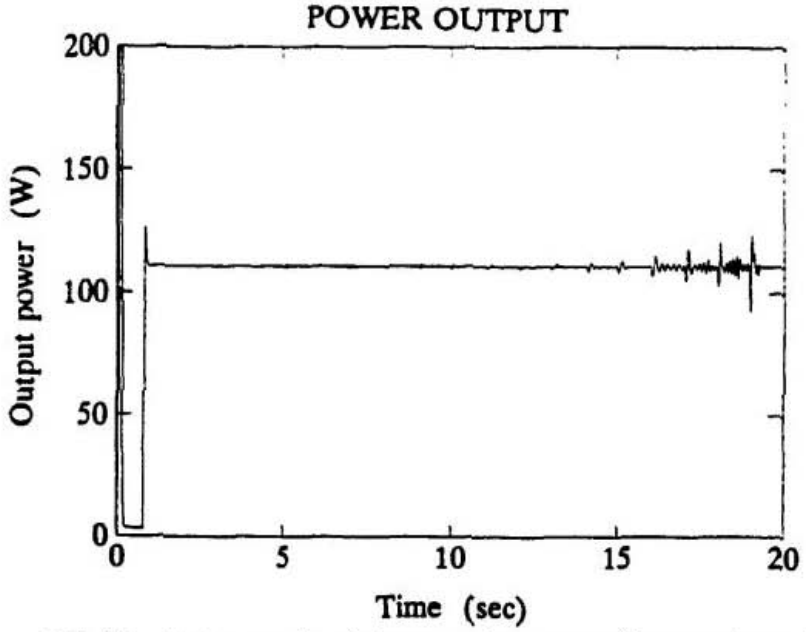

Figure 5.5: Simulation result of the open-loop test: Power output P_{out}

controller continuously decreases the flux current i_{ds} (Figure 5.6), and therefore the input power to the system (Figure 5.7). It can be seen that about 10 seconds after the adaptive controller starts working, the system operates at optimal efficiency for the given load and speed. Thus loss minimization is achieved. At 35 seconds, a large and sudden load increase is applied, which can be speed and/or torque change(s). The system detects the change and then resets the flux current i_{ds} to its rated value. The adaptive controller works again for the changed load until the new loss minimization operating point is achieved (Figures 5.6 and 5.7).

5.1.4 Sudden Load Change

In general, there are two kinds of load changes: speed and torque. For a large speed increase, a solution is proposed in [47]: i_{ds} is reset at the value corresponding to the rated flux whenever the speed controller command is the maximum value of torque current i_{qs}. The method is also suitable for large torque increase. But in lower speed case, when a larger torque increase occurs suddenly, i_{qs} can not meet the maximum value as shown in Figure 5.12. (For this simulation, the maximum value of i_{qs} is limited at 18 A.). Since the system is operating in reduced flux and lower power input situation, in the case of sudden and larger torque increase, the power input could be much less than power output required to meet the transient. Therefore, the dynamic bahaviour of the system could be poor without resetting i_{ds}.

A modified method for this case is that the system simply detects the changing value of flux current i_{ds}, and if it increases within a certain value (about 20 - 50 percent of 1 p.u. input power for this simulation), i_{ds} is reset to its rated value regardless of whether i_{qs} has reached the maximum value or not. If the change is

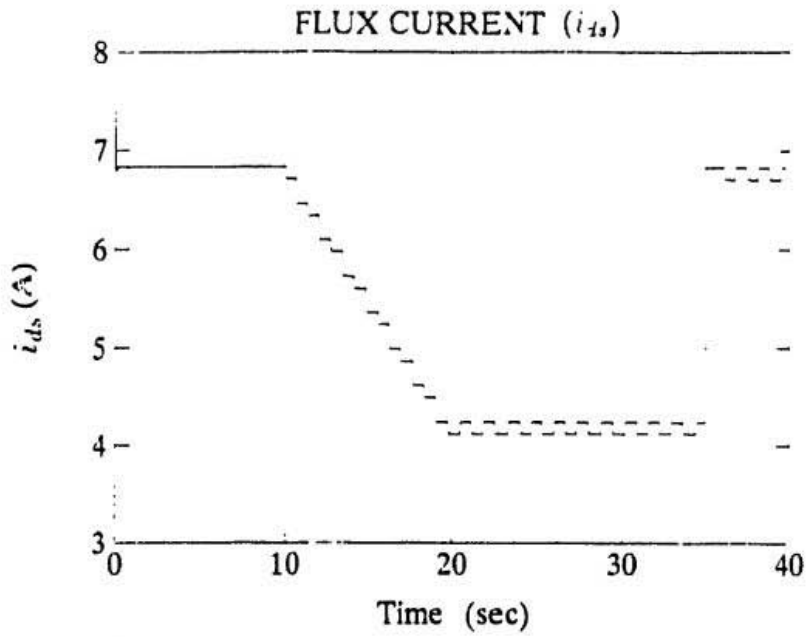

Figure 5.6: Simulation result of the proposed control system: Flux current i_{ds}.

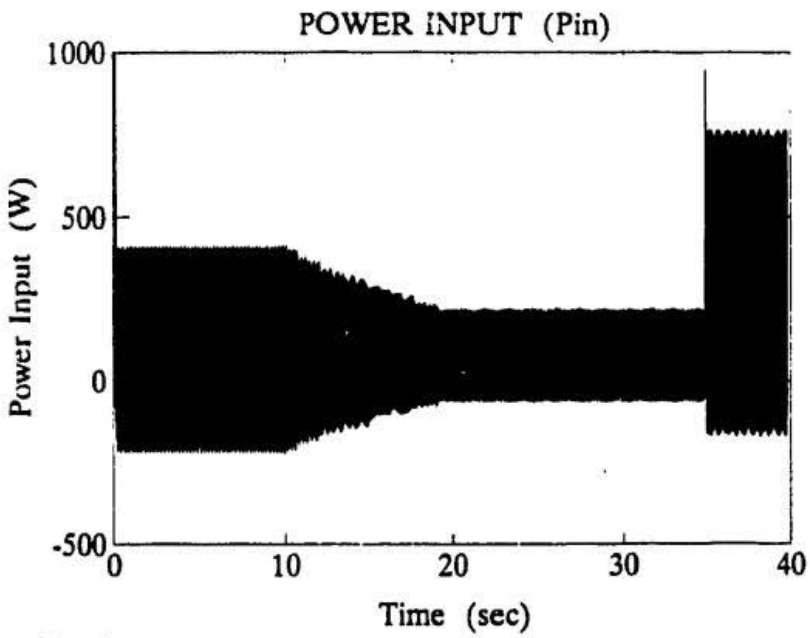

Figure 5.7: Simulation result of the proposed control system: Power input P_{in}.

less than 20 percent, the adaptive controller can handle the case without resetting.

For a large torque increase, some simulation results are presented here to demonstrate the dynamic performance of the drive for both flux resetting and rated flux conditions. In the resetting method, the adaptive controller detects the output power of the system every 10 ms; the system is reset whenever either the power input increases by more than 0.4 p.u. or as in the method in [47].

Figures 5.8–5.13 show that the system tackles a large torque increase at 3rd seconds (Figure 5.9); this can also be a large speed increase. The adaptive controller detects the load change and increases i_{ds} (Figure 5.11), thereby increasing the rotor flux (Figure 5.10) and the power input of the drive (Figure 5.13) within 10 ms. Although the delay in the worst case is 10 ms, it is still faster than i_{qs} getting its maximum value at about 3.04 seconds (Figure 5.12). Figures 5.14 – 5.19 show the simulation results in the rated flux case. Comparing Figure 5.8 with Figure 5.14, we can conclude that the dynamic performance of the decreased flux case is satisfactory, but the power consumption in the former case is much less than in the latter case (Figure 5.13 and Figure 5.19).

5.2 Experimental Results

In this section, the system description and the experimental set-up are addressed. Experimental results of the proposed scheme are reported, which verify the theory of loss minimization and to show the achievement of maximum efficiency by the proposed scheme.

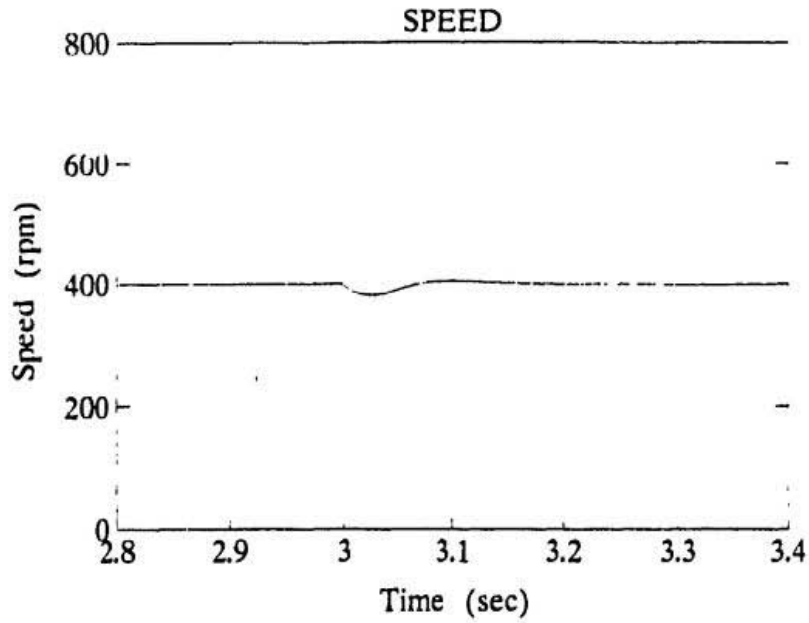

Figure 5.8: Simulation results of the proposed control system with sudden load change: Speed.

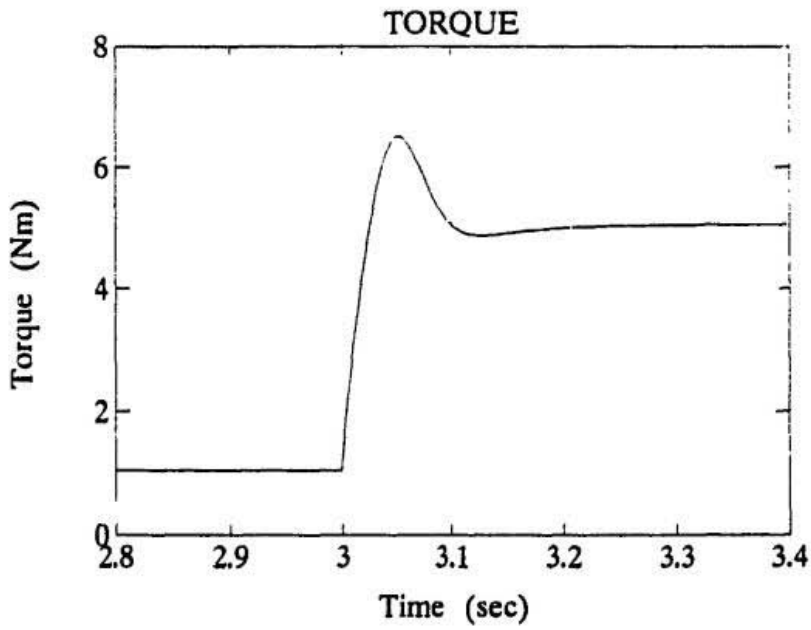

Figure 5.9: Simulation results of the proposed control system with sudden load change: Torque.

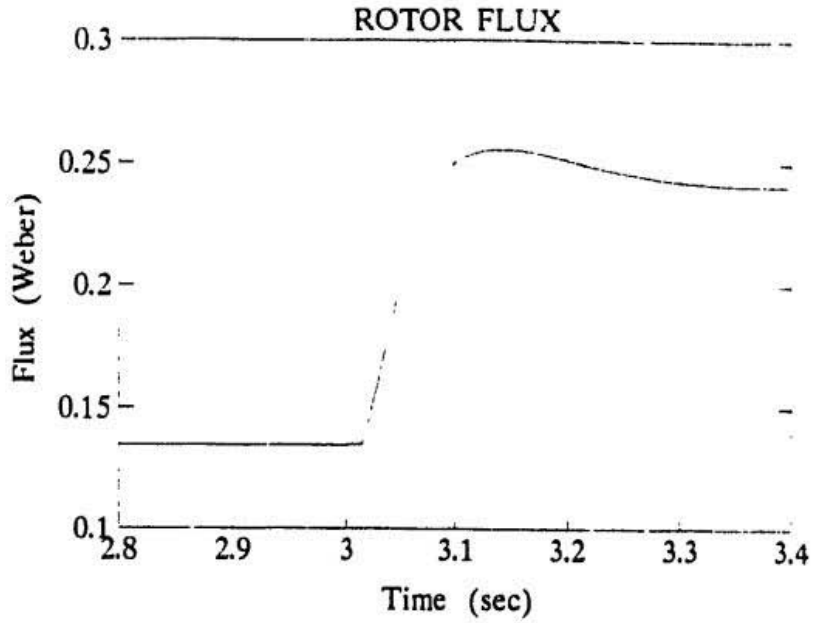

Figure 5.10: Simulation results of the proposed control system with sudden load change: Rotor flux.

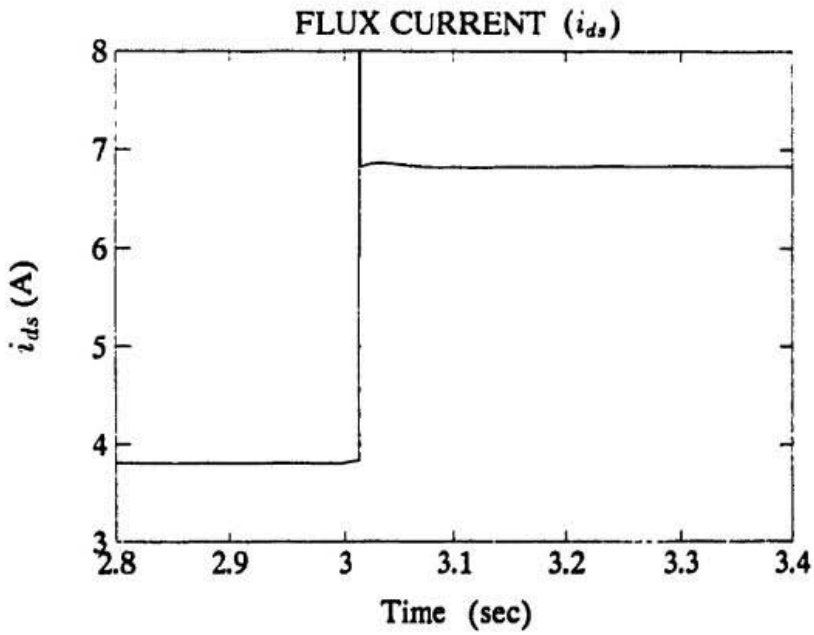

Figure 5.11: Simulation results of the proposed control system with sudden load change: Flux current i_{ds}.

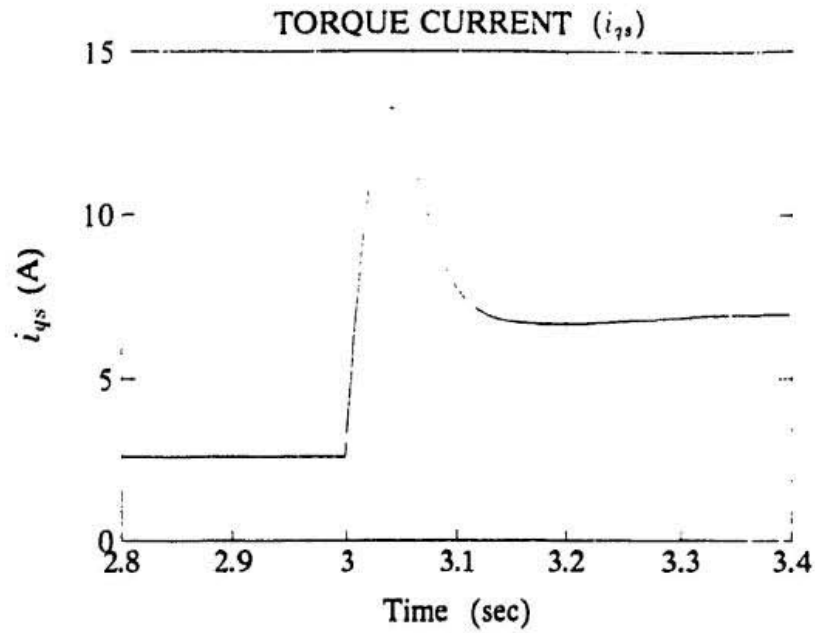

Figure 5.12: Simulation results of the proposed control system with sudden load change: Torque current i_{qs}.

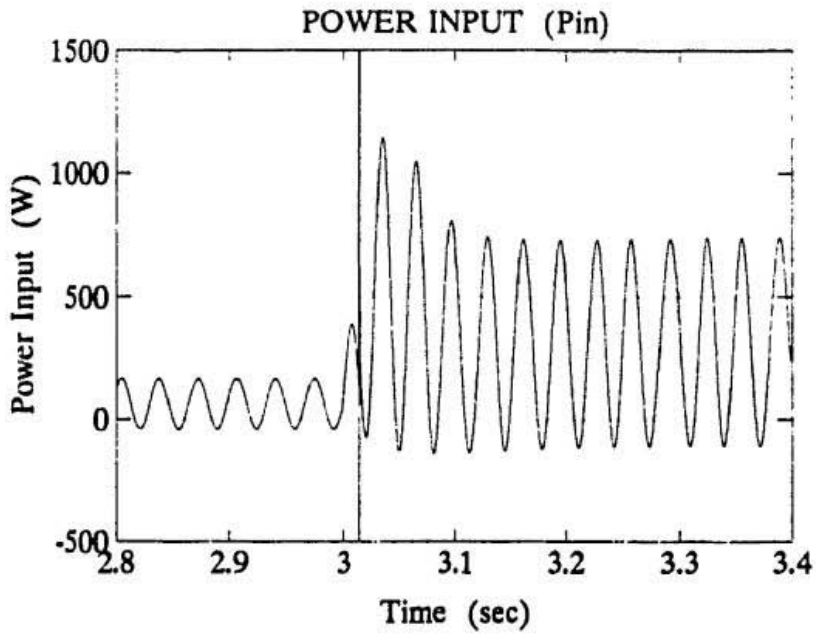

Figure 5.13: Simulation results of the proposed control system with sudden load change: Power input P_{in}.

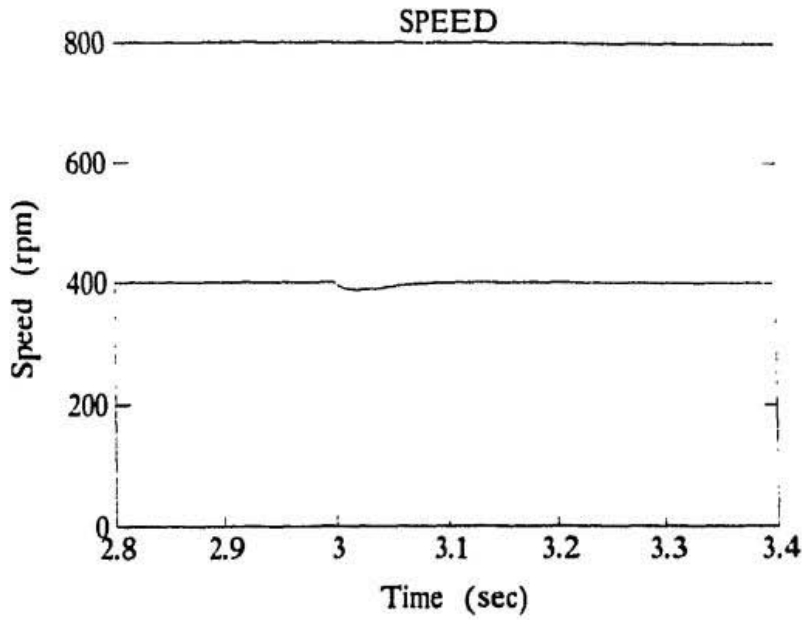

Figure 5.14: Simulation results of the system with rated flux: Speed.

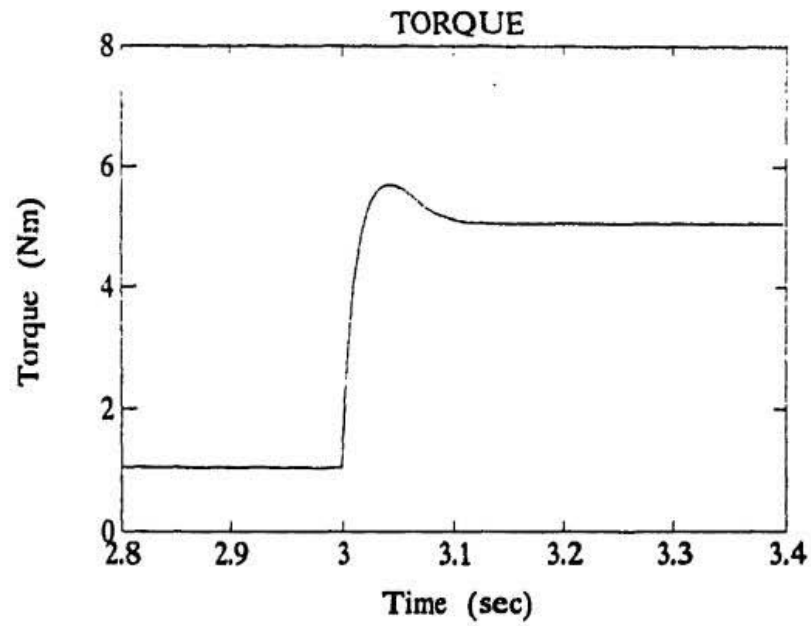

Figure 5.15: Simulation results of the system with rated flux: Torque.

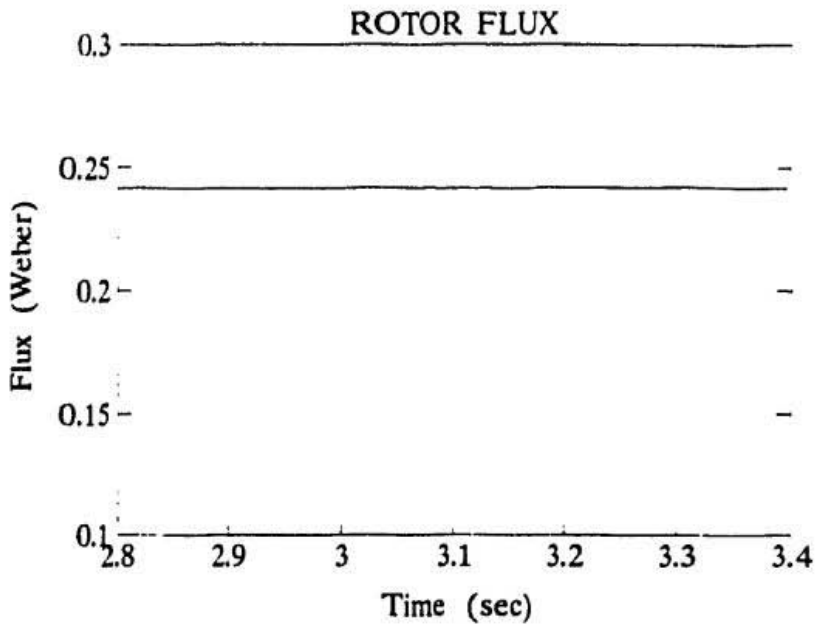

Figure 5.16: Simulation results of the system with rated flux: Rotor flux.

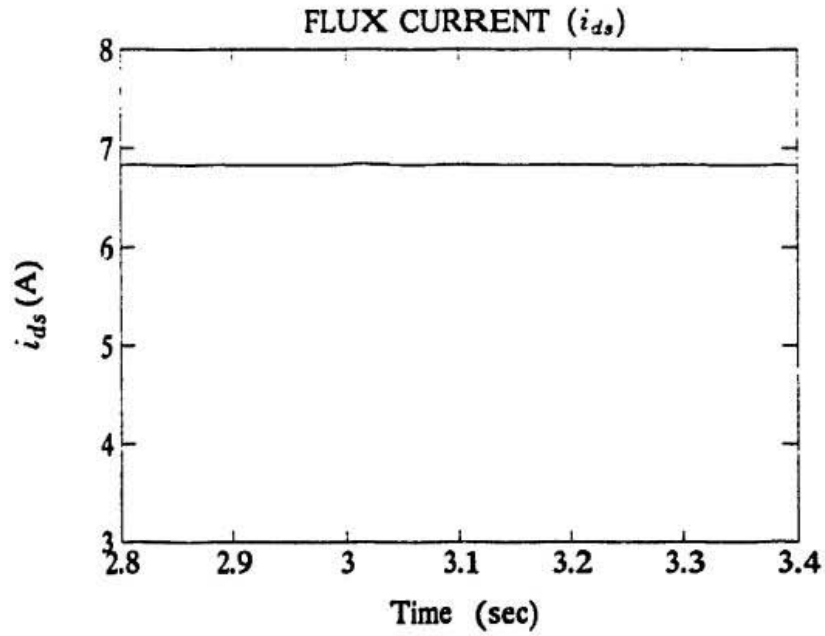

Figure 5.17: Simulation results of the system with rated flux: Flux current i_{ds}.

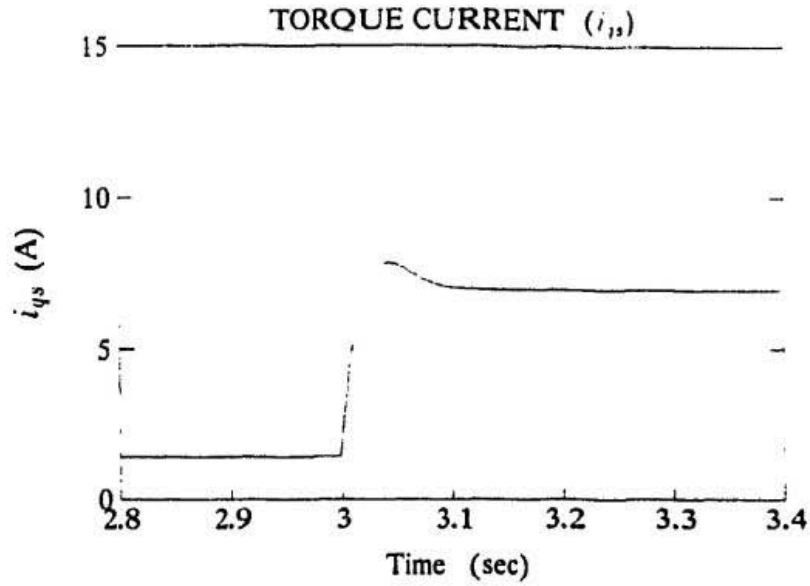

Figure 5.18: Simulation results of the system with rated flux: Torque current i_{qs}.

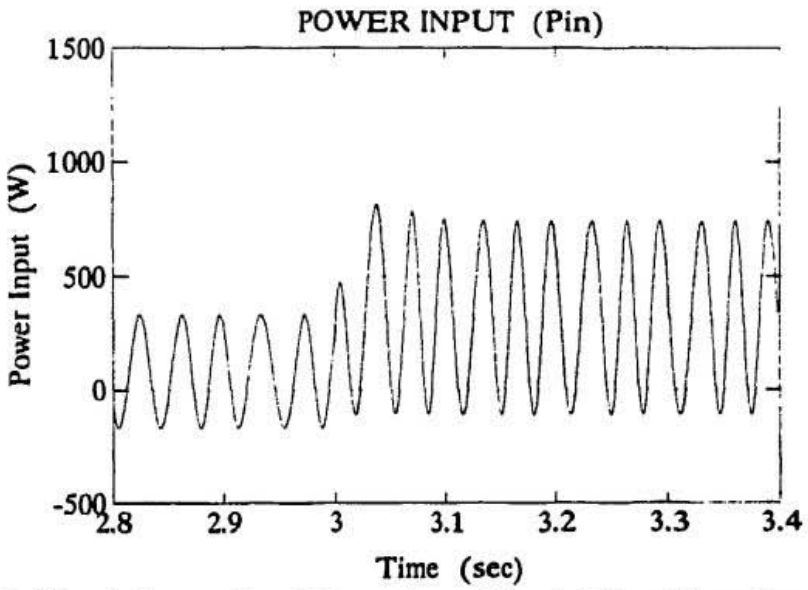

Figure 5.19: Simulation results of the system with rated flux: Power input P_{in}.

5.2.1 Experimental Set-Up

The ac motor used in the experiment is a K254T 3 hp ac motor manufactured by Brook Electric Motors of Canada Ltd. It is configured as a 4-pole, Y connection machine and its nameplate details are listed in Appendix A-1. A synchronous generator with EC609-62 Field Power Supply and EC606-01 Resistive Bank coupled to the motor provided the mechanical load for the ac motor. The generator is a 3-phase, 1.6 kW, 1.29 A and 66 field excitation, type SG-1480 synchronous generator made by CANRON Montreal Canada Ltd. A picture of the complete experimental set-up is given in Figure 5.20.

The other equipment used in the experiment are:

- CONTRONICS Personal Computer (Model 386) with four T800 Transputers (running real-time control program to obtain the execution times)
- LASER 286/2 Personal Computer
- RTI-815 Multifunction Input/Output Board with built-in A/D and D/A Converters
- INVERPOWER (Model P111 VSI) 3-Phase Voltage Source Inverter
- INVERPOWER (Model L108 SPWM) Sine PWM Logic
- 6 channel pulse amplifier
- Three phase full wave rectifier
- Two ROCKLAND (Model 10222F) Dual Hi/Lo Filters
- FF12A/9/C Tachogenerator

Figure 5.20: Experimental set-up of losses minimization control of ac motor drive

- Three INVERPOWER (Model P112 HES) isolated current transducers
- INVERPOWER (Model L109 VIB) isolated voltage transducer
- Three YEW (Type 2503) Digital AC Power Meters
- 5103N Storage Oscilloscopes
- Frequency meter
- Digital multimeters

The RTI-815 Multifunction Input/Output Board has eight built-in A/D converters and two D/A converters. The details of the board can be found in [85].

The ac motor is tested at a frequency range of 5 Hz to 60 Hz and its corresponding speeds are 160 rpm to 1720 rpm.

5.2.2 System Description

Figure 3.17 shows the block diagram of the proposed loss minimization control scheme for the experiment. Six control variables are inputted to the system through A/D converter channels; they are speed command ω_r^*, speed ω_r, ac currents i_a and i_b, dc input voltage U_{in} and current I_{in}. There is one more input signal i_{ds}^*, which is reference flux current and used for testing the field-oriented control scheme only. Two output signals, voltage $|U^*|$ and frequency f^*, connected through D/A converter channels, control the PWM pulse generator and then the PWM inverter and the ac motor.

The speed command ω_r^* as well as reference flux current i_{ds}^* are obtained from adjustable dc power supplies. Both ω_r^* and i_{ds}^* are calibrated for 0 – 10 V which

correspond to 0 - 1720 rpm (rated rotor speed) and 0 -9.5 A (rated current). The speed measurement ω_r is from the tachogenerator, which is mounted on the shaft of the ac motor. The parameters R_r and L_r used in slip angular frequency ω_s calculation were obtained from the experimental tests presented in Chapter 3 and listed in Appendix A-1.

For Y connection and with neutral point of an ac motor, we can get currents i_α and i_β by measuring two of three phase ac currents i_a and i_b in ac power supply using two isolated current transducers. The equations of the $3\phi/2\phi$ coordinate transformation are given as,

$$i_\alpha = \frac{2}{3}(i_a - \frac{1}{2}i_b + \frac{1}{2}i_a + \frac{1}{2}i_b) = i_a \tag{5.1}$$

$$i_\beta = \frac{2}{3}(\frac{\sqrt{3}}{2}i_b + \frac{\sqrt{3}}{2}i_a + \frac{\sqrt{3}}{2}i_b) = \frac{1}{\sqrt{3}}(i_a + 2i_b) \tag{5.2}$$

i_α and i_β are used for the field-oriented control.

The two power meter method is used to measure input power to the motor. However, for the loss minimization control the dc input voltage U_{in} and current I_{in} to the inverter are obtained via a dc isolated voltage and an isolated current transducers, respectively. The product of these two values is the power input P_{in}, and the average power input at every 30 cycles is needed to obtain a stable reading. The product is input to the adaptive controller for the loss minimization control.

$u_{ds}u_{qs}/u_\alpha u_\beta$ and $i_\alpha i_\beta/i_{ds}i_{qs}$ in Figure 3.17 are coordinate transformations between the rotating and stationary reference frames. KP in the figure is polar coordinate transformation. The output signals of the whole control system are voltage $|U^*|$ and frequency f^*, which are input of the SPWM pulse generator. There is a pulse amplifier between the SPWM pulse generator and the inverter for amplifying

the output values of the SPWM pulse generator. The outputs of the inverter are variable three phase ac currents and voltages to control the ac motor.

Since there are some very low frequency ripples in V_{in} and I_{in} measurements, two 1 Hz low-pass filters are used between V_{in} and I_{in} measurements and the inputs of A/D converters of the adaptive controller. For the same reason, two 80 Hz low-pass filters are applied between ac currents i_a and i_b measurements and the inputs of the A/D converters to the $3\phi/2\phi$ coordinate transformation.

In this experiment, LASER 286/2 Personal Computer is used first. Then CONTRONICS Personal Computer (Model 386) with one and four T800 Transputers are used for comparision.

5.2.3 Comparison of Different Control Schemes

Figures 5.21 and 5.22 show the experimental results of the measured power inputs for different control schemes operating at a constant speed. Figure 5.21 shows the power input for the conventional operation in which the voltage and frequency are adjusted together (constant V/Hz). Figures 5.22 shows the power input for minimum loss operation. The speed is around 864 rpm (30 Hz) for both cases. The mechanical load is maintained constant at 186 W, which electrical load is increased from 0 (Case 1) to the rated value (case 5).

These two figures show that if the input voltage is adjusted to its optimal value, more energy savings can be obtained than in the conventional method (constant V/Hz) at each constant load.

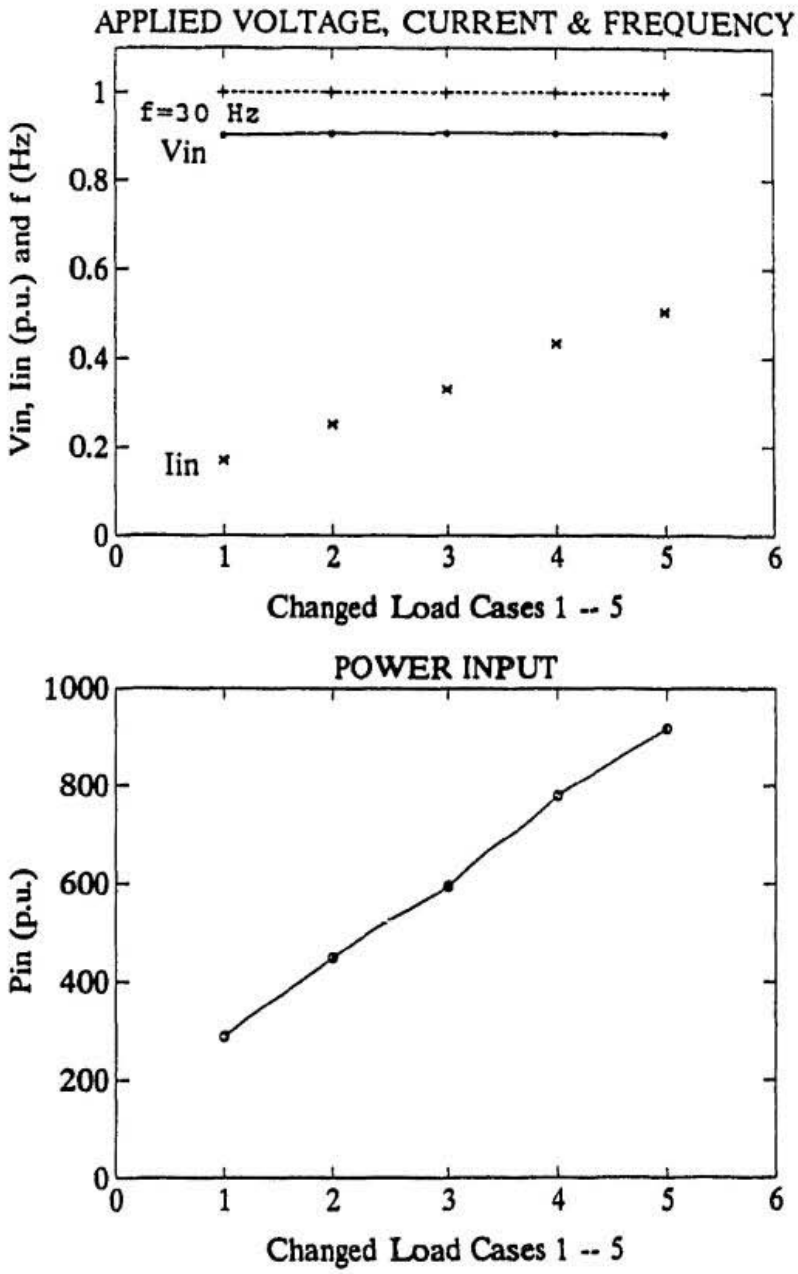

Figure 5.21: Power input for constant V/Hz operation at constant speed.

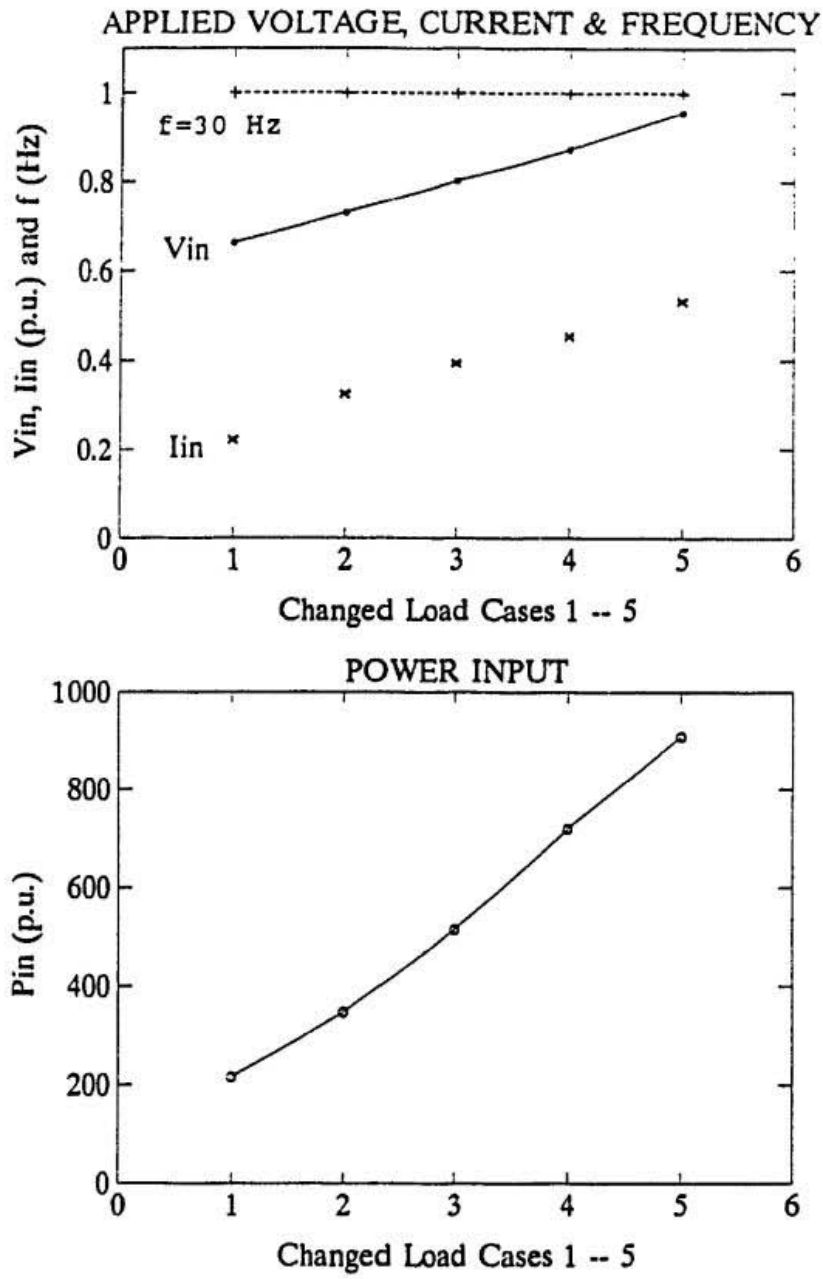

Figure 5.22: Power input for loss minimization operation at constant speed.

5.2.4 Closed-Loop Test

Figures 5.23 and 5.24 show the experimental results of the control system with and without the adaptive controller for the loss minimization control at a light load condition. The speed is at 985 rpm, and the mechamical load is kept constant at 186 W. The supply dc voltage is maintained at 294 V. Due to the voltage input $|U^*|$ of the SPWM Logic is reversal value, the lower values of $|U^*|$ in the figures are higher output from the D/A channel.

The dc current I_{in} (power input) is initially at its rated value. After the adaptive controller works, I_{in} is adjusted during the optimization in step of 3.2 % of rated value. After 26 steps and about 10 seconds, the controller decreases the power input and achieves the loss minimum point, then the system operates at optimal efficiency for the given load and speed.

Figures 5.25 shows the experimental results of the control system with and without the adaptive controller at a heavier load condition. The speed is also at 985 rpm, and the mechanical load is 186 W with a dc 0.85 A field power supply and 300 W electrical load. The supply dc voltage maintains at 294 V.

The figure illustrates that at lower speed and heavier load condition, the adaptive controller can also decrease the power input from 1068 W (read by the two wattmeters) and achieve the loss minimization at 714 W.

Figures 5.26 shows the experimental results of the proposed scheme response to a sudden and large load increase. After the adaptive controller works, the system operates at the efficiency optimization for the speed = 620 rpm and T_l = 186 W between 7.5 – 32.5 seconds. At 32.5 seconds, the speed command ω_r^* suddenly increases to 1482 rpm. The adaptive controller detects the speed changing and increases power

Table 5.1: Real Time Control Computing Times for Each Sampling Cycle Over Different Computers (Time in Microseconds).

COMPUTER	SIMULATION COMPUTING TIME
IBM - PC (Model 286)	822
One Transputer	348
Four Transputers	106

input from 108 W to 336 W. The controller works again for the changed speed until the new loss minimization operating point is achieved (power input = 285 W).

5.2.5 Execution time

Measured exeution times using similar real time control programs over different computers are listed in Table 5.1 for comparisons. The table shows that execution time of the four Transputer scheme is 106 μs, and it can meet fast dynamic servo control requirements. The table also shows that execution time of the four Transputer scheme is faster than one, as well as the one Transputer method is much faster than the PC (286).

5.3 Summary

System descriptions for both the computer simulation and experiment are disscused in this chapter. Simulation results of open- and closed-loop tests as well as the analyses of the dynamic performance of the proposed scheme are provided.

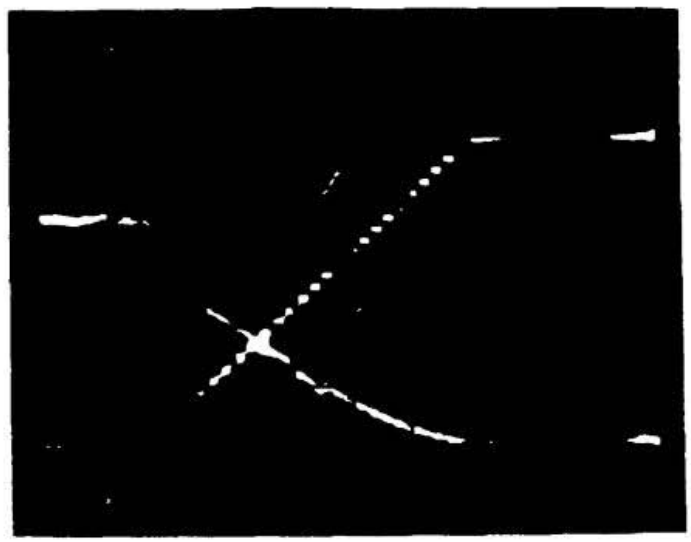

Figure 5.23: Experimental result 1: Efficiency optimization for a light load condition. ω_r = 985 rpm, T_l = 186 W. Each step in I_{in} equals 3.2 % of the rated value. (Hor: 2 sec./div)

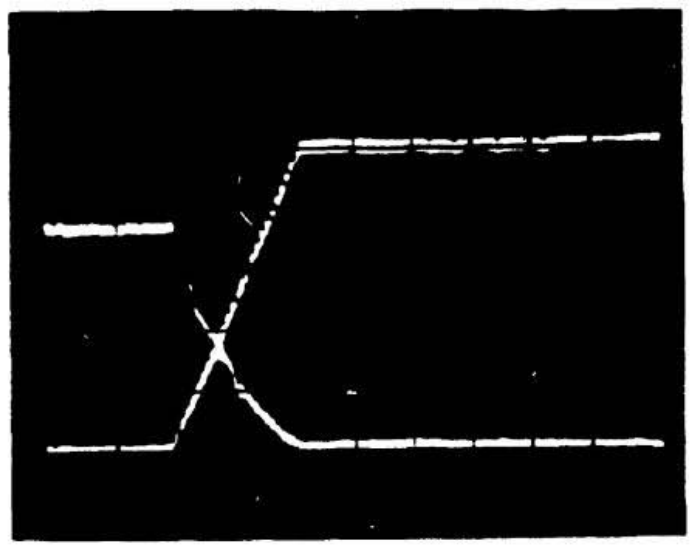

Figure 5.24: Experimental result 2: Efficiency optimization for a light load condition. ω_r = 985 rpm, T_l = 428 W. Each step in I_{in} equals 3.2 % of the rated value. (Hor: 5 sec./div)

Figure 5.25: Experimental result 3: Efficiency optimization for a heavier load condition. ω_r = 985 rpm, T_m = 186 W with a dc 0.85 A field power supply and 300 W electrical load. Each step in I_{in} equals 3.2 % of the rated value.

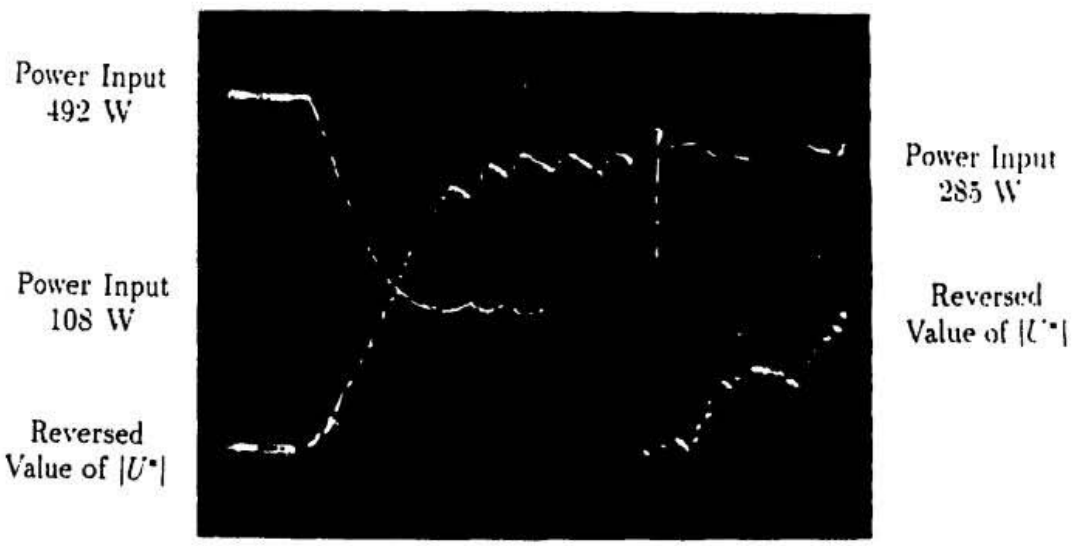

Figure 5.26: Experimental result 4: Efficiency optimization for a sudden speed increase. ω_r = 620 to 1482 rpm, T_l = 186 W. Each step in I_{in} equals 3.2 % of the rated value.

Measured execution times using similar real time control programs over different computers are also shown. According to the simulation and experimental results, some conclusions and discussions can be made as follows:

1. The loss minimization theory of ac motor drives has been verified by the open-loop tests.

2. The simulation and experimental results of the closed-loop tests show that the proposed scheme for loss minimization control can achieve significant energy savings.

3. The measured execution times demonstrate that using the adaptive controller with the indirect field-oriented scheme, both the potential for significant energy savings and high performance in ac motor drives can be achieved.

Chapter 6

Conclusions and Suggestions for Further Research

Based on the theoretical analysis, simulation and experimental results presented in this thesis, some conclusions are drawn in this chapter and suggestions for further research are listed.

6.1 Conclusions

The objectives of using multiple Transputers in the parallel processing of indirect field-oriented vector control employing loss minimization for high performance ac motor drives have been achieved. Losses in ac motor drives have been studied and verified by experiments. A new scheme based on the use of a multiple Transputer system for the real-time parallel processing implementation of indirect field-oriented control incorporating loss minimization strategy for high performance ac motor drives has been proposed. Computer simulation results of using five Transputers and experimental results of using a PC (386) and a real-time control program running on four Transputers for the parallel processing have been presented in the

thesis. It has been shown that high performance as well as significant energy savings can be achieved by the proposed scheme. The work is summarized as follows:

Losses in ac motor drives are studied in detail first by theoretical derivation in general, and then by experimental verification on a particular ac motor. The results of the study show that significant energy savings can be achieved for operation at light torque loads for all speeds, and for torque loads near the rated value under low-speed operation with a variable frequency loss minimization control system. An indirect field-oriented control method incorporating a loss minimization control strategy in an adaptive control technique has been proposed. The model of an ac motor for the field-oriented control is briefly discussed, and the parameters of the ac motor for the experiment are also calculated. It is shown that the proposed scheme can achieve the aim of significant energy savings and meet the needs of high-performance ac drive applications.

Since the complexity of control algorithms such as the indirect field-oriented control and adaptive controller lead to a heavy computational burden on computers, the execution time in a real-time control system becomes critical. The multiple Transputer system can be a good solution for parallel processing of real-time digital control of ac motor drives.

A new scheme using multiple Transputers for the parallel processing implementation of the field-orientation employing the loss minimization strategy has been proposed. The fundamental principles of parallel processing and the Transputer are presented. The hardware and software details of a parallel processing scheme using five T800 Transputers to emulate the partitioned algorithms for real-time control studies and using four Transputers for real-time control experiment are presented.

Execution times of the control process using one (and five) Transputer(s) are also investigated.

The digital simulation and experimental results of open- and closed-loop tests as well as sudden changes in load tests for the proposed scheme have been provided. System descriptions for digital computer simulation and experiment are addressed. Measured execution times using similar real time control programs over different computers are also obtained.

Based on the work described above, the following conclusions can be made:

- The loss minimization theory of ac motor drives has been verified by both simulation and experimental results of open-loop tests.
- The simulation and experimental results of closed-loop tests show that the proposed scheme for loss minimization control can achieve significant energy savings.
- The execution times of the proposed scheme using one, five (for the simulation) and four (for the experiment) T800 Transputers have been determined, and the effectiveness of the proposed scheme for parallel processing has been verified.
- The simulation and experimental results demonstrate that using the adaptive controller in the indirect field-oriented scheme and parallel processing, the proposed scheme offers both significant energy savings and high performance for ac motor drives.
- Since high performance and reliable motor drive systems often require additional features such as fault tolerance, artificial intelligence, expert systems,

self tuning, on-line diagnostics, protection, data capturing and user friendliness, and considering that modern control techniques constitute complex real-time signal processing algorithms, parallel processing using multiple Transputers is a good solution for high performance ac motor drives.

- Although hardware development and board costs are low, the Transputers are still not low-cost devices and for commercial drives, their application would be expected to be restricted to the higher power range. For low and medium powers, it is envisaged that a hardware specific parallelism involving conventional processors with a defined, restrictive specification is likely to remain the most economic option for some time.

6.2 Suggestions for Further Research

This thesis provides a brief analysis, simulation and partial implementation of multiple Transputer-based parallel processing of indirect field-oriented vector control employing loss minimization for high performance ac motor drives. This subject needs much detailed study. The suggestions for further research are outlined as follows:

- It has been noted in [22][24][35] that the performance of indirect vector control strategies is sensitive to the rotor time constant. When applying variable flux control for loss minimization, the motor parameters should change more widely. Although some researchers have studied the problem[56], further work needs to be carried out by digital simulations and experimental implementations.

- Since speed measurement is very important to the indirect field-oriented control for the slip calculation and speed control, a more accurate tachogenerator is recommended for further experimentation.

- The transient performance of the proposed scheme should be studied in more detail through further experimentation using different control schemes. A design of four quadrant operation of the scheme is recommended.

- More D/A channels are needed to obtain more internal parameters of the control system such as flux current, torque current, calculated slip, rotor flux and variables in coordinate transformations in order to analyze the system characteristics in detail.

- Although a flux controller can reduce some losses in ac motors such as the fundamental core and ohmic losses, it is difficult to reduce the harmonic and load-independent converter losses. A further reduction in losses could be achieved if a multiple variable optimization is applied.

- The software of control algorithm must be partitioned in an optimum manner for parallel processing. On the other hand, other parallel strategies should be investigated in order to fully explore the inherent advantages of real-time digital control of ac motor drives.

- Since each T800 Transputer has only four links with which to interconnect the processors, this implies that a limited amount of interconnection is possible. The optimum number of Transputers needed for different applications should be determined.

- With development of VLSI technology as well as with decreasing prices and increasing system functions, it is desirable that some special VLSI chips be manufactured for parallel processing of ac motor control for commercial purpose.

- As mentioned earlier, for high performance and reliable ac motor drive systems, more additional features such as fault tolerance, artificial intelligence, expert systems, self tuning, on-line diagnostics, protection, data capturing and user friendliness, sliding model control, modern control techniques and their complex real-time signal processing algorithms are needed to be considered along with the parallel processing.

References

[1] P.C. Sen, " Electric Motor Drives and Control—Past, Present and Future", *IEEE Trans. on Industrial Electronics*, vol.37, no.6, pp.562-575, Dec. 1990.

[2] B.K. Bose, "Technology Trends in Microcomputer Control of Electrical Machines", *IEEE Trans. on Industrial Electronics*, vol.35, no.1, pp.160-177, Feb. 1988.

[3] R.G. Harley, M.R. Webster, G. Diana and D.C. Levy, "A High Performance, Interactive, Real-Time Controller for a Field Oriented Controlled AC Servo Drive", *IEEE Conf. Rec. IAS Annu. Meeting*, pp.613-618, 1990.

[4] R.G. Harley, A.W.M. Hemme, D.C. Levy and M.R. Webster, "Real-Time Issues of Transputers in High Performance Motion Control Systems", *IEEE Conf. Rec. IAS Annu. Meeting* pp.324-330, 1991.

[5] P.J. Tsitvitse and E.A. Klingshirn, "Optimum Voltage and Frequency for Polyphase Induction Motors Operating with Variable Frequency Power Supplies", *IEEE Conf. Rec. Annu. Meeting in Ind. Gen. Applic. Soc.*, pp. 815-823, 1970.

[6] F.J. Nola, "Save Power in AC Induction Motor", *NASA Tech. Brief N. MFS-23280*, Summer, 1977.

[7] F.J. Nola, "Power Factor Control System for AC Induction Motor", *U.S. Patent 4,052,648*, Oct. 4, 1977.

[8] F.J. Nola, "Power Factor Controller – an Energy Saver", *IEEE Conf. Rec. IAS Annu. Meeting*, pp. 194-198, 1980.

[9] D. Galler, "Energy Efficient Control of AC Induction Motor Driven Vehicles", *IEEE Conf. Rec. ISA Annu. Meeting*, pp. 301-308, 1980.

[10] T.W. Jian, D.W. Novotny and N.L. Schmitz, "Characteristic Induction Motor Slip Values for Variable Voltage Part Load Performance Optimization", *IEEE Trans. Power Appar. System*, vol.102, pp.38-46, 1983.

[11] A. Kusko and D. Galler, "Control Means for Minimization of Losses in AC and DC Motor Drives", *IEEE Trans. on Industry Applications*, vol.19, no.4, pp.561-570, July-Aug, 1983.

[12] M.H. Park, S.K. Sul, D.Y. Yoon and T.W. Chun, "Optimal Efficiency Drive of Induction Motors with Current Source Inverter", *Proc. Inter. Power Elec. Conf.* Tokyo, pp.450-460, 1983.

[13] M.H. Park and S.K. Sul, "Microprocessor-Based Optimal-Efficiency Drive of an Induction Motor", *IEEE Trans. on Industrial Electronics*, vol.31, no.1, pp.69-73, Feb. 1984.

[14] P. Famouri and J.J. Cathey, "Loss Minimization Control of an Induction Motor Drive", *IEEE Trans. on Industry Applications*, vol.27, no.1, pp.32-37, Jan./Feb. 1991.

[15] F. Blaschke, "The Principle of Field Orientation as Applied to the New Transisor Closed-Loop Control System for Rotating-Field Machines", *Siemens Review*, No.5, pp.217-220, 1972.

[16] K. Hasse, "Zur Dynamik Drehzajlgeregelter Antriebemit Stromrichtergespeisten Asynchron-Kurzschlusslau Fermaschinen", *Dissertation*, Techn. Hochsch., Darmasadt, West Germany, 1969.

[17] L.J. Garces, "Parameter Adaption for the Speed-Controlled Static AC Drive with a Squirrel-Cage Induction Motor", *IEEE Trans. on Industry Applications*, vol.16, no.2, pp.173-178, Mar./Apr. 1980.

[18] V.B. Honsinger, "Induction Motors Operating from Inverters", *IEEE Conf. Rec. ISA Annu. Meeting*, pp.1276-1285, 1980.

[19] N. Mutoh, H. Nagase et al., "High Response Digital Speed Control System for Induction Motors", *Proc. 1984 IECON*, pp. 839-844, 1984.

[20] S. Sathiakumar and J. Vithayathil, "Digital Simulation of Field-Oriented Control of Induction Motor", *IEEE Trans. on Industrial Electronics*, vol.31, no.2, pp.141-148, May 1984.

[21] F. Harashima, S. Konda and K. Ohnishi, "Multimicroprocessor-Based Control System for Quick Response Induction Motor Drive", *IEEE Trans. on Industry Applications*, vol.21, no.4, pp.603-609, May/June 1985.

[22] T. Matsuo and T.A. Lipo, "A Rotor Parameter Identification Scheme for Vector-Controlled Induction Motor Drives", *IEEE Trans. on Industry Applications*, vol.21, no.4, pp.624-632, May/June 1985.

[23] K. Kubo, M. Watanabe and T. Ohmae, "A Fully Digitalized Speed Regulator Using Multimicroprocessor System for Induction Motor Drives", *IEEE Trans. on Industry Applications*, vol.21, no.5, pp.1001-1007, July/Aug. 1985.

[24] K.B. Nordin, D.W. Novotny, D.S. Zinger, "The Influence of Moter Parameters in Feed-Forward Field Orientation Drive Systems", *IEEE Trans. on Industry Applications*, vol.21, no.5, pp.1009-1015, July/Aug. 1985.

[25] B.K. Bose, "Motion Control Technology Present and Future", *IEEE Trans. on Industry Applications*, vol.21, no.6, pp.1337-1342, Nov./Dec. 1985.

[26] P.P. Acarnley, J.W. Finch and D.J. Atkinson, "Field Orientation in AC Drives: State of the Art and Future Prospects", *IEE Conf. Publ. 282*, pp.285-289, 1987.

[27] P.P. Acarnley and J.W. Finch, "Review of Control Techniques for Field-Orientation in AC Drives", *22 Universities Power Engineering Conference*, Sunderland, paper 9.08, 1987.

[28] S.N. Ghani, "Digital Computer Simulation of Three-Phase Induction Machine Dynamics—a Generalized Approach", *IEEE Trans. on Industry Applications*, vol.24, no.1, pp.106-114, Jan./Feb. 1988.

[29] T.A. Lipo, "Recent Progress in the Development of Solid-State AC Motor Drives", *IEEE Trans. on Power Electronics*, vol.3, no.2, pp.105-117, Apr. 1988.

[30] E.Y.Y. Ho and P.C. Sen, "Decoupling Control of Induction Motor Drives", *IEEE Trans. on Industrial Electronics*, vol.35, no.2, pp.253-262, May 1988.

[31] C.H. Liu, C.C. Hwu and Y.F. Feng, "Modelling and Implementation of a Microprocessor-Based CSI-Fed Induction Motor Drive Using Field-Oriented

Control", *IEEE Trans. on Industry Applications*, vol.25, no.4, pp.588-597, Jul/Aug. 1989.

[32] G.R. Slemon, "Modelling of Induction Machines for Electric Drives", *IEEE Trans. on Industry Applications*, vol.25, no.6, pp.1126-1131, Nov./Dec. 1989.

[33] R.D. Lorenz and D.B. Lawson, "A Simplified Approach to Continuous On-Line Tuning of Field-Oriented Induction Machine Drives", *IEEE Trans. on Industry Applications*, vol.26, no.3, pp.420-424, May/June 1990.

[34] T. Murata, T. Tsuchiya and I. Takeda, "Vector Control for Induction Machine on the Application of Optimal Control Theory", *IEEE Trans. on Industrial Electronics*, vol.37, no.4, pp.283-290, Aug. 1990.

[35] C.C. Chan and H.Q. Wang, "An Effective Method for Rotor Resistance Indentification for High-Performance Induction Motor Vector Control", *IEEE Trans. on Industrial Electronics*, vol.37, no.6, pp.477-482, Dec. 1990.

[36] IEEE Standard 112-1978, *"IEEE Test Procedures for Polyphase Induction Motors and Generators"*, No. 112, 1978.

[37] A.E. Fitzgerald, Charles Kingsley, Jr. and S.D. Umans, *"Electric Machinery"*, Fourth edition, McGraw-Hill Book Co. 1983.

[38] S.A. Nasar, *"Electric Machines and Transformers"*, MacMillan Publishing Co., 1986.

[39] S. Yamamura, *"AC Motors for High-Performance Applications"*, Marcel Dekker, Inc., 1986.

[40] P. Vas, "*Vector Control of AC Machines*", Oxford Science Publications, 1990.

[41] B.K. Bose, "*Power Electronics and AC Drives*", Englewood Cliffs, NJ: Prentice-Hall, 1987.

[42] J.M.D. Murphy and F.G. Turnbull, "*Power Electronic Control of AC Motors*", Pergamon Press, 1988.

[43] W. Li, "*Field Oriented Control and its Parallel Processing Using Transputers for Induction Motor*", M.Eng. thesis, Memorial University of Newfoundland, 1991.

[44] S.C. Peak and J.L. Oldenkamp, "A Study of System Losses in a Transistorized Inverter-Induction Motor Drive System", *IEEE Conf. Rec. ISA Annu. Meeting*, 1983.

[45] D.S. Kirschen, D.W. Novotny, and W. Suwanwisoot, "Minimizing Induction Motor Losses by Excitation Control on Variable Frequency Drives", *IEEE Trans. on Industry Applications*, vol.20, no.5, pp.1244-1250, Sep.-Oct. 1984.

[46] H.G. Kim, S.K. Sul and M.H. Park, "Optimal Efficiency Drive of a Current Source Inverter Fed Induction Motor by Flux Control", *IEEE Trans. on Industry Applications*, vol.20, no.6, pp.1453-1459, Nov./Dec. 1984.

[47] D.S. Kirschen, D.W. Novotny and T.A. Lipo, "Optimal Efficiency Control of an Induction Motor Drive", *IEEE Trans. on Energy Conversion*, vol.2, no.1, pp.70-76, Mar. 1987.

[48] S. Chen and S.M. Yeh, "Efficiency Control of Field Oriented Operation Based on the Open-Loop VVVF Drives", *IEEE Conf. Rec. ISA Annu. Meeting*, pp.58-64. 1991.

[49] R.D. Lorenz and S.M. Yang, "Efficiency-Optimized Flux Trajectories for Closed-Cycle Operation of Field-Orientation Induction Machine Drives", *IEEE Trans. on Industrial Applications*, vol.28, no.3, pp.574-580, May/June 1992.

[50] R.D. Lorenz and S.M. Yang, "AC Induction Servo Sizing for Motion Control Applications Via Loss Minimizing Real-Time Flux Control", *IEEE Trans. on Industrial Applications*, vol.28, no.3, pp.589-593, May/June 1992.

[51] T.Egami and T. Tsuchiya, "Efficiency-Optimized Speed Control System with Feed-Forward Compensation", *IEEE Trans. on Industrial Electronics*, vol.34, no.2, pp.216-226, May. 1987.

[52] K.S. Su and S.N. Yeh, "Deep-Bar Effect Analysis of Induction Motors", *Proc. of the 9th symposium on Electrical Power Engineering*, pp. 359-379, 1988.

[53] R.S. Lu, R. Venkatesan and J.E. Quaicoe,"Loss Minimization Control of AC Motor Drives", *The Third Newfoundland Electrical and Computer Engineering Conference (NECEC '92)*, St. John's, NF, Canada, May, 1992.

[54] G.S. Kim, I.J. Ha and M.S. Ko, "Control of Induction Motors for both High Dynamic Performance and High Power Efficiency", *IEEE Trans. on Industrial Electronics*, vol.39, no.4, pp.323-333, Aug. 1992.

[55] R.S. Lu, R. Venkatesan and J.E. Quaicoe, "Transputer-Based Parallel Processing for Loss Minimization Control of AC Motor Drives", the *Canadian Con-*

ference on Electrical and Computer Engineering(CCECE'92), Toronto, Canada, Sep., 1992.

[56] S. Chen and S.M. Yeh, "Optimal Efficiency Analysis of Induction Motors Fed by Variable-Voltage and Variable-Frequency Source", *IEEE Trans. on Energy Conversion*, vol.7, no.3, pp.537-543, Sep. 1992.

[57] D.S. Kirschen "*Optimal Efficiency Control of Induction Machines*", Ph.D. thesis, University of Wisconsin-Madison, 1985.

[58] S.R. Bowes, "Recent Developments in PWM Switching Strategies for Microprocessor-Controlled Inverter Drives", *Motor-Con. Proceedings*, pp. 10-22, June 1988.

[59] D.I. Jones and P.J. Fleming, "Control Applications of Transputers", Personal communication with D.I. Jones, Bristol University, United Kingdom, Mar. 1988.

[60] P.J. Fleming, "*Parallel Processing in Control — the Transputer and other Architectures*", Peter Peregrinus Limited, 1988.

[61] S.R. Bowes and P.R. Clark, "Transputer-Based Harmonic Elimination PWM Control of Inverter Drives", *IEEE Conf. Rec. IAS Annu. Meeting*, pp.744-752, 1989.

[62] G.M. Asher, "Real-Time Motor Control Using a Transputer Parallel Processing Network", *EPE 89 Proceedings*, Aachen, West Germany, pp. 433-438, Oct. 1989.

[63] Inmos, "Performance Maximisation", *The Transputer Applications Notebook, Systems and Performance*, 1st Edition, pp. 280-298, 1989.

[64] G.M. Asher and M. Summer, " Parallelism and the Transputer for Real-Time High Performance Control of AC Induction Motors", *IEE Proceedings*, vol.137 pt. D, no.4, pp.179-188, July 1990.

[65] J.W. Ponton and R. Mckinnel, "Nonlinear Process Simulation and Control Using Transputers", *IEE Proceedings*, vol.137, Pt.D, no.4, pp.189-195, July 1990.

[66] H.A. Thompson and P.J. Fleming, "Fault-Tolerant Transputer-Based Controller Configurations for Gas-Turbine Engines", *IEE Proceedings*, vol.137 pt. D, no.4, pp.253-260, July 1990.

[67] S.R. Bowes and P.R. Clark, "Transputer-Based Harmonic-Elimination PWM Control of Inverter Drives", *IEEE Trans. on Industry Applications*, vol.28, no.1, pp.72-80, Jan./Feb. 1992.

[68] S.R. Bowes and P.R. Clark, "Transputer-Based Optimal PWM Control of Inverter Drives", *IEEE Trans. on Industry Applications*, vol.28, no.1, pp.81-88, Jan./Feb. 1992.

[69] W.L. Li and R. Venkatesan, "A Highly Reliable Parallel Processing Controller for Vector Control of AC Induction Motor", *Ind. Elect., cont., Instr., and Auto. Int. Conf. (IECON '), Nov. 1992.*

[70] K. Hwang and F.A. Briggs, *"Computer Architecture and Parallel Processing"*, McGraw Hill Book Co., 1984.

[71] Lord, *"Advanced Computers"*, Ann Arbor Science, 1988.

[72] Meyers, *"Advances in Computer Architecture"*, JM., 1989.

[73] "*Transputer Handbook*", INMOS Limited, 1989.

[74] A. DeCegrame, "*The Technology of Parallel Processing*", Vol. 1, Prentice Hall Englewood Cliffs, New Jersey, 1989.

[75] "*Transputer Architecture and Overview, Transputer Technical Specifications, the Transputer Instruction Set: a Compiler Writer's Guide*", Computer System Architects, 1990.

[76] "*Logical Systems C for the Transputer: Version 89.1 User Manual, Periscope Transputer Network Debugger for Logical Systems C*", Computer System Architects, 1990.

[77] B.W. Johson and J.H. Aylor, "Reliability and Safety Analysis of a Fault-Tolerant Controller", *IEEE Trans. on Reliability*, vol. R-35, no.4, Oct. 1986.

[78] Z.K. Wu, and E.G. Strangas, "Feed Forward Field Orientation Control of an Induction Motor Using a PWM Voltage Source Inverter and Standardized Single-Board Computers", *IEEE Trans. on Industrial Electronics*, vol.35, no.1, pp.75-79, Feb. 1988.

[79] A. Sabanovic and F. Bilalovic, "Sliding Mode Control of AC Drives", *IEEE Trans. on Industry Applications*, vol.25, no.1, pp.70-75, Jan./Feb. 1989.

[80] I. Takahashi and Y. Ohmori, "High-Performance Direct Torque Control of an Induction Motor", *IEEE Trans. on Industry Applications*, vol.25, no.2, pp.257-264, Mar./Apr. 1989.

[81] J. Zhang and T.H. Barton, "A Fast Variable Structure Current Controller for an Induction Machine Drive", *IEEE Trans. on Industry Applications*, vol.26, no.3, pp.415-419, May/Jun. 1990.

[82] R.D. Lorenz and D.B. Lawson, "A Simplified Approach to Continuous On-Line Tuning of Field-Oriented Induction Machine Drives", *IEEE Trans. on Industry Applications*, vol.26, no.3, pp.420-424, May/Jun. 1990.

[83] H.H. Huffman, "Introduction to Solid-State Adjustable Speed Drives", *IEEE Trans. on Industry Applications*, vol.26, no.4, pp.671-678, Jul./Aug. 1990.

[84] J.M.D. Murphy and V.B. Honsinger, "Efficiency Optimization of Inverter-Fed Induction Motor Drives", *IEEE Conf. Rec. ISA Annu. Meeting*, pp. 544-552, 1982.

[85] *"RTI-800/815 Multifunction Input/Output Board, User's Manual"*, Analog Devices and IBM Co., 1986.

[86] *"PRO-MATLAB for VAX/VXS Computers, User's Guide"*, The MathWorks Inc., June 1989.

Appendix A-1: Motor Parameters for Experiment

Nameplate Data:

Frame	K254T
Type	DP
F.L.Speed	1720/1120/870/550
Volts	208
F.L.Amps	6/9.5
Hz	60
Phase	3
HP	3/2/1.5/1

Equivalent Circuit Parameters:

Connection	Y
R_s	1.04 Ω
R_r	0.56 Ω
X_s	2.45 Ω
X_r	3.67 Ω
X_c	35.0 Ω

Appendix A-2: Motor Parameters for Simulations

rated power	1 kW
rated speed	1710 r/min
number of poles	4
R_s	0.49 Ω
R_r	0.45 Ω
L_s	0.0388 H
L_r	0.0354 H
M	0.0354 H
rated i_{ds}	6.83 A
rated i_{qs}	11.54 A
total inertia J	0.024 Nm s^2/rad
viscous friction coefficient D	0.0011 Nm s/rad